An Investigation of Surface Water Sediment Source Tracking Using Bacterial Metagenomics and Elemental Fingerprinting

A Dissertation Presented for the

Doctor of Philosophy

Degree

The University of Tennessee, Knoxville

Yanchong Huangfu

December 2018

Copyright © 2018 by Yanchong Huangfu

All rights reserved.

DEDICATION

I dedicate this dissertation to my Mom and Dad, who have been my cheerleaders all of my life.

ACKNOWLEDGEMENTS

I would like to thank my advisor Dr. Shawn Hawkins for his tremendous support to my academic career. My co-advisor, Dr. Michael Essington spent copious amounts of time advising me on my dissertation, and I feel appreciative for his input. Thanks to my committee members Drs. Alice Layton, Forbes Walker and John Schwartz. The completion of my doctoral study would not happen without your guidance and knowledge. Dr. Layton provided me with enormous assistance in doing research on microbial communities. Thanks to Dr. Walker, the PI of our project, for assigning me to work on this project. Thanks to Dr. Schwartz for helping me to collect samples, building up my connections and extending my research in a broad scope. Working under all of your supervision was such an incredible experience for me.

I would like to thank Dr. Julie Carrier, the head of our department in assigning Li Xiuwen and helping with my manuscripts. I am thankful for Li Xiuwen and Zeng Xiangfeng's great advice on my dissertation. I also want to thank Jessica Oetting and the couple (Robin and Woody Smith) in helping me with improving the grammar and vocabulary in this dissertation. A special thank you to Ms. Lena Beth, the staff of UT Extension, who graciously helped in accessing the sampling sites. I am also grateful for the assistance of Dan Williams, Melanie Stewart and Karina Costa in helping me with all the experimental work.

This project was funded by the U.S. National Institute of Food and Agriculture (NIFA)'s Program (Grant No. 2012-51130-20246). My doctoral program was also supported by the hardship grant of Society for Applied Microbiology (SfAM). I was

also sponsored by the Crenshaw Scholarship from our university. I am very thankful for their financial support in covering my tuition and living expenses.

I would like to thank my landlady Natalie Harris for allowing me to stay at her house as a student boarder, from whom I learnt a lot of American culture. I also would like to thank my mentor, Sherry Wang, who invited me to come to Tennessee and gave me much help since moving to here.

Thanks to my darling, Qu Ziyu, who dove right in my life during my doctoral study. I feel appreciative that our love drove me through the dark, even though we are thousands of miles away. I am grateful you are the one waiting for me.

Lastly, thanks to my family members, particularly my parents, Su Yingying and Huangfu Yuanzhou for their unconditional love, support and encouragement in my life. They sent me to school in Hong Kong (Bachelor and Master study) and the United States (Doctoral study). They are the people who changed my life. I feel honored to be their son.

ABSTRACT

Excess suspended sediment in river systems commonly degrades surface water quality. A sediment source tracking approach is necessary to target management practices that will reduce significant sources of sediment in rainfall runoff and restore water quality. Sediment source tracking utilizes the biogeochemical characteristics of sediment, often paired with a mathematical model, to link eroding source materials and in-stream suspended sediment. However, there are still many questions left unanswered in using this approach, including simultaneously identifying fecal contamination sources, quantifying the reliability of sediment tracers, and methods to assess the accuracy of sediment source identification. The research herein utilized the microbial communities and elemental fingerprinting techniques associated with an impaired watershed's eroding source materials and suspended sediment; these sediment source tracking methods were employed using two Bayesian-based models, SourceTracker for metagenomic bacterial community data, and Stable Isotope Analysis in R (SIAR) for the sediment elemental composition. Bacterial metagenomic data from sources of both upland eroding soil (i.e., cropland and cattle paths) and eroding bank soil were more similar to the bacterial metagenomic community within in-stream suspended sediment than manure; this indicates that certain microbial communities in upland eroding soils can be used to identify important sources of in-stream suspended sediment. Eroding source material elemental composition data indicated that bank erosion was an important source of suspended sediment within the watershed. This knowledge can be used to more efficiently improve water quality by

focusing on stream bank stabilization projects. Additional research herein evaluated the performance of nitric acid extraction versus total dissolution for sediment elemental analysis; the results clearly showed that the safer nitric acid extraction provided an elemental analysis that was as effective for sediment source tracking as total dissolution with hydrofluoric acid.

TABLE OF CONTENTS

CHAPTER 1: INTRODUCTION 1

Background 2

Sediment Source Tracking 4

Objectives 7

Organization of the Dissertation 9

Reference 10

Appendix 1: Table in Chapter 1 13

CHAPTER 2: SEDIMENT-MICROBIAL SOURCE TRACKING (MST): A PROOF OF CONCEPT STUDY USING SEDIMENT METAGENOMIC DATA IN AN IMPAIRED WATERSHED 15

Abstract 16

Introduction 17

Materials and Methods 21

Study Site and Sample Collection 21

DNA Extraction and Purification 22

Library Preparation and High-throughput Sequencing 22

Bioinformatics 24

Multivariate Analysis 25

SourceTracker Apportionment 25

Results 27

Physicochemical and Water Quality Parameters 27

Soil and Sediment Microbiomes 27
Alpha Diversity 28
Bacterial Community Composition 28
Bacterial Community Beta Diversity 30
Sediment-Microbial Source Tracking (MST) 31
Discussion 32
References 34
Appendix 2: Tables in Chapter 2 38
Appendix 3: Figures in Chapter 2 49
CHAPTER 3: ASSESSING THE VALIDITY OF SEDIMENT FINGERPRINTING USING ARTIFICIAL MIXTURES 55
Abstract 56
Introduction 58
Materials and Methods 62
Study Area 62
Sampling and Analysis 63
Tracer Selection Methods 64
Source Group Classification 65
Artificial Mixtures 65
SIAR Simulations 66
Results and Discussion 68
Sediment Source Discrimination 68

Evaluation of Apportionment Results 70

Suspended Sediment Source Apportionment 72

Conclusions 73

References 75

Appendix 4: Tables in Chapter 3 78

Appendix 5: Figures in Chapter 3 94

Appendix 6: Total Dissolution Element Concentrations 100

Appendix 7: Nitric Acid Extraction (HNO_3) Element Concentrations 106

CHAPTER 4: EVALUATION OF NITRIC ACID EXTRACTION OF ELEMENTS FROM SOIL AND SEDIMENTS FROM TWO WATERSHEDS IN EAST TENNESSEE 112

Abstract 113

Introduction 114

Materials and Methods 116

Study Area 116

Soil Properties 116

Sample Collection and Processing 117

Total Dissolution 117

Nitric Acid Extraction 118

ICP-OES Measurements 118

Statistical Analyses 119

Results and Discussion 120

Summary 123

Reference 124

Appendix 8: Tables in Chapter 4 126

Appendix 9: Figures in Chapter 4 130

CHAPTER 5: CONCLUSIONS 138

VITA 142

LIST OF TABLES

Table 1.1 Adverse surface water quality impacts of excess sediment…….....……....14

Table 2.1 Water sample physicochemical parameters…….…….....39

Table 2.2 Alpha diversity metrics by sample type…….……...…40

Table A. 2.1 OTU summary for Oostanaula Creek sink samples ranked by OTUs……41

Table A. 2.2 Description of Oostanaula Creek sampling sites.....42

Table A. 2.3 OTU summary for Oostanaula Creek upland soils……..……....….44

Table A. 2.4 OTU summary for Oostanaula Creek bank soils……..…….…….....45

Table A. 2.5 OTU summary for manure samples …….……....……46

Table A. 2.6 Core microbiomes for sediment source and sink samples.……..…..47

Table 3.1 Sediment elemental fingerprinting research……..…….……...79

Table 3.2 Summary of trial sets validating sediment elemental fingerprinting……..80

Table 3.3 Artificial mixture content of different source group sample classification schemes: aa (Surface + Subsurface) and bb (Bank + Forest + Pasture + Path)……...81

Table 3.4 Trial set tracer misclassification percentage in discriminant analysis.……..82

Table 3.5 Percent root mean square errors (RMSEs) between actual and predicted mean proportional source contribution for 12 artificial sediment mixtures, trial sets I through IV…….……83

Table 3.6 Percent root mean square errors (RMSEs) between actual and predicted mean proportional source contributions for 12 artificial sediment mixtures, trial sets V through VIII……...…….……..84

Table A. 3.1 Total dissolution and HNO_3 procedures…….....85

Table A. 3.2 Wavelengths and detection limits for elemental analysis by ICP-OES…..86

Table A. 3.3 Percent absolute residual errors between actual and predicted mean proportional source contributions for 12 artificial sediment mixtures, trial sets I through IV……..……..87

Table A. 3.4 Percent absolute residual errors between actual and predicted mean proportional source contributions for 12 artificial sediment mixtures, trial set V…..……...……...……...……88

Table A. 3.5 Percent absolute residual errors between actual and predicted mean proportional source contributions for 12 artificial sediment mixtures, trial set VI.…….……...…….89

Table A. 3.6 Percent absolute residual errors between actual and predicted mean proportional source contributions for 12 artificial sediment mixtures, trial set VII. ……..…….…….90

Table A. 3.7 Percent absolute residual errors between actual and predicted mean proportional source contributions for 12 artificial mixtures, trial set VIII. ……..……...……91

Table A. 3.8 T-test results comparing Total and HNO_3 extraction of soils and sediment…….....92

Table A. 3.9 T-test results comparing statistical selection and all tracers selection.……..……...……..93

Table 4.1 Comparison of 21 elements in Oostanaula Creek and Pond Creek soils with uncontaminated soils collected worldwide …….....127

Table 4.2 Heterogeneity, HNO_3-extraction efficiency and r-value for 21 elements in Oostanaula Creek and Pond Creek soils…….....128

Table 4.3 Geochemical association for major and trace elements in Oostanaula Creek and Pond Creek soils…….……..129

LIST OF FIGURES

Figure 2.1 Oostanaula Creek watershed sampling sites……...……50

Figure 2.2 Bacterial community OTU abundance, at the phylum level, for suspended sediment and potential eroding materials in upland and bank soils in Oostanaula Creek….....51

Figure 2.3 Bacterial community OTU abundance, at the family level, for suspended sediment and potential eroding materials in upland and bank soils in Oostanaula Creek….....52

Figure 2.4 Multivariate correlation analysis of suspended sediment and soil 16S rRNA gene sequences……...……..…53

Figure 2.5 Average predicted percentage of bacterial community composition attributable to different land-based source communities determined by SourceTracker.....54

Figure 3.1 Comparison of mean absolute residual errors for trial sets I through IV....95

Figure 3.2 Comparison of mean absolute residual errors for trial sets V through VIII.....96

Figure 3.3 Comparison of average mean absolute residual errors for trial sets I through VIII..……...…….……97

Figure 3.4 Proportional mean subsurface and surface source contributions in Oostanaula Creek watershed..……...…….…….…….98

Figure 3.5 Proportional mean upland source contributions in Oostanaula Creek watershed…….99

Figure 4.1 (a) Correlation and regression plots for Al, K, and Ti between total dissolution and nitric acid extraction for Oostanaula Creek and Pond Creek watersheds…….....…131

Figure 4.1 (b) Correlation and regression plots for Ba, Co, and Fe between total dissolution and nitric acid extraction in Oostanaula Creek and Pond Creek watersheds...……...132

Figure 4.1 (c) Correlation and regression plots for Ca, P, and Mg between total dissolution and nitric acid extraction in Oostanaula Creek and Pond Creek watersheds...…….……..133

Figure 4.1 (d) Correlation and regression plots for Zn, Nd, and Mn between total dissolution and nitric acid extraction in Oostanaula Creek and Pond Creek watersheds…….…….134

Figure 4.1 (e) Correlation and regression plots for Cr, Cu, and La between total dissolution and nitric acid extraction in Oostanaula Creek and Pond Creek watershed….……..…….135

Figure 4.1 (f) Correlation and regression plots for Li, Sr, and Zr between total dissolution and nitric acid extraction in Oostanaula Creek and Pond Creek watersheds…….……..136

Figure 4.2 Total dissolution element dendrograms for measured elements in total dissolution for Oostanaula Creek (a) and Pond Creek (b) soils…… 137

LIST OF ABBREVIATIONS

Abbreviation	Definition
Al	Aluminum
Ba	Barium
BIOM	Biological Observation Matrix
BMPs	Best Management Practices
Ca	Calcium
CDA	Canonical Discriminant Analysis
Co	Cobalt
Cr	Chromium
Cu	Copper
DFA	Discriminant Function Analysis
DO	Dissolved Oxygen
Fe	Iron
ICP-OES	Inductively Coupled Plasma - Optical Emission Spectrometry
K	Potassium
KW	Kruskal-Wallis rank test
La	Lanthanum
Li	Lithium
MCMC	Monte Carlo Markov Chains
Mg	Magnesium
Mn	Manganese

MST	Microbial Source Tracking
Nd	Neodymium
NGS	Next Generation Sequencing techniques
NTU	Nephelometric Turbidity Units
OC	Oostanaula Creek
OTUs	Operational Taxonomic Units
P	Phosphorous
PC	Pond Creek
QIIME	Quantitative Insights Into Microbial Ecology
S	Sulfur
Si	Silica
Sr	Strontium
SIAR	Stable Isotope Analysis in R
S-MST	Sediment-Microbial Source Tracking
Ti	Titanium
TDEC	Tennessee Department of Environment and Conservation
TMDLs	Total Maximum Daily Loads
V	Vanadium
Zn	Zinc
Zr	Zirconium

CHAPTER 1: INTRODUCTION

Background

Some amount of sediment will always be present in surface waters as a result of naturally occurring erosion. A given waterbody may only be of acceptable quality if the concentration of deposited and suspended sediment does not increase significantly beyond natural levels. The change from natural ecosystems to managed land use, such as pasture, can significantly increase watershed sediment loads (Blake et al., 2012). Excess sediment and siltation are a primary cause of waterbody impairment in almost one-third of impaired stream miles in the U.S., leading to a significant degradation of overall water quality (EPA, 2002; Kemp et al., 2011). Due to the fact that sediment also serves as a vector for the transport of nutrients, pathogens, and toxic environmental contaminants (Allan, 1986; Horowitz, 1991), the presence of excess suspended sediment negatively impacts water quality on a broad scope, including biological, chemical, and physical properties as indicated in Table 1.1 (Milliman and Meade, 1983; TDEC, 2008a). Furthermore, excess sediment can increase both the likelihood of flooding as well as water treatment cost substantially (TDEC, 2002). In North America, the damage associated with fluvial sediment within waterbodies have been estimated to range from $20 to $50 billion annually (Lal and Stewart, 2013; Mukundan et al., 2012).

Sediment transportation occurs following the erosion of soil and depends on a series of dynamic relationships between slope length and gradient, weather events, vegetative cover, drainage pathways, and sediment characteristics (Rickson, 2014; TDEC, 2002). Poor land management and modification of soils will interrupt these

relationships and cause significant changes in sediment yield (Brooks et al., 2012). In order to minimize the negative impacts of excess sediment in surface waters, certain national strategies have been implemented to reduce upland sediment delivery including the implementation of targeted Best Management Practices (BMP's) (EPA, 2002; TDEC, 2002). An important regulatory tool for improving sediment impaired water quality is the implementation of Total Maximum Daily Loads (TMDLs), which lists loads from all point and non-point source pollutants in an impaired stream (TDEC, 2002). In the U.S., so-called "303(d) lists" of impaired streams are published (TDEC, 2002). Because there are any number of differing sediment sources (e.g. cropland, stream bank, pasture, and cow path) which can vary in relative importance over time, identifying eroding sediment source materials is a difficult task. Therefore, methods that provide for the accurate identification of suspended sediment sources is critical and, in fact, required for TMDL development and BMP placement. Techniques that can categorize the origin of suspended sediment would improve BMPs placement and more quickly and efficiently improve water quality. Many methods have been developed for sediment source identification.

Sediment Source Tracking

This research investigated two methods for identifying the origin of surface water sediment, which utilized sediment source and sink bacterial metagenomic and elemental composition data: Sediment-Microbial Source Tracking (Sediment-MST) and elemental fingerprinting, respectively.

Sediment-MST is a term modified from "Microbial Source Tracking (MST) (Santo Domingo & Sadowsky, 2007). The difference between the two terms lies in the source objective. The traditional term, MST, refers to determining sources of fecal contamination, while Sediment-MST refers to determining sources of suspended sediment. Declaration of the differentiation between these two terms is crucial within this research, although MST and Sediment-MST may prove to be correlated in some areas dominated by animal agriculture. The research herein attempts to relate the bacterial community structure of eroding source materials to that of suspended sediment using the v4 region of 16S ribosomal RNA gene (Lee, Lee, Sung, & Ko, 2011).

There are two clear advantages of Sediment-MST using bacterial metagenomic data: it is suitable for all genetic material recovered directly from environmental samples and it can lead to the identification of different sources of contamination, both for fecal bacteria and sediment. The current limitation of this technique is the experimental cost of DNA sequencing. However, as sequencing technologies have advanced quickly, the price has steadily decreased. The increasing accuracy, speed,

and read lengths now possible with downstream processing of metagenomic datasets may provide a significant advantage in favor of Sediment-MST (Unno et al., 2018).

Sediment fingerprinting is an approach which assesses the provenance, movement, and ultimate fate of sediment within river systems using a group of "tracers" (Miller et al., 2015; Owens et al., 2016). The term tracer is associated with a specific sediment property (e.g. physical, chemical, or biological in nature) that is used to track the movement of sediment from origin to deposition (Miller et al., 2015). However, there are numerous chemical, biological, and hydraulic processes involved in the transportation of sediment that alter sediment properties from the source to suspended or deposited downstream solids.

The process of sediment fingerprinting involves the use of a fingerprint property as well as a combination of field sample collection, laboratory work, multivariate analysis and un-mixing model application to allocate suspended sediment to different source categories. The presence of a group of elements is necessary to make an inference about the sources of any given sediment (Foster and Lees, 2000). However, sediment element concentrations can be measured using different dissolution techniques (e.g. total dissolution or nitric acid extraction) (Essington, 2015) and the effect of these different extraction methods on fingerprinting effectiveness is not well qualified.

Statistical tests and un-mixing models are critical steps for converting collective sediment element concentration data to meaningful estimates of source contribution. The Kruskal-Wallis (KW) and Discriminant Function Analysis (DFA) tests have been

used in two-step approaches in selecting sediment tracers (Collins and Walling, 2002; Walling et al., 1999). Un-mixing models, such as Stable Isotope Analysis in R (SIAR) are commonly used to estimate the proportional source contributions and also report the level of uncertainty (Barthod et al., 2015; Koiter et al., 2013; Parnell et al., 2013), but have not been employed for validating the techniques of sediment source identification. SIAR could be used to evaluate the relative importance of mixed sediment sources. However, there is lack of practice in research which could validate the role of un-mixing models for sediment element datasets. The use of artificial sediment mixtures (known quantities of different sediment sources) would be an efficient way to evaluate the performance of un-mixing models using the sediment elemental fingerprinting approach (Hughes et al., 2009; Palazón et al., 2015; Poulenard et al., 2012).

Objectives

The primary goals of this research were to: (1) apply and evaluate a tool for sediment microbial source tracking and (2) to validate sediment elemental fingerprinting using artificial sediment source mixtures.

Specific objectives for sediment microbial source tracking included: (1) sampling suspended stream sediment and different land-based source materials in an impaired watershed; (2) investigating the microbial communities of source materials and suspended sediment; (3) evaluating whether microbial communities discriminate between suspended sediment source materials; (4) applying the features of microbial communities in a model for an impaired watershed to estimate the proportional contribution of different source materials.

Specific objectives for sediment elemental fingerprinting included: (1) sampling the eroding soils in an impaired watershed; (2) determining the elemental content of soil and suspended sediment samples by both total dissolution and nitric acid (HNO_3) extraction; (3) creating artificial sediment mixtures using different classes of source materials; (4) validating the sediment fingerprinting method using the elemental content of artificial mixtures; (5) estimating the relative contribution of sediment in an impaired watershed.

It was hypothesized that sediment source bacterial communities in different sediment source materials were distinguishable using multivariate statistical analysis. It was postulated that an elemental fingerprint would discriminate of between different categories of sediment source materials when using both total dissolution

and HNO_3 extraction datasets; it was further hypothesized that the un-mixing model could be successfully used to distinquich between surface soils (i.e., upland soils) vand subsurface soils (i.e., stream bank).

Organization of the Dissertation

The background, technique, and objectives for this research are presented in Chapter 1.

A proof of concept study using sediment-microbial source tracking (Sediment-MST) linking sediment source materials and in-stream suspended sediment is presented in Chapter 2, formatted as a manuscript for peer review. Metagenomic data are incorporated into SourceTracker for a proportional source contribution evaluation in a sediment impaired watershed.

Validation of the sediment elemental fingerprinting approach is made in Chapter 3 fusing artificial sediment source mixtures with three different comparisons: two digestion procedures, objective source groupings, and tracer selections. Chapter 3 is formatted as a manuscript for peer review.

The HNO_3 extraction method is compared with the total dissolution procedure for sediment source materials in two sediment impaired watershed in Chapter 4. Chapter 4 is formatted as a manuscript for peer review.

Conclusions for the collective sediment source tracking study are presented in Chapter 5, along with suggestions for future study.

Reference

Allan, R. J. (1986). "Role of particulate matter in the fate of contaminants in aquatic ecosystems," IWD.

Barthod, L. R., Liu, K., Lobb, D. A., Owens, P. N., Martínez-Carreras, N., Koiter, A. J., Petticrew, E. L., McCullough, G. K., Liu, C., and Gaspar, L. (2015). Selecting Color-based Tracers and Classifying Sediment Sources in the Assessment of Sediment Dynamics Using Sediment Source Fingerprinting. Journal of Environmental Quality 44, 1605-1616.

Blake, W. H., Ficken, K. J., Taylor, P., Russell, M. A., and Walling, D. E. (2012). Tracing crop-specific sediment sources in agricultural catchments. Geomorphology 139, 322-329.

Brooks, K. N., Ffolliott, P. F., and Magner, J. A. (2012). "Hydrology and the Management of Watersheds," John Wiley and Sons.

Collins, A., and Walling, D. (2002). Selecting fingerprint properties for discriminating potential suspended sediment sources in river basins. Journal of Hydrology 261, 218-244.

EPA, U. S. (2002). National Assessment Database.

Essington, M. E. (2015). Soil and water chemistry: An integrative approach, CRC press.

Foster, I., and Lees, J. (2000). Tracers in Geomorphology: theory and applications in tracing fine particulate sediments. PP: 3–20. Tracers in Geomorphology. Chichester Wiley, John Wiley, Chichester, UK.

Horowitz, A. J. (1991). Primer on sediment-trace element chemistry, Lewis Publishers.

Hughes, A. O., Olley, J. M., Croke, J. C., and McKergow, L. A. (2009). Sediment source changes over the last 250 years in a dry-tropical catchment, central Queensland, Australia. Geomorphology 104, 262-275.

Kemp, P., Sear, D., Collins, A., Naden, P., and Jones, I. (2011). The impacts of fine sediment on riverine fish. Hydrological Processes 25, 1800-1821.

Koiter, A., Owens, P., Petticrew, E., and Lobb, D. (2013). The behavioural characteristics of sediment properties and their implications for sediment

fingerprinting as an approach for identifying sediment sources in river basins. Earth-Science Reviews 125, 24-42.

Lal, R., and Stewart, B. A. (2013). "Principles of sustainable soil management in agroecosystems," CRC Press.

Miller, J. R., Mackin, G., and Miller, S. M. O. (2015). Application of Geochemical Tracers to Fluvial Sediment, Springer.

Milliman, J. D., and Meade, R. H. (1983). World-wide delivery of river sediment to the oceans. The Journal of Geology 91, 1-21.

Mukundan, R., Walling, D. E., Gellis, A. C., Slattery, M. C., and Radcliffe, D. E. (2012). Sediment Source Fingerprinting: Transforming From a Research Tool to a Management Tool1. Wiley Online Library.

Owens, P. N., Blake, W. H., Gaspar, L., Gateuille, D., Koiter, A. J., Lobb, D. A., Petticrew, E. L., Reiffarth, D. G., Smith, H. G., and Woodward, J. C. (2016). Fingerprinting and tracing the sources of soils and sediments: Earth and ocean science, geoarchaeological, forensic, and human health applications. Earth Science Reviews 162, 1-23.

Palazón, L., Latorre, B., Gaspar, L., Blake, W. H., Smith, H. G., and Navas, A. (2015). Comparing catchment sediment fingerprinting procedures using an auto-evaluation approach with virtual sample mixtures. Science of the Total Environment 532, 456-466.

Parnell, A. C., Phillips, D. L., Bearhop, S., Semmens, B. X., Ward, E. J., Moore, J. W., Jackson, A. L., Grey, J., Kelly, D. J., and Inger, R. (2013). Bayesian stable isotope mixing models. Environmetrics 24, 387-399.

Poulenard, J., Legout, C., Nemery, J., Bramorski, J., Navratil, O., Douchin, A., Fanget, B., Perrette, Y., Evrard, O., and Esteves, M. (2012). Tracing sediment sources during floods using Diffuse Reflectance Infrared Fourier Transform Spectrometry (DRIFTS): a case study in a highly erosive mountainous catchment (Southern French Alps). Journal of Hydrology 414, 452-462.

Rickson, R. (2014). Can control of soil erosion mitigate water pollution by sediments? Science of the Total Environment 468, 1187-1197.

TDEC (2002). Total Maximum Daily Load (TMDL) for Fecal Coliform in Oostanaula Creek, Hiwasse River Watershed (HUC 06020002), McMinn and Monroe Counties, Tennessee. Division of Water Pollution Control.

TDEC (2008a). 2008 305(b) Report. The Status of Water Quality in Tennessee Division of Water Pollution Control.

Unno, T., Staley, C., Brown, C. M., Han, D., Sadowksy, M. J., & Hur, H. G. (2018). Fecal Pollution: New Trends and Challenges in Microbial Source Tracking Using Next‐Generation‐Sequencing. Environmental Microbiology.

Walling, D. E., Owens, P. N., and Leeks, G. J. (1999). Fingerprinting suspended sediment sources in the catchment of the River Ouse, Yorkshire, UK. Hydrological Processes 13, 955-975.

Appendix 1: Table in Chapter 1

Table 1.1 Adverse surface water quality impact of excess sediment (TDEC, 2008a)

Property	Description
Biological	1)Restricting oxygen transfer for nests containing the eggs of fish and other species. 2)Transferring pollutants that can become toxic as they concentrate in the food chain. 3)Choking the gills of aquatic species. 4)Covering and deteriorating the habitat of aquatic insects on which fish feed. 5)Creating habitats beneficial that is beneficial to undesirable burrowing species. 6)Decreasing biological diversity. 7)Supplying underwater plants and algae nutrients and a favorable substrate, thereby promoting their growth.
Chemical	1)Impeding photosynthesis. 2)Reducing dissolved oxygen concentrations. 3)Stimulating eutrophication by increasing nutrients levels. 4)Transporting toxins into surface waters.
Physical	1)Reducing the penetration of sun light. 2)Changing temperature regimes. 3)Decreasing water depths. 4)Altering stream flow patterns.

CHAPTER 2: SEDIMENT-MICROBIAL SOURCE TRACKING (MST): A PROOF OF CONCEPT STUDY USING SEDIMENT METAGENOMIC DATA IN AN IMPAIRED WATERSHED

Abstract

Excess suspended sediment and siltation commonly degrade surface water quality in the United States. Although removal of primary sediment sources is critical to restoring surface water quality, techniques for accurately identifying eroding sediment source materials are lacking. This study investigated Next Generation Sequencing (NGS) based Sediment Microbial Source Tracking (S-MST). The goals were to characterise bacterial metagenomes for eroding sediment sources (cattle paths, pasture and cropland) and suspended stream sediment along with manure and to match the bacterial consortia within suspended surface water sediments to differentiate sediment sources categories. The V4 region of the 16S rRNA gene was targeted within land-based source materials and surface water suspended sediment in the Oostanaula Creek (OC) watershed, a sediment impaired watershed in southeastern Tennessee. Multivariate statistical analysis revealed a significant segregation between the bacterial community structures of suspended sediment, manure, and other eroding source materials. A SourceTracker analysis indicated that upland soils, as opposed to eroded bank soils, were more similar to a larger portion (74±15.4 %) of the suspended sediment microbiome. The results indicate that it may be possible to use bacterial communities from different land-based source materials to establish a predominant origin for suspended sediment in upland watersheds. S-MST could thereby improve placement of best management practices to more quickly and efficiently improve surface water quality.

Introduction

Nonpoint source pollution from anthropogenic activities, such as crop production and agricultural livestock operations, can cause surface water impairment via eroding soil (sediment) and fecal bacteria. The crucial role that sediment in particular plays in contaminant transfer and surface water quality has been recognized and incorporated into water quality management systems (Taylor and Owens, 2009). To improve water quality, particularly when nonpoint sources of sediment and fecal bacteria are present, it is important to pinpoint the sources of these pollutants within watersheds (McLellan and Eren, 2014). In the case of fecal pollution, microbial source tracking (MST) has been previously used to identify and prioritize fecal pollution sources (e.g., sewage/septic systems, livestock, wildlife) in impaired watersheds (McLellan and Eren, 2014).

In fact, to reliably and accurately identify eroding sediment source materials, a combination of source tracking/fingerprinting methods may be preferred. Sediment source tracking methods have been proposed using a variety of tracers, or fingerprinting techniques, including grain size, color, plant pollen, mineral magnetism, organic and inorganic elements, radionuclides, and stable isotopes (Collins and Walling, 2002; Davis and Fox, 2009; Foster and Lees, 2000; Mukundan et al., 2012; Walling, 2005; Walling, 2013). The strengths of the fingerprinting methods lie in the stability of elemental geochemsitry, however their sensitivity is limited by the heterogeneity of geological parent material. Also, these past attempts at

sediment source tracking do not provide information on the sources of fecal pollution sources.

Microorganisms, such as bacteria and fungi, can be transported with eroded soil particles during long transit periods and over wide geographical distances (Gonzalez-Martin et al., 2014). This indicates that the eroded soil particles may provide a protective niche environment that enables microorganisms to survive. Even when conditions are unfavorable for survival, microorganisms in eroded soil particles can still survive to seed populations in new environments by forming endospores (Nicholson et al., 2000). Cells that do not survive may serve as a nutrient source for the surviving population after favorable growth conditions are re-established. Harsh transport conditions do, in fact, select microorganisms and influence colonization of new environments (Barberán et al., 2014). This indicates that different types of soil may select different microbial communities' structure from the microbiome of the eroding parent material, and unique surviving communities may be harbored in stream suspended sediment that could serve as source tracers.

Microbial community analysis using next generation sequencing (NGS) technology has been successfully used to assess fecal pollution sources directly (Henry et al., 2016; McCarthy et al., 2017; McLellan and Eren, 2014; Unno et al., 2010). NGS has recently advanced fecal source tracking, particularly in the case of complex watersheds (Casanovas-Massana et al., 2015; Ervin et al., 2014; Henry et al., 2016; Korajkic et al., 2015; Neave et al., 2014; Newton et al., 2013). Many of these studies have sequenced the V4 hypervariable region of the bacterial 16S rRNA gene

in an attempt to identify and link characteristic bacterial consortia from sources to identify fecal sources within contaminated water bodies (Newton et al., 2013). Employing the 16S rRNA gene has several advantages: (1) it is universally present in bacterial genomes, with hypervariable regions that can be used distinguish between closely related organisms; (2) this gene provides better sensitivity because it typically occurs in multiple copies; (3) the 16S gene has long provided accurate classification between host sources, while defining community structure; and (4) the gene provides information that defines multiple phylogenetic levels (kingdom, phylum, classes, order, families, genus, and species), all with potential use as source identifiers (McLellan and Eren, 2014).

The current study attempts to build on the success of NGS based fecal source tracking assays. Specifically, we perform a proof of concept study of Sediment-Microbial Source Tracking (S-MST) by identifying and indexing the bacterial communities of suspended sediment in an impaired surface waterbody with different categories of eroding source materials. Instead of investigating general genetic markers of specific organisms, this study examines the microbial community structure of both different land-based soils and suspended sediment. This new strategy relies on an entire bacterial community, or characteristic taxonomic consortia of that overall community, to serve as a sediment source fingerprint. Specifically, operational taxonomic units (OTUs) were generated by assembling and analyzing metagenomic data (McLellan and Eren, 2014) and subsequently analyzed using the Quantitative Insights Into Microbial Ecology (QIIME) software package (Caporaso et al., 2010),

along with statistical tools to analyze the multiple large sample metagenomic datasets using multivariate analysis (Parks et al., 2014). The end-goal was to assess the primary sediment source material within a target sediment impaired stream, utilizing a Bayesian based SourceTracker analysis that assigned OTUs from source to sink bacterial metagenomic communities (Korajkic et al., 2015; McCarthy et al., 2017; Unno et al., 2010; Unno et al., 2018).

Materials and Methods

Study Site and Sample Collection

Samples of eroding soils and streambanks and stream suspended sediment were collected within the Oostanaula Creek (OC) watershed (Figure 2.1), which encompasses 44,864 acres in Monroe and McMinn counties in the Valley and Ridge physiographic region of southeast, Tennessee. A prior water quality assessment indicated OC was unable to fully support fish, aquatic life and recreation use, partly as a result of excess sedimentation (TDEC, 2008a). Agricultural land dominates the northern and southern portions of the watershed land use, mainly including pastures (beef cattle forage production), row crops (primarily corn, soybeans, and tobacco), and dairy farms. A small urban area (Athens, TN) (population 13,615) is located in the center of the watershed (USCB, 2017).

Samples were collected within the OC watershed between March and November 2013. A 250 ml volume of creek water was collected from 9 sampling locations (Figure 2.1) and immediately placed on ice in a cooler. A 100 ml aliquot of the creek water sample was subsequently filtered through 0.2 μM, 47mm cellulose nitrate filters (Whatman Ltd., England) to retain suspended sediment, which was then preserved at -80°C for later DNA extraction (Table A. 2.1). Land-based source samples from eroding soils were collected from 50 GPS coordinated locations assigned to one of two groupings (upland soil and bank soil), as illustrated in Table A. 2.2. The top 2 cm

of the soil (100 grams) was collected using a shovel and placed immediately on ice and later preserved at -80°C for DNA extraction.

DNA Extraction and Purification

Total genomic DNA was isolated from 0.5 grams of soil or suspended sediment captured with 0.2 μM, 47mm cellulose nitrate filters (Whatman, England, United Kingdom) using a FastDNA^{TM} Spin kit for soil (MP Biomedicals, LLC, Solon, OH) per the manufacture's instructions. Subsequent DNA purification was conducted with the Genomic DNA Clean & Concentrator kit (Zymo Research, Irvine, CA). Purified DNA was eluted using 50 μL of the kit DNA Elution Buffer. The DNA concentration was measured using a NANO DropTM 2000 (ThermoScientific, Wilmington, DE). The ratio of absorbance at 260 and 280 nm wavelengths (260/280 Ratio) was used as a quality control check for DNA purity. A ratio of $\geqslant$1.8 was acceptable. Extracted and purified DNA samples with a 260/280 absorbance ratio below 1.8 were re-purified with the Genomic DNA Clean & Concentrator kit and the 260/280 ratio confirmed to be $\geqslant$1.8. Extracted and purified DNA was stored at -20°C pending further analysis.

Library Preparation and High-throughput Sequencing

The V4 region of the bacterial 16S gene was amplified within the purified DNA extracts using barcoded PCR primers. Briefly, the PCR mixture included: the 515f forward primer with 5' Illumina adapter (AATGATACGGCGACCACCGAGATCTACAC), forward primer

(GTGCCAGCMGCCGCGGTAA), the reverse primer (GGACTACHVGGGTWTCTAAT) and reverse complement for the 3' Illumina adapter (CAAGCAGAAGACGGCATACGAGAT), reverse primer pad (AGTCAGTCAG), and reverse primer-linker (CC). PCR reaction mixes were made as master mixes containing 5μL Invitrogen Pfx50™ buffer (Invitrogen, Carlstead, CA), 1μL CAP 515f, 1μL dNTP (Invitrogen, Carlstead, CA), 5μL Invitrogen Pfx50™ Polymerase, 0.5 μL DMSO (Sigma, St. Louis, MO), and 37μL de-ionized water (5 PRIME, Gaithersburg, MD). The barcode primer and DNA sample were individually added to each PCR reaction tube separately. A 2 μL aliquot of deionized water was included as a negative control. PCR thermocycling was performed on a GenePro thermocycler (Bulldog Bio, Portsmouth, NH) using the following protocol: initial denaturation at 94°C (3 min), followed by 35 cycles of denaturation at 94°C (45 sec), annealing at 48°C (45 sec), with a final extension at 72 °C (7 min).

A high sensitivity Chromatin immunoprecipitation (ChIP) analysis was performed on the PCR products using a model 2100 Bioanalyzer (Agilent, Santa Clara, CA) and the High Sensitive DNA kit. PCR samples having products of the correct size ($\approx$ 400 bp) were pooled and purified using Agencour AMPure XP magnetic beads (Beckman Coulter, Inc., Indianapolis, IN). The quality of pooled and purified PCR mixtures was re-verified using the high sensitivity CHIP procedure.

Before high-throughput sequencing, amplifiable 16S genes in the pooled PCR library were measured using quantitative PCR with the KAPA SYBR® FAST qPCR Master Mix, 6 DNA standards (20 pM, 2 pM, 0.2 pM, 0.02 pM, 0.002 pM, and 0.0002

pM), and the Illumina Library Quantification kit (KAPA Biosystems, Boston, MA). Specifically, the sample libraries were diluted 1:1,000, 1:5,000, and 1:10,000 in 10 mM TRIS/0.05% TWEEN and the quantitative PCR assay was performed on a DNA Engine Opticon Continuous Fluorescence Detection System (MJ Research, Waltham, MA) following the kit's recommended cycling protocol. The amplifiable DNA copies were then used to accurately dilute the sample library to 10 nM, which served as the high-throughput sequencing input for the Illumina MiSeq Sequencer platform (Illumina, Inc., San Diego, CA) using the 300 cycle V2 kit. Following sequencing, sequences were automatically demulitplexed into Fastq files using the internal MiSeq software.

Bioinformatics

Sequence reads contained in sample fastq files were assembled and analyzed using Quantitative Insights Into Microbial Ecology (QIIME) (V1.8.0) (Caporaso et al., 2010). The raw metagenomic dataset was transformed to a matrix dataset using Operational Taxonomic Units (OTUs) via a tab-delimited mapping file that contained the sample ID, barcode sequences, primer sequences, and category information. The forward and reverse reads were concatenated and parsed barcode sequences were used to join multiple reads. Chimeras were filtered using the wrapped "usearch61" package and the UCHIME algorithm. OTUs were chosen using "UCLUST" with 97% similarity to the reference sequence collection. Sequences were assigned using RDP classifier based on the Greengenes reference database. OTUs less than 0.005% were

eliminated and the remaining sequences reads rarified to 32,000 sequences per sample. This created an equal depth of sequence analysis to prevent an incorrect assignment of increased richness due to high concentration sequences.

Multivariate Analysis

Multivariate analysis of the sequence data was conducted in Calypso (V5.4) (Zakrzewski et al., 2017), an online platform for mining, visualizing and comparing microbial community composition data across multiple samples. Specifically, a "Shannon index" was used to measure the overall alpha diversity of each sample category, including the number and evenness of OTUs. Sediment source discrimination, a visual qualitative assessment, was performed as a prerequisite for running SourceTracker, using both Principal Component Analysis (PCA) and Principal Coordinate Analysis (PCoA) in Calypso (V5.4). All other statistical tests, including Welch's t-test to determine whether certain bacterial taxa differed significantly between samples, were performed in Statistical Analysis of Metagenomics Profiles (STAMP, V2.1.3) (Parks et al., 2014). All statistical methods utilized $\alpha=0.05$ as a threshold for statistical significance.

SourceTracker Apportionment

From the viewpoint of watershed managers, it would be helpful to decide whether the sediment is predominantly from stream banks or upland sediment sources. Hence, it would be necessary to provide a breakdown of the suspended sediment bacterial communities into presumptive manure, upland sources, and bank soil. Thus, output

from QIIME, a Biological Observation Matrix (BIOM) file, was subjected to a source apportionment analysis using the R-based program SourceTracker (V1.0.1) (Knights et al., 2011). SourceTracker incorporated a Bayesian algorithm with Monte Carlo Markov Chains (MCMC) and was used to identify OTUs from source communities (e.g., bank or upland soils) found in sink communities (OC suspended sediment). Estimate of contribution in percent from (1) manures (2) upland sources and (3) bank soils were made at the following conditions: rarefaction to 1,000 sequence reads, burn-in 100, restart 10, alpha (0.001) and beta (0.01) dirichlet hyperparameter.

Results

Physicochemical and Water Quality Parameters

Water samples, collected from sites 1 to 9 (Figure 2.1), differed significantly in turbidity, dissolved oxygen (DO), and conductivity (p-value < 0.01) (Table 2.1), but not for other physicochemical parameters including temperature, log *E. coli*, and pH (p-value >0.05). Closest to the creek mouth, Site 1 displayed the highest average level of turbidity (32.5±8.4 NTU) among all sampling sites. Site 9, near the creek headwaters, had the lowest turbidity (4.3±0.5 NTU) and conductivity (66.9±17.9). The highest DO occurred at site 6 (97.6±21.4,%), and the lowest DO occurred at site 5 (82.1±25, %).

Soil and Sediment Microbiomes

A total of 45 sequenced amplicon libraries with 5,560,000 OTUs were successfully processed using QIIME and assembled into a taxonomic table using a 97% average neighbor sequence similarity. A suspended sediment collected at Site 1 did not produce enough sequence reads and was excluded from analysis. The final BIOM file provided a basis for direct comparison of the bacterial community structure in different land-based categories within the watershed. A total of 183,896 ± 32,666 OTUs were found in manure, 178,454 ± 82,258 OTUs in upland soils and 149,207 ± 37,611 OTUs in bank soils, which were not differing significantly (p-value >0.05) (Table 2.2).

Alpha Diversity

Bacterial diversity is a critical parameter for analyzing microbial communities, because diversity enables discrimination between host environments based on their microbial signatures (Knights et al., 2011; Korajkic et al., 2015; Torsvik et al., 1996). All of the alpha diversity metrics, including richness, evenness, Shannon index, and Chao 1, differed significantly among manure, upland and bank soil sample categories (p-value < 0.05) (Table 2.3). The upland soil sequence richness (14.1 ± 1.2) was greater than bank soil sequence richness (13.2 ± 0.9) and manure richness (11.8±1.3). Likewise, the evenness, Shannon index, and Chao 1 estimates indicated that samples collected from bank soils had significantly lower alpha diversity than the manure and upland soils. The sediment Shannon indices for the present study were lower (3.5± 0.3 for manure, 4.4 ± 0.3 for upland soils and 4.1 ± 0.2 for bank soils) than previously found in a German drinking water reservoir (6.9 ± 0.2) (Röske et al., 2012) and sediment in a Brazil mangrove wetland (5.6 ± 0.2) (Dos Santos et al., 2011).

Bacterial Community Composition

The bacterial community composition was similar among all environmental water samples (suspended sediment) collected at stream sites 2 to 9, with high relative abundances of *Proteobacteria* and *Actinobacteria* (Figure 2.2). In contrast, the bacterial community composition varied significantly between upland soil and manure samples. For instance, manures, which are present on some upland soils, were predominantly comprised of *Firmicutes* and *Bacteroidetes*. Sub-samples of upland

soils associated with cattle walkways and cropland had a greater relative abundance of *Acidobacteria* as compared to other land-based source samples.

At the family level, a higher taxonomic resolution, the most abundant phyla across all soil and water samples were *Proteobacteria* and *Bacteroidetes*. The percentage of *Microbacteriaceae* significantly varied among upland and bank source samples (p-value <0.05) and tended to be more abundant in manure samples. *Chthoniobacteraceae* and *Sphingomonadaceae* are also two families which can significantly between cattle walkways, cropland soils, manure and bank soil) (p-value <0.05) (Figure 2.3). Members of the families *Comamonadaceae* and *Microbacteriaceae* were abundant in suspended sediment samples but not the soil samples. *Oxalobacteraceae* between the upstream and downstream suspended sediment samples due perhaps, in part, to changes in physicochemical parameters (like turbidity) (Table 2.1). Soil samples, excluding manures contained bacterial families dominated by *Actinobacteria* and *Acidobacteria*. The bacterial communities in manures that were more abundant than for *Verrucomicrobia*, *Firmicutes*, *Bacteroidetes*, and *Euryarchaeota*. The percentage of unassigned reads was lowest for the cattle walkway samples among all upland soil samples. In general, the average percentage of unassigned reads was higher for the sink (suspended sediment) as compared to source samples.

Bacterial Community Beta Diversity

Suspended sediment and sediment source sample bacterial communities were evaluated using ordination of the Bray-Curtis distances in PCA and the Euclidian distances in PCoA (Figure 2.4). The bacterial community structure did not differ significantly between the upstream and downstream Oostanaula Creek sampling sites, however all stream sediment communities clustered separately from manure and sediment sources (p-value >0.05) (Figure 2.4). Likewise, manure samples cluster together and did not differ significantly from each other (p-value >0.05). Although the community structure of different upland soil categories (cattle path and cropland) clustered less than bank soils, they were not significantly different from bank soils (p-value >0.05).

Sediment sources categories, bank versus manure and upland soils, displayed significantly different bacterial communities (p-value < 0.01 between manure and suspended sediment, p-value < 0.01 between manure and other land-based sources, p-value < 0.01 between suspended sediment and other upland soil (p-value < 0.01) (Figure 2.4). Ordination of Bray-Curtis distances in PCA and Euclidian distances in PCoA revealed significant separation for manure, suspended sediment and other groups (Figure 2.4). These distances among sample types, as revealed by the separation of clustering, were primarily attributable to the core group of 80 shared OTUs, mainly *Acidobacteria, Actinobacteria, Bacteroidetes, Chloroflexi, Crenarchaeota, Euryarchaeota, Firmicutes, Gemmatimonadetes, Nitrospirae, Synergistetes, Tenericutes, Verrucomicrobia,* and *Proteobacteria* phyla (Table A. 2.6).

Sediment-Microbial Source Tracking (MST)

Land-based sources were divided into manure, upland and bank soils to evaluate the relative importance of upland soils versus eroding bank as sediment source contributors. It was hypothesized that there would be a difference in the suspended sediment bacterial composition upstream versus downstream of Athens, because of the effects of a centralized city and because the apparent differences in the physicochemical parameters (Table 2.1). However, a SourceTracker analysis did not reveal significant differences in the bacterial source communities of the sampling sites upstream versus downstream of Athens (p-value >0.05) (Figure 2.5). Thus, it appears the bacterial communities were homogeneously mixed along the length of Oostanaula Creek, a prerequisite for performing a subsequent Bayesian algorithm MCMC.

Among the Oostanaula Creek sampling sites, the average compositional percentage of bacterial communities from upland soil (44±12.5 %) was greater than manure and bank soil (20±3.5 %) (Figure 2.5). Unknown bacterial apportionment accounted for only (5±4.5 %) of sequences from the different sampling sites.

At the furthest upstream region, site 9 had the greatest average microbial source influence from the upland soil (51±15%), but lowest from bank soil (Figure 2.5). In contrast, site 6 had the most average microbial source influence from the bacterial communities' in manure (39±7%). Among the sampling sites downstream of the city of Athens, site 4 was sourced mainly from upland soils (54±22%).

Discussion

A proof of concept study was performed using bacterial metagenomic data to characterise and associate the bacterial communities in sediment source materials and suspended sediment from a sediment impaired watershed. The technique was similar to methods previously used to characterize fecal bacterial indicators (FBI) using next generation sequencing (NGS) based techniques (454 Pyrosequencing or Illumina-based sequencing) (Jesus et al., 2016; Trivedi et al., 2016; Zhao et al., 2014). Instead of only investigating a few cultured FIB or single gene targets, NGS based microbial source tracking (MST) allows for a community based characterization of sources (Unno et al., 2018). These studies have revealed that bacterial communities, known bacterial signature libraries (McCarthy et al., 2017), can be unique to their host environment reference. This study clearly reveals, by multivariate analysis, that sediment source and suspended sediment source-specific clustering occurs within the categories of eroded sediment source and sink or stream suspended sediment (Figure 2.4).

Fecal and non-fecal contamination from different land-based sources are associated with different microbial communities (Figure 2.2 and 2.3). For example, *Bacteroidetes*, which are gram-negative, elongated filament-like rods that form bright yellow colonies (Tamaki et al., 2003). *Bacteroidetes* suggested eroded sediment containing manure may be delivering high loads directly to sediment impaired stream, making the paths perhaps a primary source of the fecal bacteria delivered from pastures. Another fecal bacterial member, *Firmicutes* (Eckburg et al., 2005),

demonstrate the consistent abundance (around 20% of the OTUs counts attributed) one within manure samples, but was only identifies 5.5%, 2.8%, and 2.4% for suspended sediment, cattle walkway and other potential eroding soils, respectively.

The family of *Flavobacterium* has been isolated from freshwater sediment and abundant in organic-polymer-degrading bacterium (Tamaki et al., 2003). As illustrated in Figure 2.2, *Chloroflexi* is abundant and highly diverse in the aquifer sediments (Hug et al., 2013). *Nitrospirae* are key players in the nitrogen cycle in which they perform nitrite oxidation (Hawkins et al., 2012). Even though *Acidobacteria*, *Actinobacteria*, *Chloroflexi*, and *Nitrospirae*, have been found in other parallel sediment sequencing studies (Feng et al., 2009), but additional research is needed to address the main sediment source associated with other non-fecal bacterial members.

The sediment-MST in this study was used to assess whether suspended sediment were more likely derived from bank or upland soils. SourceTracker predicted the primary source of microbial populations in the suspended sediment was from upland eroding source materials. These results suggest that stream bank itself plays a less significant role with respect to determine the microbial community structure of suspended sediment. Therefore, the water remediation efforts should focus on the minimization of upland sediment runoff into the river. Solutions to this issue would be to enhance the water-holding capacity of soils and reduce the sheet and rill erosion occurring in the upland area of watershed. Also, stream bank buffers could protect and enhance infiltration from cropland and pastures, and along with cattle watershed prevent cattle's paths directly contributing sediment to the stream.

References

Barberán, A., Henley, J., Fierer, N., and Casamayor, E. O. (2014). Structure, inter-annual recurrence, and global-scale connectivity of airborne microbial communities. Science of the Total Environment 487, 187-195.

Caporaso, J. G., Kuczynski, J., Stombaugh, J., Bittinger, K., Bushman, F. D., Costello, E. K., Fierer, N., Pena, A. G., Goodrich, J. K., and Gordon, J. I. (2010). QIIME allows analysis of high-throughput community sequencing data. Nature Methods 7, 335-336.

Casanovas-Massana, A., Gómez-Doñate, M., Sánchez, D., Belanche-Muñoz, L. A., Muniesa, M., and Blanch, A. R. (2015). Predicting fecal sources in waters with diverse pollution loads using general and molecular host-specific indicators and applying machine learning methods. Journal of Environmental Management 151, 317-325.

Collins, A., and Walling, D. (2002). Selecting fingerprint properties for discriminating potential suspended sediment sources in river basins. Journal of Hydrology 261, 218-244.

Davis, C. M., and Fox, J. F. (2009). Sediment fingerprinting: review of the method and future improvements for allocating nonpoint source pollution. Journal of Environmental Engineering 135, 490-504.

Dos Santos, H. F., Cury, J. C., Do Carmo, F. L., Dos Santos, A. L., Tiedje, J., Van Elsas, J. D., Rosado, A. S., and Peixoto, R. S. (2011). Mangrove bacterial diversity and the impact of oil contamination revealed by pyrosequencing: bacterial proxies for oil pollution. PLoS One 6, e16943.

Eckburg, P. B., Bik, E. M., Bernstein, C. N., Purdom, E., Dethlefsen, L., Sargent, M., Gill, S. R., Nelson, K. E., and Relman, D. A. (2005). Diversity of the human intestinal microbial flora. Science 308, 1635-1638.

Ervin, J. S., Van De Werfhorst, L. C., Murray, J. L., and Holden, P. A. (2014). Microbial source tracking in a coastal California watershed reveals canines as controllable sources of fecal contamination. Environmental Science and Technology 48, 9043-9052.

Feng, B.-W., Li, X.-R., Wang, J.-H., Hu, Z.-Y., Meng, H., Xiang, L.-Y., and Quan, Z.-X. (2009). Bacterial diversity of water and sediment in the Changjiang estuary and coastal area of the East China Sea. FEMS Microbiology Ecology 70, 236-248.

Foster, I., and Lees, J. (2000). Tracers in Geomorphology: theory and applications in tracing fine particulate sediments. PP: 3–20. Tracers in Geomorphology. Chichester Wiley, John Wiley, Chichester, UK.

Gonzalez-Martin, C., Teigell-Perez, N., Valladares, B., and Griffin, D. W. (2014). The Global Dispersion of Pathogenic Microorganisms by Dust Storms and Its Relevance to Agriculture. Advances in Agronomy, Vol 127 127, 1-41.

Hawkins, S., Robinson, K., Layton, A., and Sayler, G. (2012). Molecular indicators of Nitrobacter spp. population and growth activity during an induced inhibition event in a bench scale nitrification reactor. Water Research 46, 1793-1802.

Henry, R., Schang, C., Coutts, S., Kolotelo, P., Prosser, T., Crosbie, N., Grant, T., Cottam, D., O'Brien, P., and Deletic, A. (2016). Into the deep: Evaluation of SourceTracker for assessment of faecal contamination of coastal waters. Water Research 93, 242-253.

Hug, L. A., Castelle, C. J., Wrighton, K. C., Thomas, B. C., Sharon, I., Frischkorn, K. R., Williams, K. H., Tringe, S. G., and Banfield, J. F. (2013). Community genomic analyses constrain the distribution of metabolic traits across the Chloroflexi phylum and indicate roles in sediment carbon cycling. Microbiome 1, 1.

Jesus, E. d. C., Liang, C., Quensen, J. F., Susilawati, E., Jackson, R. D., Balser, T. C., and Tiedje, J. M. (2016). Influence of corn, switchgrass, and prairie cropping systems on soil microbial communities in the upper Midwest of the United States. Gcb Bioenergy 8, 481-494.

Knights, D., Kuczynski, J., Charlson, E. S., Zaneveld, J., Mozer, M. C., Collman, R. G., Bushman, F. D., Knight, R., and Kelley, S. T. (2011). Bayesian community-wide culture-independent microbial source tracking. Nature Methods 8, 761-763.

Korajkic, A., Parfrey, L. W., McMinn, B. R., Baeza, Y. V., VanTeuren, W., Knight, R., and Shanks, O. C. (2015). Changes in bacterial and eukaryotic communities during sewage decomposition in Mississippi river water. Water Research 69, 30-39.

McCarthy, D., Jovanovic, D., Lintern, A., Teakle, I., Barnes, M., Deletic, A., Coleman, R., Rooney, G., Prosser, T., and Coutts, S. (2017). Source tracking using microbial community fingerprints: Method comparison with hydrodynamic modelling. Water Research 109, 253-265.

McLellan, S. L., and Eren, A. M. (2014). Discovering new indicators of fecal pollution. Trends in Microbiology 22, 697-706.

Mukundan, R., Walling, D. E., Gellis, A. C., Slattery, M. C., and Radcliffe, D. E. (2012). Sediment Source Fingerprinting: Transforming From a Research Tool to a Management Tool1. Wiley Online Library.

Neave, M., Luter, H., Padovan, A., Townsend, S., Schobben, X., and Gibb, K. (2014). Multiple approaches to microbial source tracking in tropical northern Australia. Microbiology Open 3, 860-874.

Newton, R. J., Bootsma, M. J., Morrison, H. G., Sogin, M. L., and McLellan, S. L. (2013). A microbial signature approach to identify fecal pollution in the waters off an urbanized coast of Lake Michigan. Microbial Ecology 65, 1011-1023.

Nicholson, W. L., Munakata, N., Horneck, G., Melosh, H. J., and Setlow, P. (2000). Resistance of Bacillus endospores to extreme terrestrial and extraterrestrial environments. Microbiology and Molecular Biology Reviews 64, 548-572.

Parks, D. H., Tyson, G. W., Hugenholtz, P., and Beiko, R. G. (2014). STAMP: statistical analysis of taxonomic and functional profiles. Bioinformatics 30, 3123-3124.

Röske, K., Sachse, R., Scheerer, C., and Röske, I. (2012). Microbial diversity and composition of the sediment in the drinking water reservoir Saidenbach (Saxonia, Germany). Systematic and Applied Microbiology 35, 35-44.

Santo Domingo, J. W., and Sadowsky, M. J. (2007). Microbial source tracking, ASM Press Washington, DC.

Scott, T. M., Rose, J. B., Jenkins, T. M., Farrah, S. R., and Lukasik, J. (2002). Microbial source tracking: current methodology and future directions. Applied and Environmental Microbiology 68, 5796-5803.

Tamaki, H., Hanada, S., Kamagata, Y., Nakamura, K., Nomura, N., Nakano, K., and Matsumura, M. (2003). Flavobacterium limicola sp. nov., a psychrophilic, organic-polymer-degrading bacterium isolated from freshwater sediments. International Journal of Systematic and Evolutionary Microbiology 53, 519-526.

Taylor, K. G., and Owens, P. N. (2009). Sediments in urban river basins: a review of sediment–contaminant dynamics in an environmental system conditioned by human activities. Journal of Soils and Sediments 9, 281-303.

TDEC (2008a). 2008 305(b) Report. The Status of Water Quality in Tennessee Division of Water Pollution Control.

Torsvik, V., Sørheim, R., and Goksøyr, J. (1996). Total bacterial diversity in soil and sediment communities—a review. Journal of Industrial Microbiology and Biotechnology 17, 170-178.

Trivedi, P., Delgado-Baquerizo, M., Anderson, I. C., and Singh, B. K. (2016). Response of soil properties and microbial communities to agriculture: implications for primary

productivity and soil health indicators. Frontiers in Plant Science 7.

U.S. Census Bureau. (2017). Demographics of the United States: City of Athens in Tennessee. https://www.census.gov/

Unno, T., Jang, J., Han, D., Kim, J. H., Sadowsky, M. J., Kim, O.-S., Chun, J., and Hur, H.-G. (2010). Use of barcoded pyrosequencing and shared OTUs to determine sources of fecal bacteria in watersheds. Environmental Science & Technology 44, 7777-7782.

Unno, T., Staley, C., Brown, C. M., Han, D., Sadowksy, M. J., and Hur, H. G. (2018). Fecal Pollution: New Trends and Challenges in Microbial Source Tracking Using Next‐Generation‐Sequencing. Environmental Microbiology.

Walling, D. (2005). Tracing suspended sediment sources in catchments and river systems. Science of the Total Environment 344, 159-184.

Walling, D. E. (2013). The evolution of sediment source fingerprinting investigations in fluvial systems. Journal of Soils and Sediments 13, 1658-1675.

Zakrzewski, M., Proietti, C., Ellis, J. J., Hasan, S., Brion, M.-J., Berger, B., and Krause, L. (2017). Calypso: a user-friendly web-server for mining and visualizing microbiome–environment interactions. Bioinformatics 33, 782-783.

Zhao, J., Zhang, R., Xue, C., Xun, W., Sun, L., Xu, Y., and Shen, Q. (2014). Pyrosequencing Reveals Contrasting Soil Bacterial Diversity and Community Structure of Two Main Winter Wheat Cropping Systems in China. Microbial Ecology 67, 443-453.

Appendix 2: Tables in Chapter 2

Table 2.1 Water sample physicochemical parameters [†‡].

Site No.	n	Temperature (°C)	Turbidity (NTU)	DO (%)	Log *E. coli*	pH	Conductivity	Region
1	**7**	16.3±4.1	32.5±8.4	91.4±13.1	2.5±0.4	7.4±1.0	278±28.5	Downstream of Athens
2	**7**	16.4±4.2	32.0±6.5	95.6±21.9	2.5±0.6	7.2±0.6	267±38.7	Downstream of Athens
3	**7**	16.4±4.2	20±3.3	87.0±17.2	2.6±0.6	7.0±0.7	283±44.5	Downstream of Athens
4	**7**	16.2±3.7	11.7±2.2	94.9±26.8	2.6±0.5	7.2±0.9	285±34.2	Downstream of Athens
5	**7**	14.9±2.8	8.7±3.1	82.1±25.0	2.4±0.2	7.1±1.1	272±27.2	Downstream of Athens
6	**7**	14.8±2.6	11.6±2.4	97.6±21.4	2.7±0.4	7.7±1.6	255±33.3	Upstream of Athens
7	**7**	15.3±2.3	5.3±1.2	97.0±11.2	2.5±0.5	7.4±1.2	254±21.8	Upstream of Athens
8	**7**	15.8±3.7	14.7±3.8	123±26.5	2.8±0.4	6.9±0.8	303±22.9	Upstream of Athens
9	**7**	17.1±5.3	4.3±0.5	95.5±22.7	2.8±0.5	6.8±1.0	66.9±17.9	Upstream of Athens

[†]Values are mean ± standard deviation among all samples.

[‡]Parameters measured include temperature, turbidity, dissolved oxygen (DO), Log *E.coli*, pH, and conductivity.

Table 2.2 Alpha diversity metrics by sample type[a].

Sample Type	**n**	**Richness**	**Evenness**	**Shannon**	**Chao1 Estimate**	**OTUs**[b]
Manure	7	11.8±1.3	0.7±0.05	3.5±0.3	230±31	183,896±32,666
Upland Soil	15	14.1±1.2	0.8±0.05	4.4±0.3	349±32	178,454±82,258
Bank Soil	11	13.2±0.9	0.7±0.08	4.1±0.2	308±23	149,207±37,611
	p-value[c]	0.0235	0.002	0.002	0.0003	0.107

[a] Values are mean ± standard deviation among all samples.

[b] Number of OTUs observed.

[c] Sample groups did not differ significantly in alpha diversity by Welch's t test (P>0.05).

[c] Manure is counted separately. Upland soils consist of crop land and cattle path samples. Bank soils are soil eroding stream bank soils.

Table A. 2.1 OTU summary for Oostanaula Creek sink samples ranked by OTUs

Sampling Site	No. of OTUs	Region
6	35,341	Upstream
2	36,660	Downstream
5	38,991	Downstream
9	53,075	Upstream
4	53,643	Downstream
8	58,216	Upstream
3	83,717	Downstream
4	141,558	Downstream
7	142,311	Upstream
9	147,552	Upstream
5	150,795	Downstream
8	176,224	Upstream

Table A. 2.2 Description of Oostanaula Creek sampling sites

Site #	Description of sample collection location	Latitude	Longitude
01	A cattle path entering an unnamed tributary of Oostanaula Creek;	35.5141	-84.4842
02	A cattle path crossing an unnamed tributary of Oostanaula Creek and approximately 50 meters E of site (01);	35.5132	-84.4841
03	A cattle path leading to a trampled area in an alfalfa field;	35.5806	-84.6023
04	Alfalfa/fescue forage pasture;	35.5130	-84.4845
05	A cattle path along the edge of an unnamed tributary of Oostanaula Creek adjacent to a dairy farm;	35.5128	-84.4840
06	A cattle path with a head cut along the edge of an unnamed tributary of Oostanaula Creek (05);	35.5126	-84.4842
07	In-stream deposited sediment from the bottom of an unnamed tributary of Oostanaula Creek (05);	35.5127	-84.4843
08	Eroding stream bank upstream of an unnamed tributary of Oostanaula Creek (05);	35.5127	-84.4846
09	Former cattle path being revegetated and was situated approximately 100 meters NW of site 008;	35.5133	-84.4841
10	A tilled wheat field sampled 50 meters from Oostanaula Creek;	35.5121	-84.4842
12	A cut bank adjoining a dirt road situated approximately 10 meters from Oostanaula Creek;	35.5118	-84.4838
13	A tilled field situated in an eroded hill approximately 50 meters from a small unnamed tributary of Oostanaula Creek;	35.5138	-84.4820
14	A cattle travel path on a dairy farm;	35.4973	-84.4945
15	A former heavily traveled cattle path 200 meters E of a small unnamed tributary of Oostanaula Creek (13);	35.4974	-84.4936
16	A stream wash close to site 015 and approximately 100 meters from Oostanaula Creek;	35.4977	-84.4932
17	A cattle path that was completely non-vegetated and that entered into the Oostanaula Creek;	35.4979	-84.4931
18	Long-term pasture situated close to a small unnamed tributary of Oostanaula Creek;	35.4981	-84.4928
19	A stream bank of Oostanaula Creek immediately adjacent to the pasture land at the site (18);	35.4980	-84.4934
20	A cattle path adjacent to pasture land (18);	35.4968	-84.4929
21	A pasture field on a dairy farm;	35.4966	-84.4928
22	A pasture field on a dairy farm;	35.4948	-84.5043
23	A streambank at the corner of an unnamed tributary of Oostanaula Creek;	35.4952	-84.5047

Table A. 2.2 Continued

Site #	Description of sample collection location	Latitude	Longitude
24	Stream bank located at the main stem of a tributary of Oostanaula Creek (23);	35.5000	-84.5049
25	Heavily trampled cattle path;	35.5020	-84.5052
26	Pasture surrounding a cattle path (25);	35.5022	-84.5055
27	Cut bank along a ditch approximately 100 meters from a cattle path near sampling site (25);	35.5021	-84.5057
28	Pasture adjacent to the cut bank at sampling site (27);	35.5020	-84.5047
29	Instream sediment deposit along the inside edge of the meander adjacent to the main stem of Oostanaula Creek;	35.4870	-84.5247
30	Tilled field in a corn/soybean rotation on which biosolids had been applied;	35.4870	-84.5244
31	Construction site with fill;	35.4164	-84.5843
32	Construction site without fill adjacent to the sampling site (31);	35.4165	-84.5842
33	Construction site sample;	35.4227	-84.5826
34	Construction site near (33);	35.4229	-84.5828
35	Construction site near (33), collected at the top of a hill with dark soil;	35.4230	-84.5823
36	Eroding hill;	35.4257	-84.5826
37	Construction site near sampling site (36);	35.4391	-84.6229
38	Railroad track cut dirt;	35.4515	-84.5987
39	Railroad track cut dirt;	35.4513	-84.5985
40	Streambank on the main stem of Oostanaula Creek;	35.4400	-84.5891
41	Streambank on the main stem of Oostanaula Creek;	35.4302	-84.5947
42	A road cut adjacent to a housing development;	35.4542	-84.5673
43	Streambank located on the main stem of Oostanaula Creek restoration;	35.4583	-84.5773
44	Flood plain situated at a goat farm;	35.4580	-84.5797
45	Construction site situated above a TDEC restoration site;	35.4565	-84.5771
46	Stream bank located at a local library;	35.4545	-84.5820
47	Stream bank located at a local library;	35.4542	-84.5820
48	Stream bank at wetland on Oostanaula Creek;	35.4531	-84.5820
49	Stream bank on the Walker Branch tributary Oostanaula Creek;	35.4274	-84.5790
50	Stream bank on the Black's Branch tributary Oostanaula Creek.	35.4241	-84.5882

Table A. 2.3 OTU summary for Oostanaula Creek upland soils

Sample ID	No. of OTUs	Latitude	Longitude	Group	Origin
Cattle path					
OostCP10	48,191	35.4968	-84.4929	Source	Upland Soil
OostCP11	89,016	35.4979	-84.4931	Source	Upland Soil
OostCP12	123,568	35.4973	-84.4945	Source	Upland Soil
OostCP5	150,172	35.5128	-84.484	Source	Upland Soil
OostCP3	171,768	35.5132	-84.4841	Source	Upland Soil
OostCP4	192,751	35.5141	-84.4842	Source	Upland Soil
OostCP6	223,681	35.502	-84.5052	Source	Upland Soil
OostCP1	232,005	35.4979	-84.4931	Source	Upland Soil
OostCP2	275,136	35.5126	-84.4842	Source	Upland Soil
OostCP7	387,859	35.5806	-84.6023	Source	Upland Soil
Cropland					
Oostsoil14	113,662	35.5138	-84.482	Source	Upland Soil
Oostsoil18	128,105	35.4981	-84.4928	Source	Upland Soil
Oostsoil13	161,935	35.5138	-84.482	Source	Upland Soil
Oostsoil17	176,457	35.4979	-84.4931	Source	Upland Soil
Oostsoil15	202,505	35.4974	-84.4936	Source	Upland Soil

Table A. 2.4 OTU summary for Oostanaula Creek bank soils

Sample ID	No. of OTUs	Latitude	Longitude	Group	Origin
Oostsoil19	210,850	35.498	-84.4934	Source	Bank Soil
Oostsoil24	169,067	35.5	-84.5049	Source	Bank Soil
Oostsoil27	142,853	35.5021	-84.5057	Source	Bank Soil
Oostsoil33	148,151	35.4227	-84.5826	Source	Bank Soil
Oostsoil35	167,115	35.423	-84.5823	Source	Bank Soil
Oostsoil39	162,365	35.4513	-84.5985	Source	Bank Soil
Oostsoil40	135,892	35.44	-84.5891	Source	Bank Soil
Oostsoil41	126,536	35.4302	-84.5947	Source	Bank Soil
Oostsoil46	89,938	35.4545	-84.582	Source	Bank Soil
Oostsoil49	195,064	35.4274	-84.579	Source	Bank Soil
Oostsoil50	93,443	35.4241	-84.5882	Source	Bank Soil

Table A.2.5 OTU summary for manure samples

Sample ID	No. of OTUs	Latitude	Longitude	Group	Origin
Manure					
Manure111613B	139,185	35.4966	-84.4928	Source	Upland area
Manure523142	166,826	35.4966	-84.4928	Source	Upland area
Manure111613C	170,154	35.4966	-84.4928	Source	Upland area
Manure523141	171,018	35.4966	-84.4928	Source	Upland area
Manure521142	189,429	35.4966	-84.4928	Source	Upland area
Manure521141	213,216	35.4966	-84.4928	Source	Upland area
Manure111613A	237,442	35.4966	-84.4928	Source	Upland area

Table A. 2.6 Core microbiomes for sediment source and sink samples

Core microbiomes			
p__Acidobacteria__o__iii1.15_311603	*p__Actinobacteria__f__Microccaceae_4401816*	*p__Bacteroidetes__f__Cytophagaceae_103802*	*p__Euryarchaeota__g__Methanobrevibacter_842598*
p__Acidobacteria__o__iii1.15_368890	*p__Actinobacteria__f__Micromonosporaceae_265094*	*p__Bacteroidetes__g__Flavobacterium_141447*	*p__Euryarchaeota__g__Methanocorpusculum_108525*
p__Acidobacteria__o__iii1.15_4024062	*p__Actinobacteria__f__Micromonosporaceae_931593*	*p__Bacteroidetes__g__Flavobacterium_158263*	*p__Firmicutes__f__Carnobacteriaceae_4482376*
p__Acidobacteria__o__iii1.15_4329544	*p__Actinobacteria__f__Nocardioidaceae_1088254*	*p__Bacteroidetes__g__Flavobacterium_4354769*	*p__Firmicutes__g__Bacillus_826250*
p__Acidobacteria__o__iii1.15_4341171	*p__Actinobacteria__f__Solirubrobacteraceae_1129425*	*p__Bacteroidetes__g__Flavobacterium_4438548*	*p__Firmicutes__o__Bacillales_137561*
p__Acidobacteria__o__iii1.15_717396	*p__Actinobacteria__f__Solirubrobacteraceae_873887*	*p__Bacteroidetes__o__Sphingobacteriales_4477202*	*p__Gemmatimonadetes__c__Gemm.1_2984011*
p__Actinobacteria__f__Gaiellaceae_1000512	*p__Actinobacteria__g__Pseudonocardia_114587*	*p__Chloroflexi__c__Ellin6529_112867*	*p__Nitrospirae__f__0319.6A21_241078*
p__Actinobacteria__f__Gaiellaceae_1143223	*p__Actinobacteria__g__Streptomyces_3761170*	*p__Chloroflexi__c__Ellin6529_849821*	*p__Nitrospirae__f__0319.6A21_4314932*
p__Actinobacteria__f__Gaiellaceae_368218	*p__Actinobacteria__o__0319.7L14_1142871*	*p__Chloroflexi__o__JG30.KF.CM45_549954*	*p__Synergistetes__g__vadinCA02_70446*
p__Actinobacteria__f__Gaiellaceae_816291	*p__Actinobacteria__o__Solirubrobacterales_240715*	*p__Crenarchaeota__g__Candidatus_Nitrososphaera_4400134*	*p__Tenericutes__g__Acholeplasma_106506*
p__Actinobacteria__f__Intrasporangiaceae_4432889	*p__Actinobacteria__o__Solirubrobacterales_968261*	*p__Crenarchaeota__g__Candidatus_Nitrososphaera__s__SCA1145_756973*	*p__Verrucomicrobia__g__DA101_1624*
p__Actinobacteria__f__Microbacteriaceae_826611		*p__Crenarchaeota__g__Candidatus_Nitrososphaera__s__SCA1170_556561*	

Table A. 2.6 continued

Core microbiomes	
p__Proteobacteria__f__Aeromonadaceae_829133	*p__Proteobacteria__f__Oxalobacteraceae_4363027*
p__Proteobacteria__f__Bradyrhizobiaceae_573135	*p__Proteobacteria__f__Oxalobacteraceae_4418009*
p__Proteobacteria__f__Comamonadaceae_1120966	*p__Proteobacteria__f__Rhodocyclaceae_4429771*
p__Proteobacteria__f__Comamonadaceae_1148345	*p__Proteobacteria__f__Syntrophobacteraceae_831386*
p__Proteobacteria__f__Comamonadaceae_1898675	*p__Proteobacteria__g__Acinetobacter_159711*
p__Proteobacteria__f__Comamonadaceae_1932541	*p__Proteobacteria__g__Acinetobacter_2797395*
p__Proteobacteria__f__Comamonadaceae_315609	*p__Proteobacteria__g__Allochromatium_821874*
p__Proteobacteria__f__Comamonadaceae_3926677	*p__Proteobacteria__g__Comamonas_808203*
p__Proteobacteria__f__Comamonadaceae_4170464	*p__Proteobacteria__g__Hydrogenophaga_4472017*
p__Proteobacteria__f__Comamonadaceae_4388545	*p__Proteobacteria__g__Janthinobacterium_818527*
p__Proteobacteria__f__Comamonadaceae_4452118	*p__Proteobacteria__g__Kaistobacter_4447334*
p__Proteobacteria__f__Comamonadaceae_4453998	*p__Proteobacteria__g__Kaistobacter_824146*
p__Proteobacteria__f__Hyphomicrobiaceae_4385422	*p__Proteobacteria__g__Methylibium_518380*
p__Proteobacteria__f__Methylophilaceae_306546	*p__Proteobacteria__g__Rhodoferax_4479347*
p__Proteobacteria__f__Methylophilaceae_4413869	*p__Proteobacteria__g__Rhodoplanes_101542*
	p__Proteobacteria__g__Rhodoplanes_1126197
	p__Proteobacteria__g__Rhodoplanes_136162
	p__Proteobacteria__g__Rhodoplanes_253167
	p__Proteobacteria__g__Roseateles__s__depolymerans_61836

Appendix 3: Figures in Chapter 2

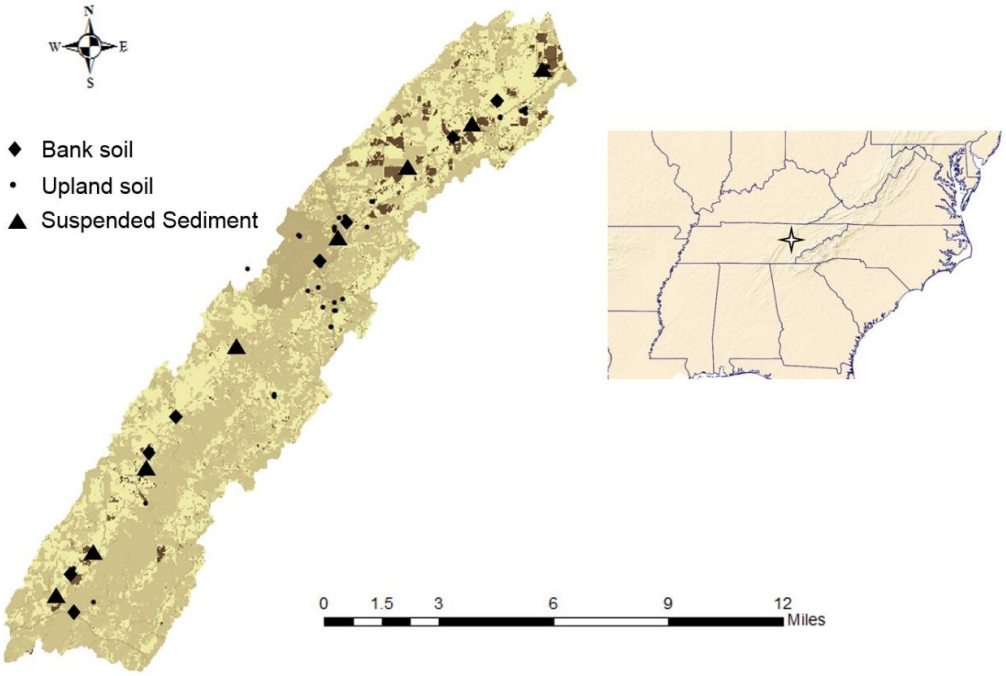


Figure 2.1 Oostanaula Creek watershed sampling sites

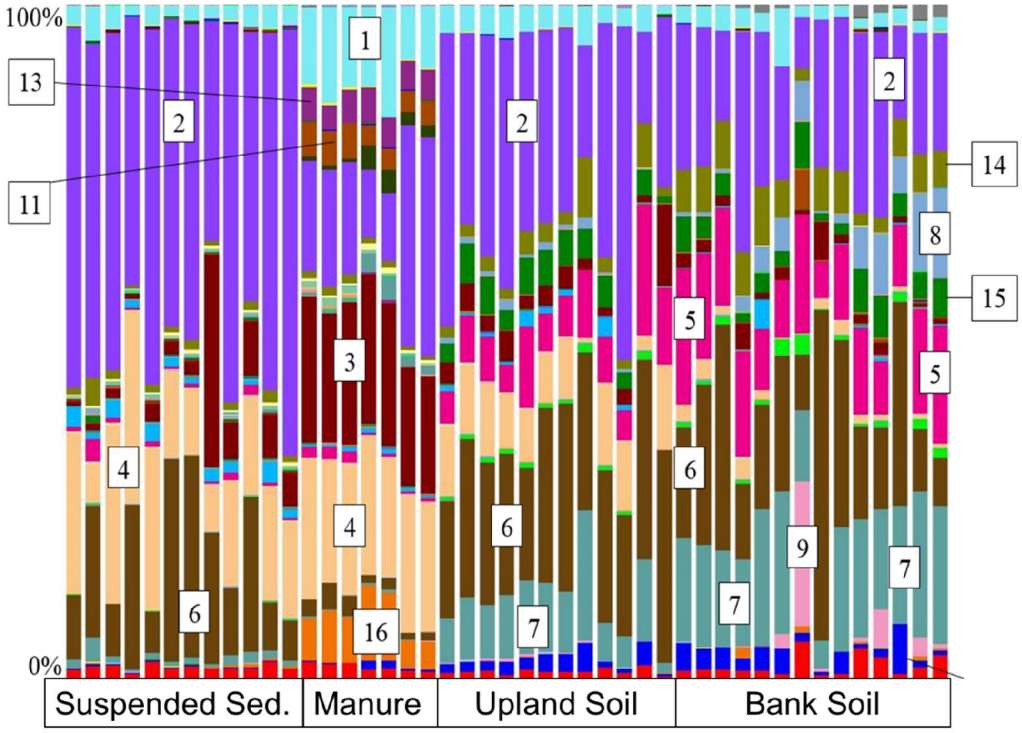


Figure 2.2 Bacterial community OTU abundance, at the phylum level, for suspended sediment and potential eroding materials in upland and bank soils in Oostanaula Creek. Select taxa are 1. *Verrucomicrobia*; 2. *Proteobacteria*; 3. *Firmicutes*; 4. *Bacteroidetes*; 5. *Chloroflexi*; 6. *Actinobacteria*; 7.*Acidobacteria*; 8. *Nitrospirae*; 9. AD3; 10. *Crenarchaeota*; 11. *Synergistetes*; 13. *Tenericutes*; 14. *Planetomycetes*; 15. *Gemmatimonadetes*; 16. *Euryarchaeota*. Full taxonomic legends for each sample are presented in the supplementary data.

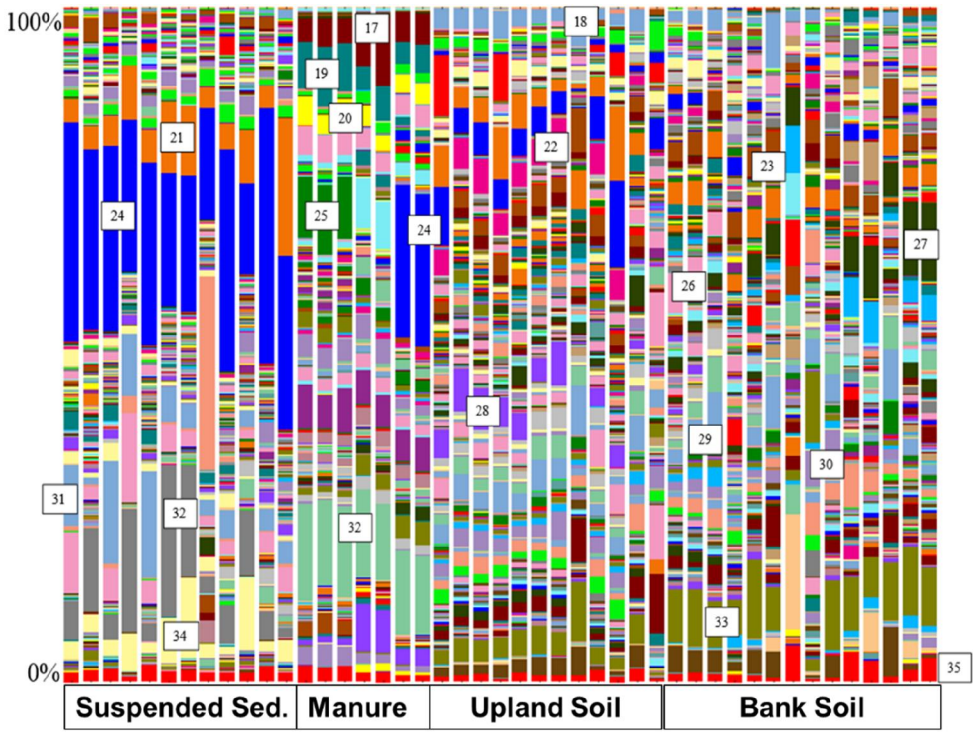
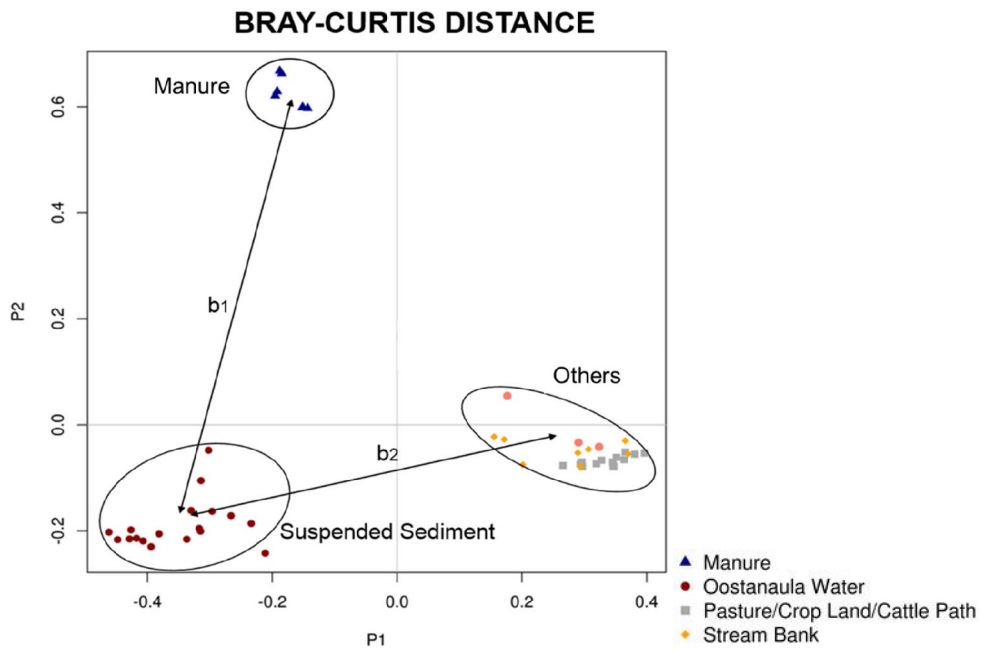
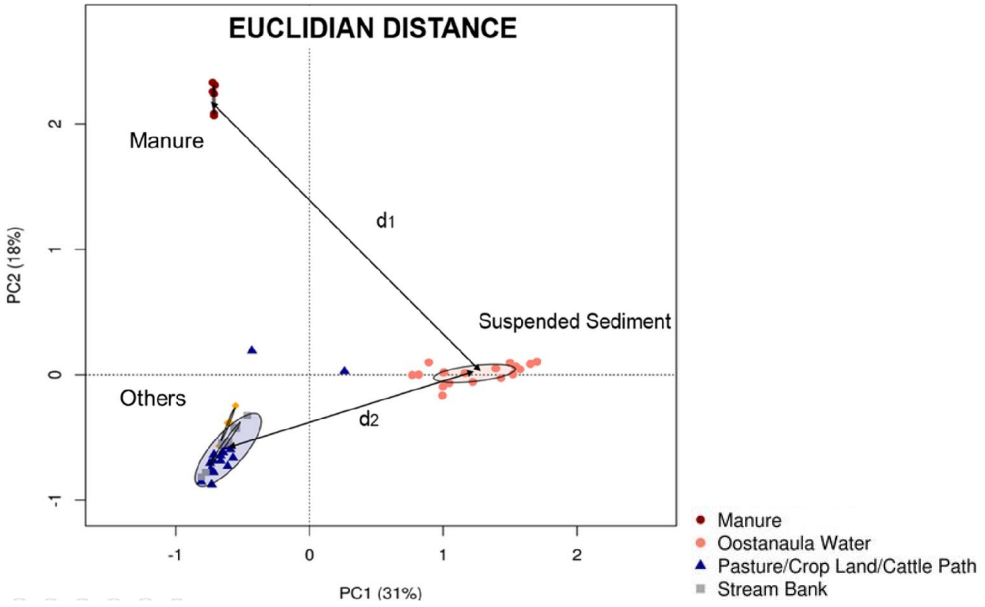


Figure 2.3 Bacterial community OTU abundance, at the family level, for suspended sediment and potential eroding materials in upland and bank soils in Oostanaula Creek. Select taxa are 18. *Chthoniobacteraceae*;; 20. *Acholeplasmataceae*; 21. *Oxalobacteraceae*; 22. *Sphingomonadaceae*; 23. *Hyphomicrobiaceae*; 24. *Comamonadaceae*; 25. *Chromatiaceae*; 28. *Chitinophagaceae*; 29. *Gaiellaceae*; 30. *Nocardioidaceae*; 31. *Flavobacteriaceae*; 32. *Microbacteriaceae*.



a. Principal Component Analysis (PCA)



b. PCoA (Principal coordinate analysis)

Figure 2.4 Multivariate correlation analysis of suspended sediment and soil 16S rRNA gene sequences. PCA and PCoA were created from Calypso (V 5.4).

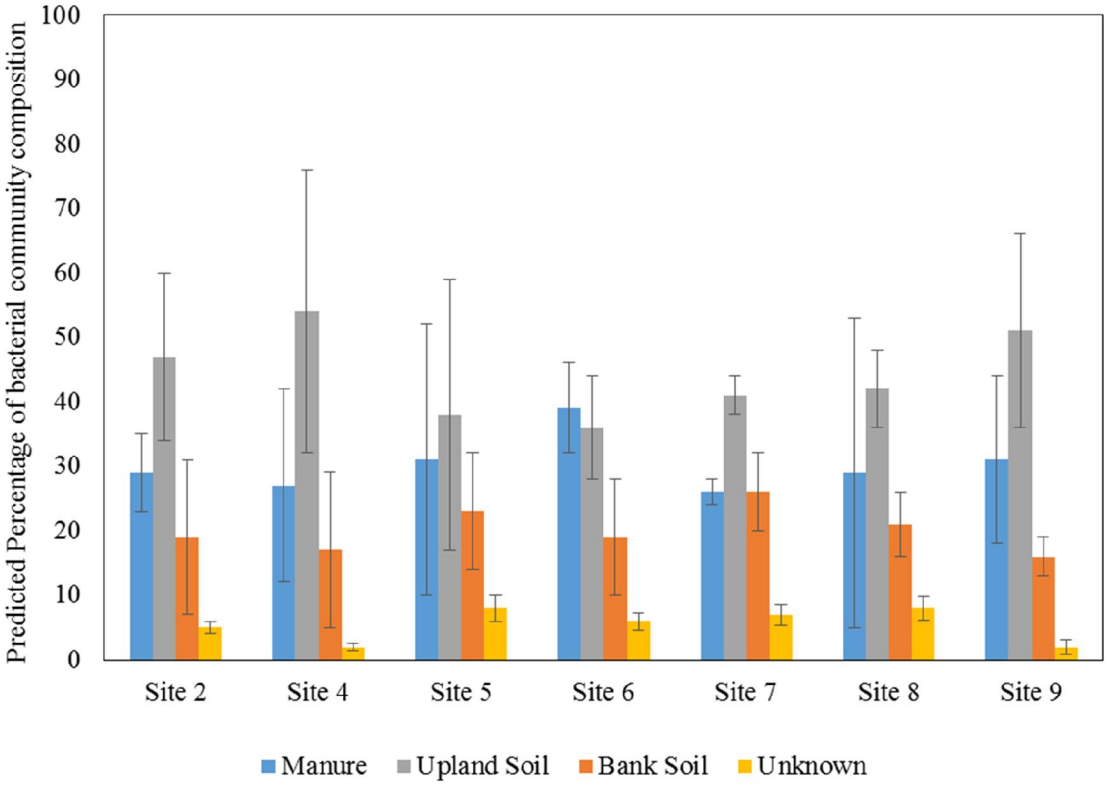


Figure 2.5 Average predicted percentage of bacterial community composition attributable to different land-based source communities determined by SourceTracker. Sites 2 to 5 are in downstream of Athens. Sites 6 to 9 are in upstream of Athens. Manure is grouped separately. Upland soils consist of crop land and cattle path. Bank soils consist the soil eroding from stream bank. Error bars represent the standard deviations.

CHAPTER 3: ASSESSING THE VALIDITY OF SEDIMENT FINGERPRINTING USING ARTIFICIAL MIXTURES

Abstract

The accurate identification of primary sediment sources in a watershed is necessary to implement targeted management practices that will reduce erosion and restore water quality. Sediment fingerprinting is a commonly-used tool to accomplish this task. However, the accuracy and precision of different procedures to select tracers for un-mixing sediment sources is still a largely uninvestigated area in relation to sediment fingerprinting. The goal of this research was to validate a sediment fingerprinting methodology by applying it to the Oostanaula Creek watershed in southeast Tennessee. We assessed three method protocols (soil digestion procedure, objective source grouping, and tracer selection) that are utilized for assessing the performance of fingerprinting in terms of apportionment outputs. The major and trace elemental composition of sediment source and suspended sediment were determined by total dissolution and nitric acid extraction followed by analysis with inductively coupled plasma - optical emission spectrometry (ICP-OES). The Kruskal-Wallis (KW) test as well as stepwise discriminant function analysis (DFA) were utilized during tracer selection. The source un-mixing model utilized was SIAR, a Bayesian mathematical model within Stable Isotope Analysis in R. Sediment fingerprinting in the Oostanaula watershed proved to be difficult due to the chemical and mineralogical similarities of the potentially erodible source material. Upon analysis, it was found that the sediment tracers identified as those with low misclassification during cluster analysis wouldn't guarantee a high degree of accuracy during source apportionment. However, there are certain outputs with low errors as compared with the real proportional contributions in

artificial mixtures, for example findings showed that bank erosion is a primary source of suspended sediment in the Oostanaula Creek. Further, it was concluded that source apportionment from sediment fingerprinting were sensitive to the digestion procedure, objective source groupings, and the tracer selection. Our research provides a quantitative approach for assessing the validity of the sediment fingerprinting technique.

Introduction

Sediment fingerprinting has been employed as a tool to identify the sources of suspended sediment within a given river system (Collins and Walling, 2002; Collins et al., 1997b). The results of the sediment fingerprinting approach can be helpful in decision making by agencies charged with managing water quality and watershed health. For instance, local governments can target their Best Management Practices (BMPs) by using this technique to identify whether a channel bank is a primary sediment source (Fox and Martin, 2014). Hence, local residents could benefit from the improved water quality due to decreased stream fine sediments after BMP implementation. Compared to conventional sediment source tracking techniques (e.g. aerial photography, watershed monitoring), fingerprinting involves a direct investigation of erodible soil materials characterizing elemental geochemical properties among different potential sediment sources. Sediment fingerprinting is based on the identifying suspended sediment properties (e.g. trace elemental concentrations, radionuclide activities) that reflect their origin (Koiter et al., 2013; Owens et al., 2016). For example, compound-specific stable isotopes can be utilized for the identification and apportionment of source soils contributing to estuarine sediments (Gibbs, 2008). However, any direct link between the fingerprint properties in the source and the sink, requires an assumption that alterations or transformations of those properties are either negligible or quantifiable, and that the fingerprint property is conservative (Belmont et al., 2014; Owens et al., 2016).

Major and trace elemental geochemistry are often utilized to identify the different

spatial sources of sediment by using the distinct elemental geochemistry among sources (Table 3.1). Eroded sediments from generation, transportation, and deposition processes are characterized by these geochemical fingerprints, allowing the relative contributions of different sources to be predicted (Caitcheon et al., 2006; D'haen et al., 2013; Hughes et al., 2009; Laceby et al., 2017). The geochemical fingerprints are composed of elemental concentrations, also called 'sediment tracers'. None of the tracers are insignificant in the sediment fingerprinting technique regardless of their attributes to the geochemical behavior. Yet, some tracers can provide more discriminatory power in differentiation of the sediment from different sources than others. Laceby et al. (2017) stated that the relationship between the sediment itself and its elemental geochemistry is complex and partly dependent on the digestion procedure (e.g. acid leached versus total digestion) used to prepare samples for analysis.

After the concentrations of sediment tracers are determined in the source and sediment material, a two-step statistical process is typically employed to select a subset of elements for sediment fingerprinting. In the first step, major and trace elements that significantly distinguish between sources are identified using the Kruskal-Wallis H-test (Collins and Walling, 2002; Collins et al., 2010). In the second step, the select subset of elements are incorporated into a mathematical model for source apportionment. Quantitative un-mixing models have recently been used to estimate sediment source contributions to river systems. Most un-mixing models are based on Bayesian mathematics, with some using multivariate mixing models (Laceby and Olley, 2015; Parnell et al., 2013).

However, there remains a need to assess the accuracy among the different methods (dependent on native geology, objective source groupings, or un-mixing models) utilized in catchment sediment fingerprinting (Owens et al., 2016), such as the influence of different subsets of elemental tracers on the final apportionment results. Vale et al. (2016) considered how the specific group of tracers employed in sediment fingerprinting accounted for the uncertainty of the model predictions. Pulley et al. (2015) also identified a mean difference of 24% associated with prediction at each source group's proportional contribution to the suspended sediment. These researchers also pointed out the impact of source group classification on the accuracy of sediment fingerprinting outputs (e.g. surface and subsurface source groups versus two-step cluster source groups) (Pulley et al., 2017).

In this study, we implement and assess several sediment fingerprinting method protocols and compare their accuracies in estimating the proportional source contribution. Specifically, the following methodologies are assessed: 1) nitric acid extraction versus total elemental dissolution for determining sediment tracers; 2) surface and subsurface groupings versus land use type based groupings (stream bank, forest, pasture, and cattle path); and 3) two-step statistically selection of tracers versus all elements as sediment tracers. The goal was to assess the errors associated with sediment fingerprinting under the three variable methodologies, and to select the approaches that generate the least root mean square error (RMSE) using pre-defined artificial suspended sediment mixtures. Applying relationships with known tracer

characteristics, natural samples from the Oostanaula Creek (OC) watershed in east Tennessee analyzed to predict the potential sources of suspended sediment.

Materials and Methods

Study Area

The Oostanaula Creek (OC) watershed encompasses 18,156 hectares (91 hectares of open water) in Monroe and McMinn counties within the Valley and Ridge physiographic region of southeast Tennessee (Figure 2.1 in Chapter 2). This sampling area was selected because it represents the primary geology of the Appalachian Mountains in the eastern United States. Oostanaula Creek is a tributary of the Hiwassee River watershed that originates in southwestern North Carolina and Northeastern Georgia. The watershed is primarily comprised of agricultural land, including cropland and pasture for local dairy and beef cattle operations.

Most of the soils in OC are derived from the underlying bedrock, which consists of Quaternary cherty clay solution residuum and Ordovician dolomite as well as limestone (USDA, 2006). The residuum is the result of long weathering over limestone and dolomite, and is categorized as a non-transported parent material (Plaster and Sherwood, 1971). Soils in the watershed include Bodine (loamy-skeletal, siliceous, semiactive, thermic Typic Paleudults), Decatur (fine, kaolinitic, thermic Rhodic Paleudults), Dewey (fine, kaolinitic, thermic Typic Paleudults), Fullerton (fine, kaolinitic, thermic Typic Paleudults), Steekee (loamy, parasesquic, thermic, shallow Ruptic-Ultic Dystrudepts), Tellico (fine, parasesquic, thermic Typic Rhodudults), and Waynesboro series (fine, kaolinitic, thermic Typic Paleudults) (USDA, 2006).

Sampling and Analysis

Sediment source samples (potential eroding soils; 0 to 3 cm depth) were collected from the study area along the creek channel banks and from adjacent upland areas (Figure 2.1 in Chapter 2). Both source (surface and subsurface soils) and sink (suspended sediment in stream water) sampling occurred between January 2013 and April 2013. Complete sampling site data including GPS coordinates and descriptions of sampling sites are listed in Table A 2.2 (in Chapter 2).

Upland topsoil samples from areas adjacent to the OC were categorized as pasture, forest, and cattle path. The soils were only obtained from the bank cut materials and topsoil directly relevant to the study. This restriction simplifies the interpretation of results for investigating the impacts of different source grouping classification schemes on sediment fingerprinting. Bulk suspended sediment-water mixtures (20 L) were collected at two locations from the stream and allowed to settle for 24 h in the laboratory at room temperature before the isolation of the sediment.

The collected soil samples were air-dried and disaggregated using a mortar and pestle. The soil sild and clay particle size fraction (<53 μm) was chosen for study to ensure that alterations or transformations of sediment fingerprinting properties remain unchanged during transportation from source to sink (Owens et al., 2001). Hence, all of the soil samples were wet-sieved through a 53-μm sieve to isolate the <53 μm material. The resulting suspension was separated by centrifuging. The suspended sediment samples were also sieved to <53 μm. Following particle size fractionation, the

soil and sediment samples were freeze-dried using a Laboconco Freezone 4.5 and stored for digestion (total dissolution or HNO_3 extraction) (Table A 3.1).

Major and trace elemental geochemistry of the source and sediment samples was determined using inductively coupled plasma- optical emission spectrometry (ICP-OES). The ICP-OES employed was a Spectro CIROS using ISO (International Organization for Standardization) certified standards. Instrument calibration was checked every 10 samples and recalibration was triggered when > 20% error was observed for any element in the standard, or when the coefficient of variation (CV) was > 20% for a single element in a single sample. Both major and trace element concentrations (mg kg-1) were obtained for each sample as the mean value of triplicate measurements. Detection limits of ICP-OES for each element with its wavelength are listed in Table A 3.2.

Tracer Selection Methods

A two-step statistical process was used to select elements for optimum fingerprint properties combination. The first process consisted of two statistical tests, Kruskal-Wallis (KW) rank test, and a discriminant function analysis (DFA) (Collins and Walling, 2002). Only elements with KW p-values <0.05 were removed from DFA analysis. In addition, all elements (without KW and DFA processing) were employed as tracers and used in the un-mixing model.

Canonical discriminant analysis (CDA) was used to create multiple correlations with groupings of tracer elements. The CDA determines how best to most effectively

separate different pre-defined groups of sediment samples (Cruz-Castillo et al., 1994). The CDA was conducted using JMP Pro 12 and summarized as the misclassification rate for each source grouping. Misclassification rate was defined as the percentage of the object clustered within a wrong group in CDA.

Source Group Classification

Sediment classification is an objective consideration for the sediment fingerprint process (Collins et al., 2017; Pulley et al., 2017). Two schemes of classification were performed (Table 3.2). In classification scheme aa, source samples were classified into two categories, surface soil and subsurface soil. This classification technique examined whether it could delineate sediment sources on a coarse scale (upland versus bank soils). Alternatively, the classification scheme bb technique attempted to differentiate among three upland sources; they were cattle path, pasture, and forest. Finally, statistical selection from apportionment output results was evaluated for the total and HNO_3-extractable element concentrations, resulting in eight final trial sets involved in the experimental design (Table 3.2). All trial sets were utilized to validate the sediment fingerprinting with artificial mixtures.

Artificial Mixtures

Sediment source samples were mixed in different ratios and labeled as mixtures 1 through 12 in order to simulate the suspended sediment samples, but with defined ratios (Table 3.3). Moreover, these mixtures were also classified into two schemes, aa and bb, corresponding to the source grouping classification schemes in Table 3.2. The un-

mixing procedure method used was similar to that described by Palazón et al. (2015).

These mixtures were analyzed using the same laboratory procedures and statistical procedures as the field-collected soil samples. Mixtures were compared to the original sample results by incorporation into the un-mixing model for validation. In addition to the total elemental composition measured by ICP-OES, the predicted concentrations of the elements in the mixtures were also computed by mass balance (Henderson, 2013). Hence, two datasets were created for the mixtures (measured and computed).

SIAR Simulations

The Stable Isotope Analysis in R (SIAR; V4.2) was the un-mixing model for sediment source applied to the sample mixtures in Table 3.3 (Parnell et al., 2008). SIAR input files contained the elemental concentration of sample mixtures as columns with grouping variables. This input file included both the elemental mean and standard deviation for each source without correction factors or trophic enrichment factors (TEF), as these may introduce additional uncertainty to in the fingerprinting process (Laceby and Olley, 2015; Smith and Blake, 2014). Output results from the un-mixing model were reported as proportions in percentages. The results were compared to the known proportions of each source group present in the artificial mixtures (Table 3.3). Each mixture in the two series dataset (measured and computed) was run five times for a total 960 runs for all eight trial sets (Table 3.2).The absolute residual error (ARE) between the mean source estimates and the known source proportional values in the mixtures was calculated (Collins et al., 1997a). These errors were utizilied to quantify how the

attributes of the different trial sets (Table 3.2) affected the fingerprint accuracy.

The SIAR was run with 200,000 iterations with a burn-in (bootstrapping) of 50,000 iterations. A Dirichlet distribution was used as the prior distribution in the multivariate Bayesian mixture model. The SIAR generates probability estimates of source proportions by accurately reflecting natural variation and uncertainty via Markov Chain Monte Carlo (MCMC), thereby producing simulations of plausible values (Parnell et al., 2008). The un-mixing mathematics model can be expressed as follows (Parnell et al., 2010):

$$X_{ij} = \sum_{k=1}^{K} p_k\left(S_{jk} + C_{jk}\right) + \varepsilon_{ij} \qquad [1]$$

$$S_{jk} \sim N\left(\mu_{jk}, \omega_{jk}^2\right) \qquad [2]$$

$$C_{jk} \sim N\left(\mu_{jk}, \tau_{jk}^2\right) \qquad [3]$$

$$\varepsilon_{jk} \sim N\left(0, \sigma_j^2\right) \qquad [4]$$

Where: X_{ij} is the measured elemental concentration j of the mixture i, in which i = 1, 2, 3, …, N and j = 1, 2, 3, …, J; p_k is the modeled value of apportionment in the source k; S_{jk} is the source value k on element j ($k = 1,2,3,\ldots,K$) under normal distribution (mean = μ_{jk}, standard deviation = ω_{jk}^2); C_{jk} is the element fractionation factor for element j ($k = 1,2,3,\ldots,K$) under normal distribution (mean = μ_{jk}, standard deviation = τ_{jk}^2); ε_{jk} is the residual error for element j ($k = 1,2,3,\ldots,K$) under normal distribution (mean = 0, standard deviation = σ_j^2)

Results and Discussion

Sediment Source Discrimination

The assumed geochemical conservative behavior of the sediment tracers provides the environmental basis for source discrimination between groups (Smith et al., 2018). The tracers listed in Table 3.4 (sets I to VIII) were selected with or without the two step KW-DFA statistical process. Pre-selecting tracers could potentially reduce within-source group variability and increase intra-group variability. Walling and Woodward (1992) performed pre-selection using a cluster analysis to classify sediment source groups. The associated misclassified percentage by canonical discriminant analysis (CDA) was used as a measure of how best to discriminate different pre-defined groups of sediment samples (Table 3.4).

The first classification scheme (aa) separated the samples into subsurface and surface sediment sources. The second classification scheme (bb) split the surface sources (upland soils) into forest, pasture, and cattle paths. Scheme aa generated a lower misclassified percentage, and the sources were easily distinguishable from one another; scheme aa resulted in a more effective separation of sources relative to scheme bb. In scheme aa, trial sets I and II, demonstrate a lower misclassified rate as compared to sets V and VI in scheme bb. The accuracy in discriminating source types may be very high with selected elemental fingerprints, although a small number of source types for efficient discrimination is suggested (Walden et al., 1997). While applying the KW-DFA statistical selection in scheme bb, the misclassified percentage was very high (41%

and 39% in sets V and VI). This phenomenon may be the result of a lack of dimensionality in the reduction of the dataset for CDA (Barthod et al., 2015). It is worth noting that the selection of all the elements as tracers provided more effective discriminatory power than the preselected elements at differentiation between different upland sources. Selecting all elemental tracers could strengthen geochemical concentrations within a sediment source group. In both schemes (aa & bb), a low misclassified rate (0, 0, 2.2 and 6.5) was observed for sets III, IV, VII and VIII (all elements entered without KW-DFA statistical selection) (Table 3.4). Within scheme aa and bb, total dissolution (sets I, III, VII) performed no worse than HNO_3 extraction (sets II, IV, and VIII) in relation to the misclassified rate. This might be attributed to the efficiency of total dissolution over that of HNO_3 extraction in delineating differences among the sources.

The KW-DFA statistical process produced composite fingerprints that could be used to classify, with high accuracy, samples into their correct source groups in scheme aa (subsurface + surface), but did not correctly segregate by identifying source categories in scheme bb (bank + forest + pasture + path). However, the strategy without statistical selections using all elements was able to discriminate categories for both schemes. On this basis, classification scheme aa is suitable for achieving basic discrimination using the available tracers, either with or without the efficient extraction of all constituents. Thus, scheme aa can provide useful information for watershed managers to effectively distinguish the surface sources from subsurface sources (e.g. soils from channel bank).

Evaluation of Apportionment Results

The un-mixing model outputs were utilized to assess how the different methods (classification scheme, tracer selection, and digestion procedure) affected the accuracy of the source apportionment results. Smith et al. (2018) stated that source apportionment with sediment fingerprinting is sensitive to both tracer selection and the number of mixture samples. The artificial mixtures of known proportions of source samples as defined in Table 3.3 were run through the SIAR un-mixing model per Eqs. [1] to [4], using the selected tracers listed in Table 3.4. Comparisons were completed for trial sets I to VIII with each associated absolute residual errors (ARE) between predicted and actual proportional source contributions. In each trial set, there were two dataset series in every mixture, the total elemental concentrations measured by ICP-OES as well as those computed from mass balance equation.

Comparing sets I to IV in scheme aa, classification of subsurface and surface soils, the mean ARE increased significantly when using all tracers for sets I and II versus sets III and IV as shown in Figure 3.1 ($p < 0.05$). Tracers sets I and II, based on KW-DFA statistical selection, and featured a smaller average mean ARE (I: 28% and II:27%) using a small number of tracers (I: 5 and II:7) than sets III & IV, based on all elements, with average mean ARE (III: 45% and IV:41%) using a large number of tracers (III: 23 and IV:25). This demonstrates the importance of removing tracers that do not provide discriminatory power.

In classification scheme bb, comparing sets V to VIII, the average mean ARE for trial sets with statistical selection (V:23% and VI:21%) with a small number of tracers

(V:4 and VI:4) was similar to the nonselective tracer trial sets (VII:25% and VIII:21%) with a large number of tracers (VII:23 and VIII:25) (Figure 3.2).

The t-test results (Table A. 3.8) indicate that there is significant difference in the error assessment between using total and HNO_3-extractable elemental data for apportionment of sediment sources. In regards to the statistical selected of tracers in classification scheme aa, there is a significant difference in the error assessment between total dissolution and HNO_3 extraction (Table A. 3.8). However, error levels depend on the individual case when referring to classification scheme bb (bank + forest + pasture + path sources).

Some model outputs, such as for mixture 8 in set VII for estimating the proportional source of forest inputs by measured mixture data, generated the lowest ARE (Table A 3.6). However, a high ARE also occurred with this estimation technique, as was found for mixture 3 (54%) in set VI for estimating the proportional source of bank. This illustrates that, even within the same mixtures, there is a difference among errors depends on the exact scheme applied. More detailed output results of ARE for every un-mixing methodology can be retrieved from the appendix 4: tables in Chapter 3. Root mean square errors (RMSEs) in percentage terms between the actual and predicted mean proportional source contributions are summarized in Tables 3.5 and 3.6. Sets I and VII with relatively low RMSEs were selected as the suitable tools for estimating source apportionment of the suspended sediment samples in Oostanaula Creek.

Suspended Sediment Source Apportionment

Estimating the proportional source contribution of suspended sediment in Oostanaula Creek (OC) was performed after evaluation of the un-mixing model results. Sets I (5 elemental tracers, Co, Cr, P, Si, and Ti, classification scheme aa) and VII (all elements as tracers, classification scheme bb) model outputs were used to determine the source contributions (Figures 3.4 and 3.5). Results for all sets indicate channel banks (subsurface soils) are the dominant sediment sources, albeit with considerable residual errors in the apportionment results of set I (Figures 3.4 and 3.5). The average mean proportional source contribution is 63% from subsurface soil (modeled by set I) and 71% from bank soils (modeled by set VII). The surface soil contribution is a secondary source of sediment in OC (37%, modeled by set I) (Figure 3.5). Two of the three outputs (set VII) predicted significant cattle path contributes as a secondary source of sediment in OC (Figure 3.5).

Conclusions

The mechanism of source apportionment in the sediment fingerprinting process is sensitive to sample digestion procedures, tracer selection, and source classification schemes. In this research, the SIAR was used to model estimate proportional source contributions to a sink environment using artificial source mixtures. The confounding effect involved in the fingerprinting process, due to particle size fraction during sediment transport and non-conservatism of tracers using artificial mixtures (Collins et al., 2017). The artificial sediment mixtures could eliminate the influence of complicated biogeochemical processes during sediment transportation.

Source and suspended sediment samples were collected from Oostanaula Creek watershed in southeastern Tennessee. The evaluation of sediment apportionment was performed using SIAR, a Bayesian un-mixing model. We used the most suitable trial set (with the lowest RMSEs) in estimating the source contribution to suspended sediment samples in the watershed. The stream bank was determined to be a principal source of suspended sediment, and this result was consistent with prior field observations.

In this watershed, it was also determined that the sediment fingerprinting technique has the ability to show differences on a coarse scale (surface vs subsurface), but is not nearly as effective in differentiating between multiple upland sediment sources. For example, large residual errors were observed when predicting the relative importance of pasture, cattle path, and forest sources. The reason for this observed phenomenon might be attributed to the homogeneous geology in this region which leads to soil

uniformity in the watershed. Nonetheless, in validating the sediment fingerprinting technique, this method does provide sufficient information to potentially contribute to TMDL implementation by local governments.

References

Bacon, S. R., and Edwards, M. J. (1957). Soil survey, McMinn County, Tennessee.

Barthod, L. R., Liu, K., Lobb, D. A., Owens, P. N., Martínez-Carreras, N., Koiter, A. J., Petticrew, E. L., McCullough, G. K., Liu, C., and Gaspar, L. (2015). Selecting Color-based Tracers and Classifying Sediment Sources in the Assessment of Sediment Dynamics Using Sediment Source Fingerprinting. Journal of Environmental Quality 44, 1605-1616.

Belmont, P., Willenbring, J. K., Schottler, S. P., Marquard, J., Kumarasamy, K., and Hemmis, J. M. (2014). Toward generalizable sediment fingerprinting with tracers that are conservative and nonconservative over sediment routing timescales. Journal of Soils and Sediments 14, 1479-1492.

Caitcheon, G., Douglas, G., and Palmer, M. (2006). Sediment source tracing in the Lake Burragorang catchment. Canberra: CSIRO Land and Water.

Collins, A., and Walling, D. (2002). Selecting fingerprint properties for discriminating potential suspended sediment sources in river basins. Journal of Hydrology 261, 218-244.

Collins, A., Walling, D., and Leeks, G. (1997a). Source type ascription for fluvial suspended sediment based on a quantitative composite fingerprinting technique. Catena 29, 1-27.

Collins, A., Walling, D., Webb, L., and King, P. (2010). Apportioning catchment scale sediment sources using a modified composite fingerprinting technique incorporating property weightings and prior information. Geoderma 155, 249-261.

Collins, A. L., Pulley, S., Foster, I. D. L., Gellis, A., Porto, P., and Horowitz, A. J. (2017). Sediment source fingerprinting as an aid to catchment management: A review of the current state of knowledge and a methodological decision-tree for end-users. Journal of Environmental Management 194, 86-108.

Collins, A. L., Walling, D. E., and Leeks, G. J. L. (1997b). Fingerprinting the Origin of Fluvial Suspended Sediment in Larger River Basins: Combining Assessment of Spatial Provenance and Source Type. Geografiska Annaler: Series A, Physical Geography 79, 239-254.

Cruz-Castillo, J., Ganeshanandam, S., MacKay, B., Lawes, G., Lawoko, C., and Woolley, D. (1994). Applications of canonical discriminant analysis in horticultural research. HortScience 29, 1115-1119.

D'haen, K., Verstraeten, G., Dusar, B., Degryse, P., Haex, J., and Waelkens, M. (2013). Unravelling changing sediment sources in a Mediterranean mountain catchment: a Bayesian fingerprinting approach. Hydrological Processes 27, 896-910.

Fox, J. F., and Martin, D. K. (2014). Sediment fingerprinting for calibrating a soil erosion and sediment-yield model in mixed land-use watersheds. Journal of Hydrologic Engineering 20, C4014002.

Gibbs, M. M. (2008). Identifying Source Soils in Contemporary Estuarine Sediments: A New Compound-Specific Isotope Method. Estuaries and Coasts 31, 344-359.

Henderson, P. (2013). Rare earth element geochemistry, Elsevier.

Hughes, A. O., Olley, J. M., Croke, J. C., and McKergow, L. A. (2009). Sediment source changes over the last 250 years in a dry-tropical catchment, central Queensland, Australia. Geomorphology 104, 262-275.

Kline, W. E., and Fogler, H. S. (1981). Dissolution of silicate minerals by hydrofluoric acid. Industrial and Engineering Chemistry Fundamentals 20, 155-161.

Koiter, A., Owens, P., Petticrew, E., and Lobb, D. (2013). The behavioural characteristics of sediment properties and their implications for sediment fingerprinting as an approach for identifying sediment sources in river basins. Earth Science Reviews 125, 24-42.

Laceby, J. P., Evrard, O., Smith, H. G., Blake, W. H., Olley, J. M., Minella, J. P., and Owens, P. N. (2017). The challenges and opportunities of addressing particle size effects in sediment source fingerprinting: a review. Earth Science Reviews 169, 85-103.

Laceby, J. P., and Olley, J. (2015). An examination of geochemical modelling approaches to tracing sediment sources incorporating distribution mixing and elemental correlations. Hydrological Processes 29, 1669-1685.

Owens, P., Walling, D., Carton, J., Meharg, A., Wright, J., and Leeks, G. (2001). Downstream changes in the transport and storage of sediment-associated contaminants (P, Cr and PCBs) in agricultural and industrialized drainage basins. Science of the Total Environment 266, 177-186.

Owens, P. N., Blake, W. H., Gaspar, L., Gateuille, D., Koiter, A. J., Lobb, D. A., Petticrew, E. L., Reiffarth, D. G., Smith, H. G., and Woodward, J. C. (2016). Fingerprinting and tracing the sources of soils and sediments: Earth and ocean science, geoarchaeological, forensic, and human health applications. Earth Science Reviews 162, 1-23.

Palazón, L., Latorre, B., Gaspar, L., Blake, W. H., Smith, H. G., and Navas, A. (2015). Comparing catchment sediment fingerprinting procedures using an auto-evaluation approach with virtual sample mixtures. Science of the Total Environment 532, 456-466.

Parnell, A., Inger, R., Bearhop, S., and Jackson, A. (2008). SIAR: Stable Isotope Analysis in R.

Parnell, A. C., Inger, R., Bearhop, S., and Jackson, A. L. (2010). Source partitioning using stable isotopes: coping with too much variation. PloS One 5, e9672.

Parnell, A. C., Phillips, D. L., Bearhop, S., Semmens, B. X., Ward, E. J., Moore, J. W., Jackson, A. L., Grey, J., Kelly, D. J., and Inger, R. (2013). Bayesian stable isotope mixing models. Environmetrics 24, 387-399.

Plaster, R., and Sherwood, W. (1971). Bedrock weathering and residual soil formation in central Virginia. Geological Society of America Bulletin 82, 2813-2826.

Pulley, S., Foster, I., and Collins, A. L. (2017). The impact of catchment source group classification on the accuracy of sediment fingerprinting outputs. Journal of Environmental Management 194, 16-26.

Smith, H. G., and Blake, W. H. (2014). Sediment fingerprinting in agricultural catchments: A critical re-examination of source discrimination and data corrections. Geomorphology 204, 177-191.

Smith, H. G., Karam, D. S., and Lennard, A. T. (2018). Evaluating tracer selection for catchment sediment fingerprinting. Journal of Soils and Sediments, 1-15.

USDA (2006). Soil Survey of Knox County, Tennessee. In "Web Soil Survey".

Walden, J., Slattery, M. C., and Burt, T. P. (1997). Use of mineral magnetic measurements to fingerprint suspended sediment sources: approaches and techniques for data analysis. Journal of Hydrology 202, 353-372.

Walker, J. H. a. F. (2007). Oostanaula Creek Watershed Restoration. University of Tennessee Extension Biosystems Engineering and Soil Science.

Walling, D., and Woodward, J. (1992). Use of radiometric fingerprints to derive information on suspended sediment sources. Erosion and sediment transport monitoring programmes in river basins 210, 153-164.

Appendix 4: Tables in Chapter 3

Table 3.1 Sediment elemental fingerprinting research

Reference	Country	Watershed Area (km^2)	Elements Analyzed (n)	Extraction Procedure	Analytical Method	Source Apportionment Model
Cooper et al., 2015a	United Kingdom	5	11	NA†	X-ray fluorescence spectroscopy (XRFS) and diffuse reflectance infrared Fourier transform spectroscopy (DRIFTS)	Bayesian mixing model
D'Haen et al., 2013	Turkey	264	18	Dissolved in *aqua regia*	Inductively coupled plasma optical emission spectroscopy (ICP-OES)	Bayesian mixing model
Douglas et al., 2003	Australia	22,000	50	Fused glass discs	XRFS	Bayesian geochemical linear mixing model
Haddadchi et al., 2015	Australia	911	41	Lithium metaborate fusion	Inductively coupled plasma mass spectroscopy (ICP-MS) and (ICP-OES)	Distribution mixing model
Hardy et al., 2010	Canada	12,000	55	Heated in HNO_3-$HClO_4$-HF to fusion	ICP-MS	NA
Laceby et al., 2015a	Australia	74	37	Lithium metaborate fusion	ICP-MS	Distribution mixing model
Laceby and Olley, 2015	Australia	75,123,311	23	Fused glass discs	XRFS	Distribution mixing model
Olley and Caitcheon, 2000	Australia	650,000	10	Lithium metaborate fusion	XRFS	NA
Vale et al., 2016	New Zealand	5,870	44	NA	XRFS and laser ablation ICP-MS	Multivariate mixing model

† NA (Not Applicable).

Table 3.2 Summary of trial sets validating sediment elemental fingerprinting

Different Source Group Classification Scheme	With statistical selection		All tracers selected	
	Total	**HNO_3**	**Total**	**HNO_3**
aa. Subsurface + Surface	I	II	III	IV
bb. Bank+Forest+Pasture+Path	V	VI	VII	VIII

Table 3.3 Artificial mixture content of different source group sample classification schemes: aa (Surface + Subsurface) and bb (Bank + Forest + Pasture + Path)

Mixture No.	Source Group Classification Scheme	
	aa	**bb**
1	100+0	0+0+50+50
2	70+30	30+0+70+0
3	11+89	89+0+11+0
4	88+12	12+0+10+78
5	79+21	21+0+59+20
6	68+32	32+0+35+33
7	100+0	0+50+0+50
8	86+14	14+11+0+75
9	43+57	56+10+34+0
10	100+0	0+46+13+41
11	58+42	42+10+48+0
12	36+65	65+0+0+35

Table 3.4 Trial set tracer misclassification percentage in discriminant analysis. Superscripts of T and N represent the digestion procedures, total dissolution (T) and nitric acid (HNO_3) extraction (N).

Classification Scheme	Trial set	Tracers *n*	Selected tracers	Misclassified %
	I	5	Co^T Cr^T P^T Si^T Ti^T	2.2
aa.	II	7	Co^N Cr^N Hf^N K^N Li^N Nd^N Zr^N	6.5
Subsurface + Surface	III	23	Al^T Ca^T Fe^T K^T Mg^T Mn^T P^T Si^T Ti^T Ba^T Co^T Cr^T Cu^T La^T Li^T Mo^T Nd^T S^T Sr^T V^T Zn^T Zr^T Rb^T	0
	IV	25	Al^N Ca^N Fe^N K^N Mg^N Mn^N P^N Si^N Ti^N Ba^N Co^N Cr^N Cu^N La^N Li^N Mo^N Nd^N S^N Sr^N V^N Zn^N Zr^N Cd^N Hf^N Na^N	0
	V	4	Co^T P^T La^T Mn^T	41
	VI	4	Co^N Cu^N Mg^N Nd^N	39
bb.	VII	23	Al^T Ca^T Fe^T K^T Mg^T Mn^T P^T Si^T Ti^T Ba^T Co^T Cr^T Cu^T La^T Li^T Mo^T Nd^T S^T Sr^T V^T Zn^T Zr^T Rb^T	2.2
Bank+Forest+Pasture+Path	VIII	25	Al^N Ca^N Fe^N K^N Mg^N Mn^N P^N Si^N Ti^N Ba^N Co^N Cr^N Cu^N La^N Li^N Mo^N Nd^N S^N Sr^N V^N Zn^N Zr^N Cd^N Hf^N Na^N	6.5

Table 3.5 Percent root mean square errors (RMSEs) between actual and predicted mean proportional source contribution for 12 artificial sediment mixtures, trial sets I through IV

Trial set	A	B	Average
I	35	33	34
II	32	31	31.5
III	60	44	52
IV	53	41	47

Table 3.6 Percent root mean square errors (RMSEs) between actual and predicted mean proportional source contributions for 12 artificial sediment mixtures, trial sets V through VIII. Series A and B represent the elemental datasets for each mixture measured by ICP-OES and computed by mass balance equation.

Trial set	**A**				**B**				
	Bank	Forest	Pasture	Path	Bank	Forest	Pasture	Path	Average
V	33	37	27	34	33	29	25	34	32
VI	26	22	21	22	25	21	24	28	24
VII	44	41	26	34	22	17	25	24	29
VIII	25	20	22	27	23	17	25	27	23

Table A. 3.1 Total dissolution and HNO_3 procedures

Step	Reagents	pH	Volume (ml)	% Power (W)	Time (min)
Total dissolution					
1 Add	HF	3.27	2	NA†	16 hr
2 Add and stir	*Aqua Regia*	≈ 0	5	NA	10
3 Microwave	Sample		7	80% (800)	3
4 Neutralize	HB	6.12	1 gram	NA	30
5 Microwave	Sample		7	20% (200)	10
6 Filter	Sample		NA	NA	30
			Total time of digestion		16hr + 83mins
HNO_3 extraction					
1 Digest	HNO_3	3.01	21	NA	16 hrs
2 Dilute	Deionized water		35	NA	10
3 Filter	Sample		NA	NA	10
			Total time of digestion		16 hrs + 20 min

† NA = not applicable.

Table A. 3.2 Wavelengths and detection limits for elemental analysis by ICP-OES

Element	Wavelength (nm)	Solid detection limit (mg kg^{-1})
Al	394	10
Ba	455	0.25
Ca	317	0.25
Cd	230	2.5
Co	230	2.5
Cr	267	2.5
Cu	327	2.5
Fe	259	2.5
Hf	277	25
K	766	50
La	408	5
Li	670	2.5
Mg	285	0.25
Mn	257	0.5
Mo	202	5
Na	589	25
Nd	417	25
P	177	25
Rb	780	5
S	182	20
Si	251	10
Sr	421	0.25
Ti	336	2.5
V	327	2.5
Zn	213	2.5
Zr	339	2.5

Table A. 3.3 Percent absolute residual errors between actual and predicted mean proportional source contributions for 12 artificial sediment mixtures, trial sets I through IV. Series A and B represent the elemental datasets for each mixture measured by ICP-OES and computed by mass balance equation.

Mixture No.	**Trial set I**		**Trial set II**		**Trial set III**		**Trial set IV**	
	A	**B**	**A**	**B**	**A**	**B**	**A**	**B**
1	47	46	N/A†	44	92	63	N/A	57
2	11	15	N/A	17	29	38	N/A	37
3	40	31	N/A	33	56	11	N/A	6
4	44	32	N/A	35	83	53	N/A	39
5	25	26	N/A	26	60	45	N/A	43
6	16	20	N/A	14	51	36	N/A	36
7	54	51	52	55	81	62	72	56
8	39	39	21	5	64	51	71	48
9	12	3	13	3	26	16	22	20
10	55	49	48	52	77	61	67	57
11	4	8	1	11	6	29	29	29
12	10	7	20	12	2	9	21	13

† N/A = not applicable.

Table A. 3.4 Percent absolute residual errors between actual and predicted mean proportional source contributions for 12 artificial sediment mixtures, trial set V. Series A and B represent the elemental datasets for each mixture measured by ICP-OES and computed by mass balance equation.

Mixture No.	**Trial set V**							
	A				**B**			
	Bank	Forest	Pasture	Path	Bank	Forest	Pasture	Path
1	8	49	28	15	10	23	5	38
2	10	30	33	27	19	34	26	10
3	11	33	45	12	78	33	35	10
4	8	45	34	12	1	32	34	65
5	9	51	29	11	11	33	12	10
6	9	44	38	9	21	38	5	22
7	12	59	15	14	11	5	34	40
8	12	57	19	12	2	29	34	61
9	11	52	22	14	46	25	12	10
10	12	63	11	13	11	4	23	30
11	10	34	45	12	28	30	14	11
12	11	14	60	15	53	40	38	24
Mean	10	44	32	14	24	27	23	28
SD	1	14	14	4	23	12	12	20

Table A. 3.5 Percent absolute residual errors between actual and predicted mean proportional source contributions for 12 artificial sediment mixtures, trial set VI. Series A and B represent the elemental datasets for each mixture measured by ICP-OES and computed by mass balance equation.

Mixture No.	**Trial set VI**							
	A				**B**			
	Bank	Forest	Pasture	Path	Bank	Forest	Pasture	Path
1	N/A†	N/A	N/A	N/A	28	20	21	26
2	N/A	N/A	N/A	N/A	0	23	42	20
3	N/A	N/A	N/A	N/A	54	26	12	16
4	N/A	N/A	N/A	N/A	15	22	19	55
5	N/A	N/A	N/A	N/A	8	23	31	0
6	N/A	N/A	N/A	N/A	3	23	6	14
7	28	33	25	19	25	28	30	27
8	9	4	26	38	12	13	29	54
9	27	15	5	18	25	14	7	18
10	30	29	16	17	32	16	11	17
11	15	18	19	17	12	13	21	20
12	36	20	28	11	31	25	24	18
Mean	24	20	20	20	20	21	21	24
SD	10	10	9	9	15	5	11	16

† N/A = not applicable.

Table A. 3.6 Percent absolute residual errors between actual and predicted mean proportional source contributions for 12 artificial sediment mixtures, trial set VII. Series A and B represent the elemental datasets for each mixture measured by ICP-OES and computed by mass balance equation.

Mixture No.	**Trial set VII**							
	A				**B**			
	Bank	Forest	Pasture	Path	Bank	Forest	Pasture	Path
1	36	21	31	26	35	20	29	25
2	5	56	56	6	14	23	51	14
3	72	46	13	13	30	16	3	11
4	51	72	3	70	24	15	8	46
5	24	37	45	16	21	21	39	3
6	22	29	23	29	11	18	17	13
7	66	45	18	38	30	18	16	28
8	45	1	20	64	22	6	17	45
9	42	38	6	10	8	14	18	12
10	61	37	6	30	31	15	5	21
11	24	34	19	9	3	14	29	13
12	25	26	19	20	13	15	15	17
Mean	39	37	22	28	20	16	21	21
SD	20	18	16	21	10	4	14	13

Table A. 3.7 Percent absolute residual errors between actual and predicted mean proportional source contributions for 12 artificial mixtures, trial set VIII. Series A and B represent the elemental datasets for each mixture measured by ICP-OES and computed by mass balance equation.

Mixture No.	**Trial set VIII**							
	A				**B**			
	Bank	Forest	Pasture	Path	Bank	Forest	Pasture	Path
1	N/A†	N/A	N/A	N/A	37	10	23	24
2	N/A	N/A	N/A	N/A	5	15	49	20
3	N/A	N/A	N/A	N/A	43	12	2	10
4	N/A	N/A	N/A	N/A	19	15	15	56
5	N/A	N/A	N/A	N/A	12	15	36	1
6	N/A	N/A	N/A	N/A	3	14	13	15
7	28	33	26	25	29	34	27	24
8	13	5	26	47	18	4	25	53
9	16	4	17	15	15	4	16	13
10	41	32	4	27	28	30	13	14
11	4	4	27	16	4	4	28	16
12	27	14	21	20	22	12	16	23
Mean	22	15	20	25	20	14	22	22
SD	13	14	9	12	13	9	12	16

† N/A = not applicable.

Table A. 3.8 T-test results comparing Total and HNO_3 extraction of soils and sediment

aa	**I vs II**	**III vs IV**
A	No	No
B	No	Yes

bb	**V vs VI**				**VII vs VIII**			
	Bank	Forest	Pasture	Path	Bank	Forest	Pasture	Path
A	Yes	Yes	No	No	Yes	Yes	Yes	No
B	No	No	No	No	No	No	No	No

Table A. 3.9 T-test results comparing statistical selection and all tracers selection

aa	**I vs III**				**II vs IV**			
A	Yes				Yes			
B	Yes				Yes			
bb	**V vs VII**				**VI vs VIII**			
	Bank	Forest	Pasture	Path	Bank	Forest	Pasture	Path
A	Yes	No	No	No	No	No	No	No
B	No	Yes	No	Yes	No	Yes	No	No

Appendix 5: Figures in Chapter 3

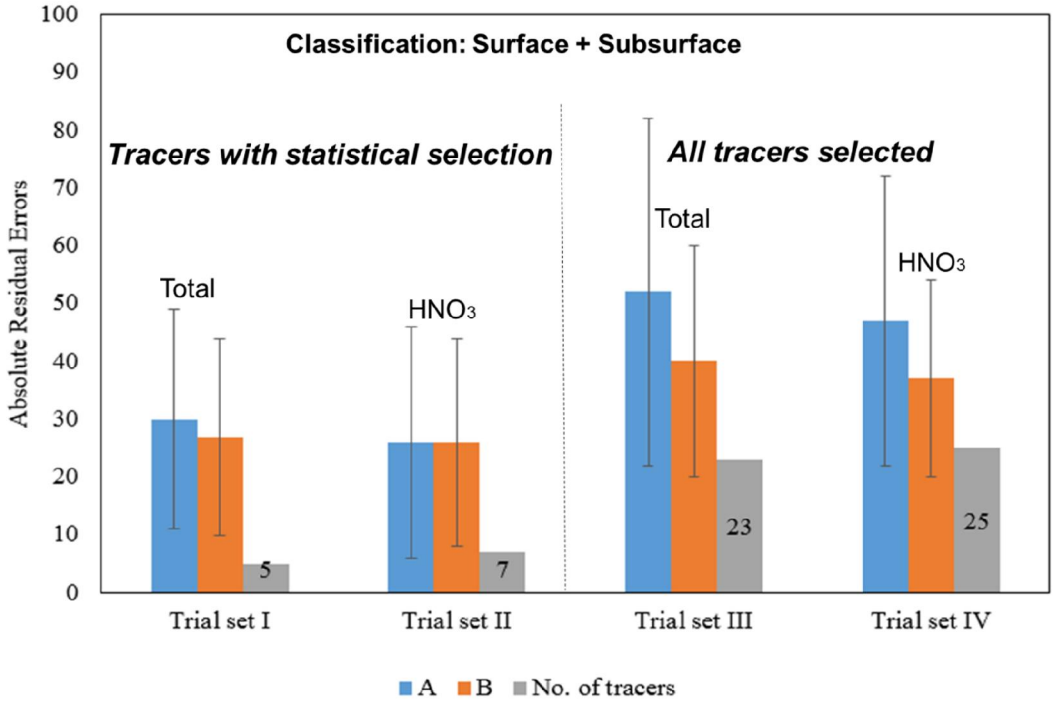


Figure 3.1 Comparison of mean absolute residual errors for trial sets I through IV. Series A represents the elemental datasets for real mixtures measured by ICP-OES. Series B represents the elemental datasets for synthetic mixtures computed by mass balance equation. Error bars represent the standard deviations.

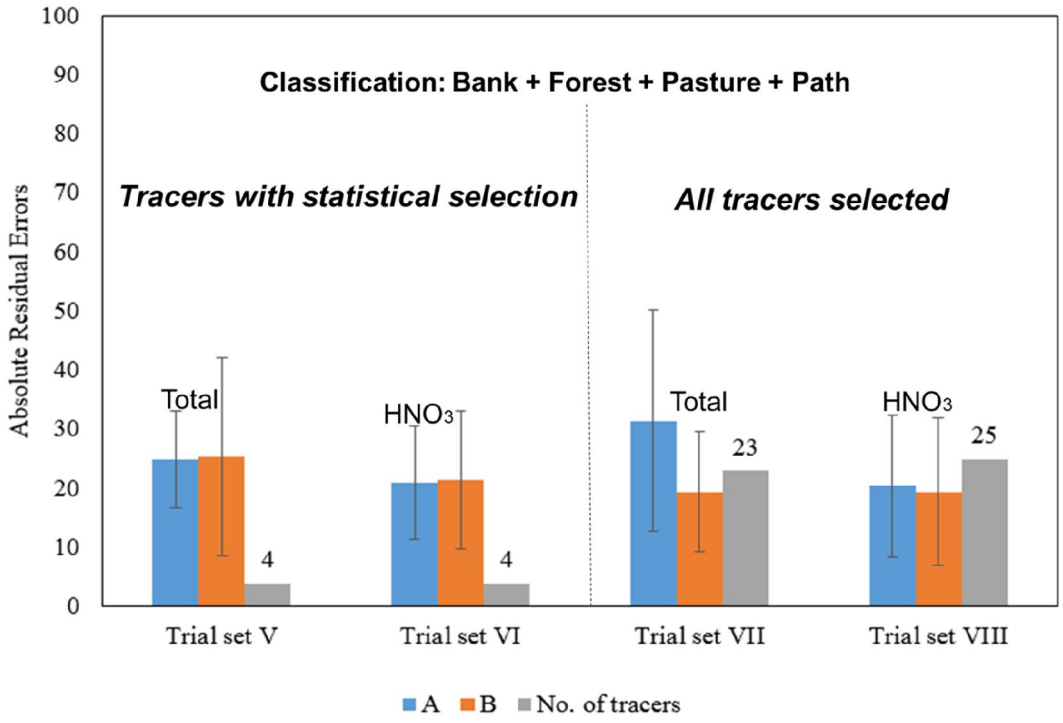


Figure 3.2 Comparison of mean absolute residual errors for trial sets V through VIII. Series A represents the elemental datasets for real mixtures measured by ICP-OES. Series B represents the elemental datasets for synthetic mixtures computed by mass balance equation. Error bars represent the standard deviations.

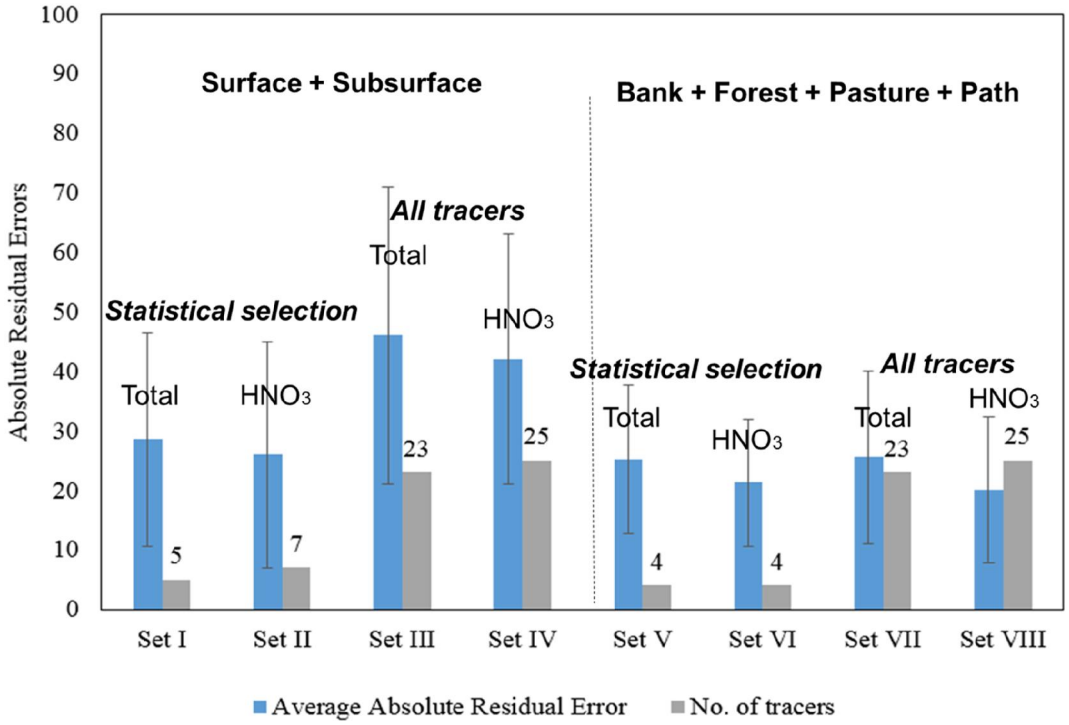


Figure 3.3 Comparison of average mean absolute residual errors for trial sets I through VIII. Error bars represent the standard deviations.

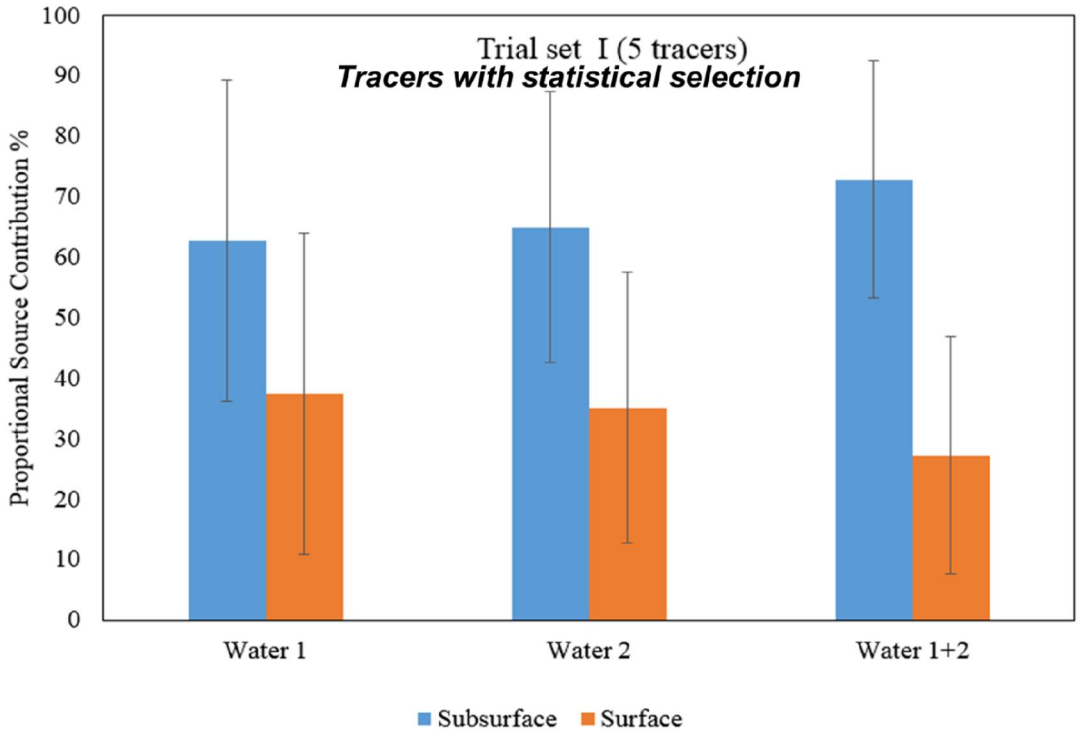


Figure 3.4 Proportional mean subsurface and surface source contributions in Oostanaula Creek watershed. Error bars represent the standard deviations.

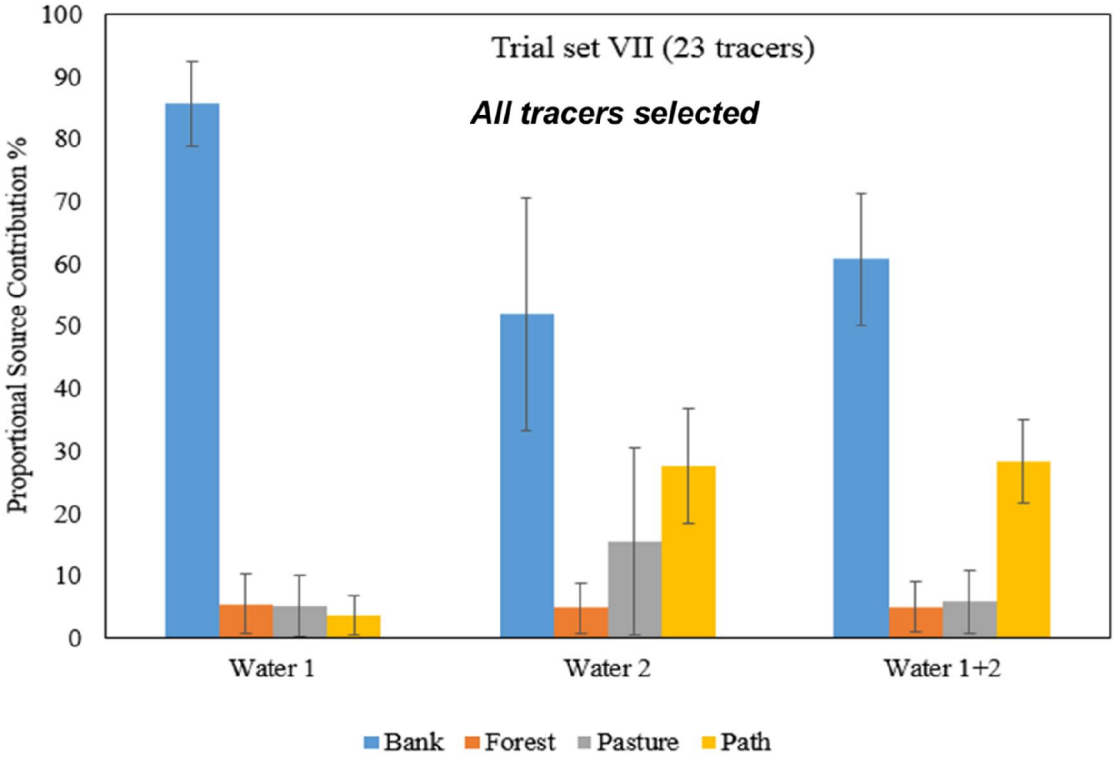


Figure 3.5 Proportional mean upland source contributions in Oostanaula Creek watershed

Appendix 6: Total Dissolution Element Concentrations

Averaged from replicates for each sample and shown in mg kg^{-1} for Oostanaula Creek watershed

Field #	Type	Al	Ba	Ca	Co	Cr
1	path	66033.33	561.33	1962.50	18.62	46.95
2	path	38633.33	528.33	3376.67	15.02	32.70
3	path	43800.00	574.17	2471.50	16.35	40.82
4	pasture	55033.33	521.33	2600.00	18.53	42.08
5	path	36066.67	487.33	3296.67	15.25	27.28
6	path	53666.67	441.67	2230.00	15.32	39.58
8	bank	49133.33	523.17	2751.67	18.75	44.83
9	path	38766.67	909.50	2936.67	14.52	32.50
13	pasture	72300.00	329.50	1942.33	8.78	62.52
14	path	37222.64	258.17	44759.93	24.71	40.27
15	path	55900.00	304.33	2060.67	10.32	40.03
17	path	52900.00	297.50	5813.33	11.45	44.58
18	pasture	43783.33	218.50	3905.00	9.77	35.30
19	bank	47600.00	181.33	6280.00	17.50	54.10
20	path	34116.67	145.50	4025.00	9.33	25.20
21	pasture	34033.33	97.50	4160.00	6.43	28.72
22	pasture	32533.33	156.50	3490.00	7.65	25.67
23	bank	53650.00	354.50	3993.33	19.92	42.47
24	bank	49150.00	370.50	5365.00	21.87	39.35
25	path	47595.45	306.56	8406.31	11.76	38.23
26	pasture	29273.50	425.76	1009.32	7.92	17.74
28	pasture	58083.33	323.67	3960.00	12.70	33.10
40	bank	57448.17	325.20	3182.20	14.74	38.61
41	bank	56563.12	306.60	2773.23	13.57	52.95
43	bank	48642.74	280.95	3841.57	15.93	37.43
46	bank	46961.35	309.52	1831.23	19.18	37.85
47	bank	45046.15	236.25	1254.98	15.02	30.77
48	bank	43460.45	257.28	2442.35	16.98	32.46
49	bank	52663.89	432.54	1492.57	12.30	30.21
50	bank	58201.32	505.12	1580.69	14.72	34.46
52	bank	41579.43	456.49	2830.01	15.56	30.13
54	bank	43646.22	460.48	3160.29	21.61	34.30
56	bank	47395.07	492.74	3152.92	18.90	33.05
57	forest	44027.70	450.37	3376.58	14.55	31.10
58	forest	27713.86	242.97	2878.32	9.88	23.09
59	bank	55365.99	328.71	2793.56	22.35	44.01
60	bank	53930.89	312.03	3956.76	25.05	43.20
62	bank	62170.58	315.07	2604.33	24.07	47.43
64	forest	40065.54	239.99	3989.47	17.02	35.09
68	pasture	45301.90	294.85	3362.66	21.11	42.18

Field #	Type	Cu	Fe	K	La	Li
1	path	41.82	41516.67	12141.67	33.35	39.97
2	path	78.47	31250.00	10880.00	31.13	26.35
3	path	55.90	45383.33	11346.67	36.37	29.57
4	pasture	67.30	54916.67	10768.33	44.50	36.00
5	path	56.03	38400.00	10190.00	28.05	24.38
6	path	74.80	42033.33	12961.67	21.12	36.33
8	bank	71.32	44416.67	12651.67	34.55	39.13
9	path	113.38	31633.33	11445.00	28.88	27.18
13	pasture	31.95	44400.00	22470.00	20.23	41.20
14	path	59.25	61792.97	14675.79	35.05	29.71
15	path	32.13	30350.00	14793.33	28.37	23.78
17	path	50.77	28816.67	13720.00	27.45	29.30
18	pasture	45.32	23883.33	10423.33	24.23	27.52
19	bank	49.35	29333.33	11395.00	35.58	26.05
20	path	46.38	18960.00	7301.67	32.63	22.17
21	pasture	48.37	23463.33	6836.67	26.33	22.90
22	pasture	49.62	15421.67	8293.33	25.03	24.98
23	bank	53.65	30015.00	13215.00	32.03	33.65
24	bank	104.13	36500.00	10398.33	38.77	36.03
25	path	76.55	27712.63	10110.66	35.33	37.40
26	pasture	119.21	14923.20	9697.15	62.50	29.69
28	pasture	76.98	30983.33	7711.67	55.67	35.77
40	bank	80.69	32542.25	13996.86	58.41	37.99
41	bank	88.68	31350.53	12643.63	57.81	34.80
43	bank	117.26	27477.06	12060.50	59.19	36.50
46	bank	91.48	31275.03	11727.55	62.16	34.26
47	bank	82.51	25994.23	10892.23	60.57	30.71
48	bank	98.81	26492.37	11468.52	59.55	32.32
49	bank	84.47	34413.23	12564.27	64.27	29.11
50	bank	89.41	34587.46	15605.61	62.72	33.50
52	bank	92.83	25503.90	10517.39	63.15	31.56
54	bank	123.31	31142.86	12356.19	65.11	31.96
56	bank	106.80	30639.58	13190.09	66.18	34.84
57	forest	102.21	28254.55	12891.12	65.63	31.12
58	forest	115.14	14320.39	5524.67	68.57	25.77
59	bank	130.43	42582.12	11383.79	85.17	42.21
60	bank	122.78	42518.28	12129.62	83.50	40.32
62	bank	132.47	46838.50	12755.18	85.93	49.04
64	forest	56.25	34166.06	6750.48	40.10	32.22
68	pasture	74.67	36576.07	10736.71	45.72	34.82

Field #	Type	Mg	Mn	Mo	Nd	P
1	path	3768.33	3036.67	2.57	33.93	884.50
2	path	2858.33	2243.50	1.63	39.08	1654.83
3	path	2796.67	2645.00	1.97	52.32	2123.67
4	pasture	3616.67	2978.33	2.53	53.98	2372.83
5	path	2499.33	2232.33	1.55	41.03	2288.00
6	path	3811.67	790.83	1.75	24.90	893.33
8	bank	3771.67	2118.83	1.78	42.85	1912.00
9	path	3010.00	1703.00	1.48	29.85	1715.00
13	pasture	7216.67	378.33	2.30	17.48	781.50
14	path	10164.36	3441.99	3.06	34.30	4248.73
15	path	4208.33	707.17	1.68	25.02	890.00
17	path	4845.00	535.33	1.43	23.15	1070.67
18	pasture	3543.33	289.33	0.85	19.18	718.17
19	bank	4350.00	1216.67	0.77	28.32	1102.00
20	path	2761.67	927.17	0.50	26.17	913.00
21	pasture	2955.00	353.00	0.83	18.22	1071.00
22	pasture	3306.67	673.33	0.53	14.32	785.83
23	bank	4386.67	1761.17	0.90	26.12	1183.50
24	bank	3941.67	2725.00	1.42	30.18	1022.17
25	path	3150.61	1266.43	1.09	17.42	1762.71
26	pasture	1623.69	564.16	0.58	13.87	657.34
28	pasture	2438.33	3013.33	1.13	36.75	1391.33
40	bank	3864.94	1339.53	1.17	31.85	625.82
41	bank	3325.00	1199.20	2.25	27.33	519.14
43	bank	3343.84	951.47	0.81	22.41	1017.09
46	bank	2916.64	2105.51	0.98	22.76	687.53
47	bank	2776.66	1943.40	0.91	20.92	390.04
48	bank	2930.15	1863.94	1.26	20.13	702.64
49	bank	2279.70	1488.45	0.64	34.89	522.74
50	bank	2866.34	1291.42	1.12	27.95	564.03
52	bank	2941.94	1575.50	0.96	21.53	1003.06
54	bank	2959.98	1755.47	0.91	22.54	1197.83
56	bank	3206.65	1777.02	1.47	22.46	1203.74
57	forest	2869.81	1189.68	0.95	18.39	1207.20
58	forest	2035.50	292.14	1.23	15.75	1046.23
59	bank	3641.37	2066.27	1.87	31.68	1091.43
60	bank	4132.90	3461.62	3.64	34.23	933.83
62	bank	3950.33	2127.19	3.34	31.85	1177.66
64	forest	2770.36	1588.66	2.49	26.92	1978.92
68	pasture	3329.45	2186.93	3.27	28.32	1654.51

Field #	Type	Rb	S	Si	Sr	Ti
1	path	195.83	186.80	373083.33	33.42	3275.00
2	path	130.50	349.17	574666.67	37.37	2633.33
3	path	231.50	239.77	575000.00	41.88	2447.17
4	pasture	269.67	235.55	529833.33	51.17	2668.33
5	path	174.67	390.50	632000.00	38.62	1898.00
6	path	206.83	111.05	615833.33	40.03	2128.50
8	bank	214.33	286.67	612833.33	44.22	2499.83
9	path	166.00	338.17	621166.67	36.57	1990.33
13	pasture	223.33	190.75	647166.67	27.60	2212.33
14	path	342.46	1320.64	237844.49	120.65	1519.54
15	path	144.33	130.90	637666.67	26.77	2405.83
17	path	125.67	1000.33	649833.33	39.28	2336.67
18	pasture	90.50	827.67	586000.00	33.82	2185.33
19	bank	123.33	464.17	313000.00	47.07	2481.83
20	path	63.17	255.20	259683.33	34.50	1977.50
21	pasture	83.83	488.67	276166.67	36.27	1856.83
22	pasture	53.33	443.67	256333.33	37.55	1768.33
23	bank	138.17	477.00	347833.33	47.87	2181.00
24	bank	170.17	706.17	253600.00	44.37	1756.33
25	path	120.54	1537.27	239806.06	35.53	1642.47
26	pasture	73.70	211.35	795138.43	16.96	1659.90
28	pasture	138.67	1346.83	227966.67	30.82	2137.33
40	bank	157.42	809.54	751193.43	34.96	2393.64
41	bank	130.82	879.29	711348.38	32.52	2115.82
43	bank	127.11	1112.50	737828.38	30.04	1991.84
46	bank	135.43	183.02	719092.09	23.23	1766.05
47	bank	106.73	61.79	713171.79	20.28	1374.07
48	bank	122.37	170.16	726959.03	21.19	1499.70
49	bank	193.43	78.61	723540.39	27.68	1647.98
50	bank	250.50	61.09	719306.93	27.77	1802.97
52	bank	158.12	241.66	722133.42	21.89	1896.15
54	bank	203.33	254.88	686493.43	24.70	1966.57
56	bank	186.86	225.90	679008.69	26.29	2046.95
57	forest	187.73	294.38	705911.47	27.16	2227.26
58	forest	63.71	453.21	293720.64	33.12	1401.66
59	bank	97.56	169.08	314628.97	35.94	2028.40
60	bank	106.36	242.71	334333.80	38.78	1848.06
62	bank	133.92	117.10	314393.38	35.53	1850.03
64	forest	176.50	631.17	225723.51	39.82	2248.99
68	pasture	193.17	471.69	243067.30	40.22	2205.62

Field #	Type	V	Zn	Zr
1	path	90.32	113.52	114.33
2	path	56.40	95.63	123.02
3	path	68.72	89.45	128.22
4	pasture	87.00	100.63	106.63
5	path	56.62	93.45	117.60
6	path	84.73	57.55	130.15
8	bank	73.22	99.05	111.70
9	path	55.90	68.62	104.30
13	pasture	101.72	75.70	116.22
14	path	65.45	177.50	119.16
15	path	70.53	59.88	149.47
17	path	61.90	118.18	134.07
18	pasture	55.63	92.28	173.80
19	bank	61.02	76.63	152.95
20	path	43.58	67.10	150.30
21	pasture	47.55	79.22	246.67
22	pasture	41.98	63.25	82.65
23	bank	67.50	106.52	132.95
24	bank	65.67	131.98	112.35
25	path	59.19	394.60	99.70
26	pasture	37.91	104.78	88.91
28	pasture	76.13	255.85	98.98
40	bank	72.96	130.77	102.46
41	bank	69.77	133.04	110.08
43	bank	62.55	233.55	106.32
46	bank	63.63	159.05	108.22
47	bank	56.85	84.41	107.44
48	bank	56.25	178.83	100.38
49	bank	60.69	58.98	120.30
50	bank	67.72	66.50	125.74
52	bank	53.10	129.46	93.57
54	bank	55.31	178.00	108.34
56	bank	57.00	157.56	117.24
57	forest	53.88	118.29	92.16
58	forest	32.05	69.97	166.79
59	bank	74.17	161.62	208.03
60	bank	76.68	99.33	168.13
62	bank	81.62	144.52	213.27
64	forest	61.26	160.91	187.27
68	pasture	65.37	157.59	148.63

Appendix 7: Nitric Acid Extraction (HNO_3) Element Concentrations

Averaged from replicates for each sample and shown in mg kg^{-1} for Oostanaula Creek watershed

Field #	Type	Al	Ba	Ca	Cd	Co
1	path	17734.26	136.81	1339.14	0.68	16.96
2	path	12546.18	160.42	2821.20	0.75	15.49
3	path	13660.32	172.42	1964.50	0.94	15.52
4	pasture	14166.90	147.96	1779.10	0.91	14.56
5	path	10704.08	154.74	2662.84	0.71	15.43
6	path	12356.84	108.29	1935.21	0.57	12.51
8	bank	15661.95	209.42	2235.62	0.76	16.86
9	path	13194.76	192.70	2640.11	0.65	17.64
13	pasture	19293.61	99.63	1606.20	0.73	9.55
14	path	12848.49	138.39	37143.33	0.72	20.46
15	path	13276.08	55.25	1797.19	0.56	11.94
17	path	15060.25	47.81	3488.83	0.53	9.40
18	pasture	10825.77	34.82	1918.09	0.41	7.34
19	bank	13209.26	74.36	3567.70	0.55	15.00
20	path	10726.49	57.84	2115.40	0.41	8.67
21	pasture	8206.18	32.67	2232.90	0.43	6.53
22	pasture	9788.09	59.66	1364.02	0.37	7.55
23	bank	10873.75	164.14	1519.75	0.49	13.46
24	bank	13921.69	230.03	3071.12	0.66	18.74
25	path	17370.58	223.64	3709.81	0.69	10.66
26	pasture	13223.57	97.37	1095.81	0.46	10.28
28	pasture	30850.20	183.19	1395.10	0.74	12.41
40	bank	15292.64	90.74	1357.11	0.57	10.22
41	bank	13678.33	83.21	817.14	0.49	9.40
43	bank	16002.21	111.58	2127.26	0.89	13.63
46	bank	15972.08	159.08	1697.61	0.85	17.20
47	bank	16582.27	96.95	1103.11	0.58	14.24
48	bank	15377.55	116.69	2275.71	0.87	14.65
49	bank	15928.47	105.08	1309.31	0.57	9.68
50	bank	15248.65	79.28	1506.52	0.56	12.32
52	bank	15919.31	137.57	2898.58	0.89	15.07
53	crop	16896.96	149.94	1170.20	0.60	12.51
54	bank	15788.29	135.72	3726.21	1.06	26.18
56	bank	14786.83	132.37	3439.61	0.96	22.22
57	forest	17397.54	107.74	4028.37	0.87	18.32
58	forest	7846.19	54.38	2031.52	0.38	10.68
59	bank	15183.20	106.49	2216.49	0.87	20.14
60	bank	13118.16	123.31	2832.10	0.64	19.91
62	bank	12660.71	101.06	2006.73	0.77	19.44

Field #	Type	Cr	Cu	Fe	Hf	K
1	path	15.01	25.49	23670.54	9.50	954.34
2	path	13.67	69.16	20597.23	9.90	1304.89
3	path	13.19	42.44	30120.03	10.89	1098.41
4	pasture	13.21	44.84	30969.56	10.89	1053.61
5	path	10.83	44.86	22420.63	11.50	1039.37
6	path	10.91	63.44	21104.13	10.17	1008.24
8	bank	16.85	60.03	25754.17	10.67	1694.62
9	path	13.08	94.70	21313.65	15.70	1523.59
13	pasture	18.40	11.37	30394.11	10.65	2459.90
14	path	12.15	25.05	23697.40	11.37	2644.07
15	path	9.34	9.97	20820.99	10.44	1789.80
17	path	12.19	11.12	20318.30	6.99	1289.97
18	pasture	8.94	6.71	14524.69	6.25	964.86
19	bank	15.08	12.37	20671.04	7.02	971.45
20	path	8.10	10.29	13088.40	7.01	923.25
21	pasture	8.57	12.22	14917.46	7.10	926.56
22	pasture	7.66	11.03	10563.78	6.10	1151.60
23	bank	11.04	11.10	17101.59	7.12	939.01
24	bank	14.69	52.67	24550.24	7.12	928.62
25	path	16.21	16.05	19653.74	6.98	1643.19
26	pasture	9.70	43.18	14285.86	7.10	832.64
28	pasture	13.86	18.61	25266.54	8.01	1427.47
40	bank	12.17	8.22	22374.19	2.74	845.42
41	bank	10.94	8.61	19812.06	2.26	705.01
43	bank	14.72	32.20	21003.56	4.87	953.62
46	bank	14.97	16.41	25299.20	3.44	859.33
47	bank	14.07	7.11	20938.76	5.14	856.44
48	bank	15.12	25.24	22786.65	1.71	902.79
49	bank	10.56	6.85	23948.67	1.52	718.47
50	bank	11.16	9.34	23053.13	3.72	807.48
52	bank	14.63	14.75	21920.06	4.55	852.05
53	crop	10.86	10.06	16933.60	4.48	1008.43
54	bank	22.46	44.46	27216.61	11.23	855.92
56	bank	18.06	20.69	25586.41	11.28	977.22
57	forest	17.43	20.22	26838.96	10.66	1266.35
58	forest	8.34	13.77	8741.66	10.71	757.82
59	bank	16.72	22.08	27279.41	9.36	888.17
60	bank	14.28	11.18	22830.78	10.62	1141.25
62	bank	14.37	14.24	22980.38	11.16	798.71

Field #	Type	La	Li	Mg	Mn	Mo
1	path	26.32	5.73	732.16	2954.10	0.88
2	path	25.53	5.45	1229.63	2286.13	0.83
3	path	27.48	5.67	1021.53	2587.95	0.97
4	pasture	24.51	5.83	1028.99	2572.81	0.96
5	path	23.38	4.16	986.57	2160.06	0.72
6	path	14.86	6.79	1058.92	785.98	0.78
8	bank	22.30	12.46	1315.08	1962.48	0.78
9	path	23.79	8.46	1212.69	1684.90	0.59
13	pasture	12.21	10.66	1588.63	396.62	1.09
14	path	15.20	15.15	6271.11	2731.85	0.81
15	path	17.41	6.57	1065.00	779.12	0.70
17	path	11.87	8.96	1491.36	440.77	0.81
18	pasture	9.25	6.03	908.51	234.53	0.57
19	bank	16.71	7.28	1211.95	1025.35	0.79
20	path	16.49	4.48	826.52	810.20	0.62
21	pasture	10.67	3.97	840.31	298.86	0.62
22	pasture	10.65	5.24	929.86	576.31	0.54
23	bank	12.44	6.56	764.54	1124.02	0.60
24	bank	18.95	9.26	1029.65	2459.35	0.89
25	path	15.44	8.86	1124.83	1115.47	0.94
26	pasture	19.44	6.80	648.62	717.94	0.67
28	pasture	33.45	9.35	978.73	3182.43	1.04
40	bank	17.30	7.36	800.84	1136.10	0.80
41	bank	12.72	6.05	611.51	1085.67	0.62
43	bank	15.20	9.37	934.63	929.92	0.78
46	bank	16.39	8.72	837.63	2177.81	0.88
47	bank	16.94	8.23	837.79	2068.02	0.83
48	bank	13.58	8.85	1014.11	1988.64	0.80
49	bank	13.81	6.95	627.34	1536.68	0.64
50	bank	11.73	8.24	733.07	1367.72	0.65
52	bank	16.92	9.32	1097.68	1735.81	0.82
53	crop	25.46	6.75	705.90	2923.48	0.54
54	bank	21.40	12.64	1244.66	2160.07	0.86
56	bank	19.17	13.23	1352.66	2064.86	0.85
57	forest	17.04	13.83	1329.79	1480.66	0.90
58	forest	12.52	6.37	846.06	244.06	0.40
59	bank	21.88	12.10	1110.22	1801.75	0.90
60	bank	19.42	8.66	1184.18	2636.79	0.77
62	bank	16.59	11.65	996.72	1724.89	0.63

Field #	Type	Na	Nd	P	S	Si
1	path	90.27	31.83	568.62	136.98	166624.83
2	path	105.64	31.51	1480.36	357.44	183862.16
3	path	88.94	34.63	1870.27	209.02	200245.84
4	pasture	85.59	32.14	1740.83	177.01	218976.49
5	path	101.37	33.99	1836.19	386.26	233409.33
6	path	94.58	25.11	541.70	78.99	188164.81
8	bank	97.85	30.79	1535.85	230.16	197443.44
9	path	241.71	40.23	1501.93	340.02	309539.05
13	pasture	93.99	20.82	553.55	137.40	194799.42
14	path	234.97	22.26	2233.59	717.96	128164.72
15	path	104.04	28.41	650.50	119.60	198317.52
17	path	76.92	18.88	814.53	316.61	217252.66
18	pasture	69.37	16.17	489.24	219.82	212354.72
19	bank	83.38	24.50	872.46	264.00	233151.11
20	path	76.95	25.34	722.83	280.83	189154.11
21	pasture	76.37	19.12	847.95	369.22	191240.39
22	pasture	73.48	16.36	568.31	267.35	153214.65
23	bank	71.65	19.92	708.03	248.82	169834.68
24	bank	72.56	24.20	710.98	231.60	187681.72
25	path	75.33	20.98	1355.84	417.54	157381.26
26	pasture	74.24	26.78	551.96	237.67	193778.89
28	pasture	80.26	45.23	1117.50	368.36	155192.19
40	bank	72.50	13.72	332.70	58.33	149904.46
41	bank	66.37	9.25	219.12	45.99	151543.49
43	bank	69.22	15.45	684.58	223.57	195219.64
46	bank	63.51	13.39	456.05	144.30	176003.01
47	bank	66.51	17.56	228.58	60.18	160038.47
48	bank	72.68	7.28	527.65	158.41	194010.34
49	bank	68.61	9.80	240.09	57.66	161357.16
50	bank	74.74	12.16	242.07	54.52	230598.45
52	bank	68.89	16.20	799.32	269.00	275738.76
53	crop	64.77	23.95	852.68	164.45	231904.99
54	bank	98.34	30.17	955.29	221.40	298823.56
56	bank	97.69	28.78	908.55	178.81	188481.34
57	forest	99.29	25.57	978.56	246.89	208560.65
58	forest	114.75	24.07	666.88	377.47	258202.10
59	bank	94.39	24.46	817.83	147.63	185706.27
60	bank	89.76	27.93	549.76	189.28	197897.11
62	bank	92.55	27.28	687.77	118.72	247260.81

Field #	Type	Sr	Ti	V	Zn	Zr
1	path	4.61	56.83	95.87	40.87	6.88
2	path	7.32	48.95	87.90	69.62	6.69
3	path	6.84	33.40	94.23	55.72	6.50
4	pasture	6.80	28.08	97.38	51.88	5.80
5	path	7.10	39.85	101.49	61.93	4.66
6	path	7.03	14.63	103.31	27.36	2.89
8	bank	9.99	21.18	95.69	73.08	5.70
9	path	8.72	30.17	139.57	60.90	4.75
13	pasture	5.01	11.00	103.84	43.34	3.73
14	path	59.43	19.65	59.83	88.93	5.55
15	path	5.60	9.42	90.51	41.74	3.81
17	path	7.57	8.87	98.39	47.71	4.89
18	pasture	4.88	8.14	93.42	35.25	3.68
19	bank	9.57	9.82	98.44	53.67	4.50
20	path	5.38	14.00	67.74	38.96	3.92
21	pasture	7.03	10.83	62.92	58.42	4.15
22	pasture	3.60	10.65	58.86	35.05	2.59
23	bank	5.67	10.56	65.80	46.59	3.60
24	bank	10.25	14.57	79.15	58.19	4.24
25	path	11.64	61.18	85.41	127.50	7.87
26	pasture	3.86	45.46	94.28	64.97	4.99
28	pasture	5.58	114.42	105.82	92.71	10.48
40	bank	4.92	15.79	99.46	35.16	2.84
41	bank	3.78	16.22	104.41	28.82	2.13
43	bank	5.28	20.36	110.34	115.40	4.72
46	bank	5.58	20.80	109.26	91.37	4.26
47	bank	5.14	19.31	109.21	40.54	2.46
48	bank	5.24	22.27	114.02	107.83	4.26
49	bank	6.42	18.79	104.10	24.40	2.62
50	bank	6.33	11.40	106.27	29.41	1.74
52	bank	7.64	15.91	109.24	89.21	3.78
53	crop	3.53	52.26	109.50	57.91	4.97
54	bank	9.71	23.62	111.93	148.32	4.68
56	bank	9.57	28.47	110.46	118.00	6.19
57	forest	11.15	23.01	109.74	95.69	6.66
58	forest	6.77	15.01	122.35	43.66	1.03
59	bank	7.02	20.28	110.32	111.06	5.17
60	bank	8.48	14.59	111.46	51.35	3.99
62	bank	5.80	18.00	112.41	77.37	3.13

CHAPTER 4: EVALUATION OF NITRIC ACID EXTRACTION OF ELEMENTS FROM SOIL AND SEDIMENTS FROM TWO WATERSHEDS IN EAST TENNESSEE

Abstract

The commonly used total dissolution method determines the total elemental concentrations in soils. However, this procedure is tedious and risky due to the use of dangerous reagents, such as HF (hydrofluoric acid). This study evaluates a single acid extraction technique for evaluating the total elemental concentrations in soils and sediments. We compared a nitric acid (HNO_3) extraction method to total dissolution (HF + microwave assisted *aqua regia*). The methods were used to analyze the elemental content of soils and sediments from two watersheds (Oostanaula Creek and Pond Creek) in east Tennessee. Twenty one major and trace elements (Al, Ba, Ca, Co, Cr, Cu, Fe, K, La, Li, Mg, Mn, Nd, P, S, Si, Sr, Ti, V, Zn, and Zr) were subsequently measured using inductively coupled plasma optical emission spectrometry (ICP-OES). The extraction efficiency for HNO_3 relative to the total were compared and discussed. In general, HNO_3 can extract the elements in absorbed phases and those residing in non-silicate minerals. Correlations were also investigated for each element between the two digestion procedures. Finally, the elements were grouped according to the interrelationships of their total elemental concentrations.

Introduction

Acid extraction and total dissolution methods have been used for sample preparation prior to the determination of elemental concentrations in soils. The digestion procedure can greatly influence the determination of soil elemental content, as differing digestion or dissolution methods can release differing quantities of elements (Gaudino et al., 2007). Single acid (e.g., HNO_3) extraction treats a soil sample with one reagent only, while total dissolution may involve the sequential or combined treatment of a soil sample with a series of strong and weak acids (Ammons et al., 1995).

The primary advantage for total dissolution over the use of single acid extraction is the complete decomposition of the soil and the unambiguous measure of total metal levels (Burt et al., 2000; McGrath, 1998; Nakashima et al., 1988; Sanchez et al., 1998). A comparative study of HNO_3 extraction and total digestion methods for determining the elemental content in peat material illustrated the general efficiency of concentrated HNO_3 extraction in the characterisation of Cu, Pb, and Zn. However total digestion was favored for characterizing Al, Ti, Co, Cr, and V (Yafa and Farmer, 2006).

A major limitation to the total dissolution of soil is the use of dangerous reagents, e.g., HF. A single strong acid extraction has numerous advantages relative to total dissolution, including simple reagent preparation, less tedious and safer, smaller solution-to-solid dilution factor, and reduced corrosion to analytical instrumentation. Chang et al. (1984) developed a method by using 4M HNO_3 to investigate the accumulation of trace metals in sewage sludge-amended soils. They reported that 70 to 80% of metals (Cd, Cr, Cu, Ni, Pb, and Zn) were extracted. Limited emphasis has been

placed on evaluating this extraction technique in quantifying the elemental content of soil. The goals of this work were to determine the total elemental concentrations for the soils and suspended sediment in the Oostanaula Creek (OC) and Pond Creek (PC) watersheds in east Tennessee and to compare their values to HNO_3 extractable contents.

Materials and Methods

Study Area

Oostanaula Creek (OC) and Pond Creek (PC) watersheds encompass 18,156 and 9,542 hectares in Loudon, Monroe and McMinn counties nestled within the Valley and Ridge physiographic region of east Tennessee. These sampling areas were selected due to their representation of the typical region that occupies the primary geology of the Appalachian Mountains in the eastern United States. Oostanaula Creek is a tributary of the Hiwassee River watershed of southeastern Tennessee, southwestern North Carolina, and Northeastern Georgia. Pond Creek is a sub-watershed within the Watts Bar/Fort Loudoun watershed. Most of the topography of OC and PC consists of low rolling ridges and valleys with a few steep ridges. Both OC and PC watersheds are comprised primarily of agricultural land, which includes pasture (forage) and row crops that support local dairy and beef cattle operations (Walker, 2006, 2007).

Soil Properties

Most of the soils in OC and PC are derived from bedrock, consisting of Quaternary cherty clay solution residuum and Ordovician dolomite and limestone. Soils of the two regions are primarily in the order Ultisols and of the series of Bodine (loamy-skeletal, siliceous, semiactive, thermic Typic Paleudults), Decatur (fine, kaolinitic, thermic Rhodic Paleudults), Dewey (fine, kaolinitic, thermic Typic Paleudults), Fullerton (fine, kaolinitic, thermic Typic Paleudults), Steekee (loamy, parasesquic, thermic, shallow

Ruptic-Ultic Dystrudepts), Tellico (fine, parasesquic, thermic Typic Rhodudults), and the Waynesboro (fine, kaolinitic, thermic Typic Paleudults) (USDA, 1973, 2004).

Sample Collection and Processing

A detailed list of sampling sites and relevant site information for OC (include GPS coordinates and descriptions of sampling sites) were recorded and listed in Table A. 2.2 (Appendix 2: Tables in Chapter 2), and include cattle paths, stream banks, cropland, forested areas, and construction sites. Sampling information for PC could be accessed from the Appendices in Hull (2008). At each sampling site, the top 1-2 cm of soil was collected, mixed, and stored in paper bags. The collected soil samples were air-dried and disaggregated using a mortar and pestle. The soils were then wet-sieved through a 53 μm sieve. The <53μm suspensions were then freeze-dried using a Laboconco Freezone 4.5 and stored until needed.

Total Dissolution

All chemicals used in the extractions were of analytical grade or better and solutions were prepared in > 18 Ω distilled-deionised (DDI) water. Total dissolution was performed using a modified method of Bernas (1968) (Ammons et al., 1995; ISO, 2012). Soil samples (200 mg) were placed in 50 mL polyallomer Oak Ridge type centrifuge tubes. To each tube was added 15 mL of HF. The mixture was left to react for 16 hours at room temperature. Then, 5 mL aqua regia (3:1:1 $HCl:HNO_3:H_2O$) was added to the sample mixture and stirred with a vortex mixer. The tubes were then heated in a microwave oven (800 W) for 3 min at 80% power. After cooling, 1 g boric acid

was added and the tubes heated at 20% power for 10 min in the microwave oven. After cooling, the solution was transferred to a 100-mL volumetric flask and brought to volume with DDI water. The solution was then filtered through a Whatman 42 (>2.5μm) filter and stored for analysis.

Nitric Acid Extraction

Nitric acid (HNO_3) digestion is based on the protocol for characterizing sewage sludge-amended soil (Chang et al., 1984). Soil samples (3.5 g) were placed in 40 mL glass tubes with 21 mL of 4M HNO_3. The tubes were capped with glass funnels and refluxed at 70°C for 16 hours. After cooling, DDI water was added to the tubes to bring the volume to 35 mL and mixed. The suspension was then filtered through a Whatman 42 (>2.5μm) filter and stored for analysis.

ICP-OES Measurements

A Spectro CIROS inductively coupled plasma optical emission spectrometry (ICP-OES) (Fitchburg, MA) was employed to determine the total elemental content of the dissolved and extracted samples. The samples were analyzed for 22 elements (Al, Ba, Ca, Co, Cr, Cu, Fe, K, La, Li, Mg, Mn, Nd, P, S, Si, Sr, Ti, V, Zn, and Zr). The order of sample analysis was randomized for quality assurance/quality control (QA/QC). International organization for standardization (ISO) certified standards were used to calibrate the instrument (VHG Labs, Inc.). The instrument was recalibrated every 10 samples. Each sample was analyzed in triplicate and ensured with a coefficient of

variation (% CV) less than 10%. Recalibration was also triggered when the % CV in the ICP-OES response in any element exceeded 20%.

Statistical Analyses

The data were summarized for the two watersheds using mean and standard deviation values. Heterogeneity of the soils in the watershed was also measured with the % CV. The extraction efficiency of HNO_3 was evaluated as an average ratio by dividing HNO_3-ex content by the total.

The Pearson correlation coefficient, r value, was used to evaluate the significance of the correlation (p = 0.05) between HNO_3-ex and total. To visually assess the relationship between total and HNO_3-ex, a set of scatter diagrams were constructed using data from the two watersheds and Sigma Plot V12.5. The elements with significant correlation ($|r| > 0.3$) were further assessed with a linear model. The coefficient of determination (r^2) was used to establish the goodness of fit. The elements with significant correlation between total and HNO_3 in both OC and PC, their extractabilities (slopes of the linear model) were compared between two watersheds based on Student's t-test for assessing whether there was significant difference. The dendrograms (JMP Pro, V13.2) were utilized to group the elements and explore elemental associations.

Results and Discussion

The elements in soils reside in a variety of mineral phases, in addition to organic and adsorbed phases. Typically, a fraction of these phases are extracted by HNO_3. For example, metals in silicate minerals and occurring as inclusions in silicate phases may not be extracted by HNO_3. On the other hand, elements that reside in non-silicate, such as carbonates, oxides, and adsorbed may be susceptible to HNO_3. Thus, elements that show a strong correlation between total and HNO_3-ex may principally reside in non-silicate phases.

There were 21 elements reported in this study. Means and standard deviations of elemental contents by HNO_3-ex and total were compared with median of uncontaminated soils (Table 4.1). Arithmetic means of total elemental concentrations were within the ranges and generally lower than their medians in uncontaminated soils. Exceptions to this were Co, Cu, and Li in OC and Co, Cr, Cu, and Li in PC, whose mean values significantly exceeded uncontaminated soil median values. Particularly, because sampling areas between PC and OC were different and more samples were collected from the deposited areas in PC, the average concentration of total Chromium was relative higher in PC than both OC and uncontaminated soils. Further, for all the elements the mean total was higher than the means by HNO_3-ex for both watersheds. Regarding total elemental heterogeneity in the two watersheds, elemental variability was moderately to highly variable, with a % CV values >16% (Table 4.2). Higher variability with % CV values exceeding 50% was observed for Ca, Mn, P, S, and Zn in OC, Cr, Cu, Mn, Nd, and P in PC.

The extraction efficiency of HNO_3 in the two watersheds are presented in Table 4.2. Elements that are above 80% extractable by HNO_3 are Co, Mn, and Nd in OC, and Ca, Co, Cu, Fe, Mn, P, and Zn in PC. Elements that are below 30% extractable by HNO_3 are K, Li, Mg, Ti, Sr, and Zr, and K, Ti, and Zr in PC. The elements Ti and Zr exhibit the lowest HNO_3 extraction efficiency in both OC and PC. Sulfur was partially extracted by HNO_3 because more than 90% of sulfur is in soil organic matter (SOM) (Essington, 2015).

In general, the concentrations elements that were efficiently extracted by HNO_3 were significantly correlated with their total concentrations. These HNO_3-ex elements generally do not reside in the silicate matrix, not as an isomorphic substituted element in that silicate or not included inside the silicate minerals (Essington, 2015). Pearson correlation coefficients (r values) for each element are summarized in Table 4.2. These data were paired with a significance test on correlation ($|r| > 0.3$) between total and HNO_3 were used to determine a linear regression model to relate HNO_3-ex to the total content (Figures 4.1 (a) to 4.1(f)).

Six elements (Ba, Co, Fe, Ca, Mn, and P) generated significant correlations between total and HNO_3 in both OC and PC watersheds. Another interesting finding is the differing correlation between the two watersheds. More soil samples were collected from deposited areas (e.g., drainage ditches) in PC than OC. Thus, the two watersheds underwent different sampling processes, which apparently lead to differing elemental distributions in soils. Based on the Student's t-test, there was no significant difference in HNO_3 extractabilities for elements of Ba, Fe, Ca, and P between OC and PC.

Exceptions to this were Co and Mn.

Total elements can be classified into sub-groups according to their mineralogical origin, elemental cycling processes, and geochemical processes during soil formation (Ma et al., 2011). The interactions between elements may suggest a pattern of the elemental association in soil sampling (Landajo et al., 2004). Trace elements are commonly linked to major elements, such as Al, Fe and Mn within the same geochemical matrix of sediments (Liu et al., 2003). To this end, the total elemental data were subjected to statistical analysis and a dendrograms were produced to examine the geochemical association among the major and trace elements (Einax et al., 1997). The elements can be classified into six groups (Table 4.3), based on their similarity and clustering, as indicated in the dendrograms (Figure 4.2).

Summary

We evaluated the HNO_3 procedure in determining the major and trace elemental concentrations for soils from two watershed in east Tennessee. Many of the elements can be effectively dissolved by HNO_3, but the extractant does not provide a total dissolution of the soil matrix. The elements can be efficiently extracted by HNO_3 are presented in this study. This study also examined the correlations between HON3-ex and total metal contents of soils ($p < 0.05$). A linear model was developed to relate HNO_3-ex to the total content. The elemental data obtained also suggest interrelationships between elements are associated with their geochemical groupings.

Reference

Ammons, J., Essington, M., Lewis, R., Gallagher, A., and Lessman, G. (1995). An application of a modified microwave total dissolution technique for soils. Communications in Soil Science and Plant Analysis 26, 831-842.

Bernas, B. (1968). New method for decomposition and comprehensive analysis of silicates by atomic absorption spectrometry. Analytical Chemistry 40, 1682-1686.

Burt, R., Wilson, M. A., Mays, M. D., Keck, T. J., Fillmore, M., Rodman, A. W., Alexander, E. B., and Hernandez, L. (2000). Trace and major elemental analysis applications in the US cooperative soil survey program. Communications in Soil Science and Plant Analysis 31, 1757-1771.

Chang, A., Warneke, J., Page, A., and Lund, L. (1984). Accumulation of heavy metals in sewage sludge-treated soils. Journal of Environmental Quality 13, 87-91.

Einax, J. W., Zwanziger, H. W., and Geiss, S. (1997). Chemometrics in environmental analysis, John Wiley and Sons.

Essington, M. E. (2015). Soil and Water Chemistry: An Integrative Approach, CRC press.

Gaudino, S., Galas, C., Belli, M., Barbizzi, S., de Zorzi, P., Jaćimović, R., Jeran, Z., Pati, A., and Sansone, U. (2007). The role of different soil sample digestion methods on trace elements analysis: a comparison of ICP-MS and INAA measurement results. Accreditation and Quality Assurance 12, 84-93.

Hull, A. R. (2008). The Evaluation of a Chemical Fingerprinting Technique for Identifying the Sources of In-stream Sediments. Master's Thesis. The University of Tennessee.

ISO (2012). ISO 12914:2012. Soil quality -- Microwave-assisted extraction of the aqua regia soluble fraction for the determination of elements, pp. 7. ISO, ISO.

Kabata-Pendias, A. (2010). Trace elements in soils and plants, CRC press.

Landajo, A., Arana, G., de Diego, A., Etxebarria, N., Zuloaga, O., and Amouroux, D. (2004). Analysis of heavy metal distribution in superficial estuarine sediments (estuary of Bilbao, Basque Country) by open-focused microwave-assisted extraction and ICP-OES. Chemosphere 56, 1033-1041.

Liu, W., Li, X., Shen, Z., Wang, D., Wai, O., and Li, Y. (2003). Multivariate statistical

study of heavy metal enrichment in sediments of the Pearl River Estuary. Environmental Pollution 121, 377-388.

Ma, L., Jin, L., and Brantley, S. L. (2011). Geochemical behaviors of different element groups during shale weathering at the Susquehanna/Shale Hills Critical Zone Observatory. Applied Geochemistry 26, S89-S93.

Ma, L. Q., Tan, F., and Harris, W. G. (1997). Concentrations and distributions of eleven metals in Florida soils. Journal of Environmental Quality 26, 769-775.

McGrath, D. (1998). Use of microwave digestion for estimation of heavy metal content of soils in a geochemical survey. Talanta 46, 439-448.

Nakashima, S., Sturgeon, R. E., Willie, S. N., and Berman, S. S. (1988). Acid digestion of marine samples for trace element analysis using microwave heating. Analyst 113, 159-163.

Rao, C., Sahuquillo, A., and Sanchez, J. L. (2008). A review of the different methods applied in environmental geochemistry for single and sequential extraction of trace elements in soils and related materials. Water, Air, and Soil Pollution 189, 291-333.

Sanchez, J., Marino, N., Vaquero, M., Ansorena, J., and Legorburu, I. (1998). Metal pollution by old lead-zinc mines in Urumea River valley (Basque Country, Spain). Soil, biota and sediment. Water, Air, and Soil Pollution 107, 303-319.

United States Environmental Protection Agency (US EPA). 2002. Supplemental guidance for developing soil screening levels for superfund sites. Office of Solid Waste and Emergency Response, Washington, D.C. http://www.epa.gov/superfund/health/conmedia/soil/index.htm

USDA (1973). Soil survey of Monroe County, Tennessee, 99-104.

USDA (2004). Soil survey of McMinn County, Tennessee, 213-215.

Walker, F. (2006). Pond Creek Watershed Restoration Plan. University of Tennessee Extension Biosystems Engineering and Soil Science.

Walker, F. (2007). Oostanaula Creek Watershed Restoration Plan. University of Tennessee Extension Biosystems Engineering and Soil Science.

Yafa, C., and Farmer, J. G. (2006). A comparative study of acid-extractable and total digestion methods for the determination of inorganic elements in peat material by inductively coupled plasma-optical emission spectrometry. Analytica Chimica Acta 557, 296-303.

Appendix 8: Tables in Chapter 4

Table 4.1 Comparison of 21 elements in Oostanaula Creek and Pond Creek soils with uncontaminated soils collected worldwide

Element	Oostanaula Creek n=54		Pond Creek n=43		Median (Range) of
	Total	HNO_3	Total	HNO_3	Uncontaminated
Major		g kg^{-1}			Soils[a]
Al	52.5±17.7[b]	14.8±3.70	62.6±24.7	34±12.8	71 (10−300)
Ca	4.01±6.08	2.87±5.20	3.85±1.83	3.51±1.81	15 (0.7-500)
Fe	34.6±11.8	22.2±6.14	39±17.6	33.6±13.7	40 (2−550)
K	12.3±4.29	1.07±0.39	10.9±2.89	2.83±1.23	14 (0.08−37)
Mg	3.60±1.41	1.10±0.82	4±1.51	2.22±0.85	5 (0.4−9)
Mn	1.66±1.01	1.55±0.96	1.95±1.11	1.87±1.18	1 (0.02−10)
P	1.14±0.66	0.79±0.50	1.41±0.9	1.24±0.77	0.8 (0.035−5.3)
S	0.48 ±0.36	0.20 ±0.14	−	0.46±0.32	0.7 (0.03−1.6)
Si	466 ±213	190 ±38.9	207.3±25.9	−	330 (250−410)
Ti	2.05±0.37	0.03±0.02	2.23±0.54	0.52±0.33	5 (0.15−25)
Trace		mg kg^{-1}			
Ba	347 ±143	112 ±57	427±149	357±298	500 (100−3,000)
Co	15.5±5.10	13.8±4.70	18.3±6.28	16.4±6.18	8 (0.05−65)
Cr	38.7±10.3	12.7±3.10	350±581	28.4±11.5	70 (5−1,500)
Cu	80.4±27.6	22.8±18.5	113±57.8	96.7±48.9	30 (2−250)
La	48.8±18.6	17.2±7.20	40±18.1	24.8±13.9	40 (2−180)
Li	35.0±8.70	8.60±3.00	52.9±13.6	22.3±8.09	25 (3−350)
Nd	27.3±9.10	23.5±9.80	25±13.6	18.1±12.1	35 (4−63)
Sr	35.6±14.3	7.30±7.70	34.1±13	14.1±9.64	250 (4−2,000)
V	−	−	80.1±30.1	48.6±18.5	90 (3−500)
Zn	135 ±70.7	62.9±29.3	151±67.9	127±54.6	90 (1−900)
Zr	131 ±37.2	4.30±1.90	118±26.8	7.78±3.03	400 (60−2,000)

[a] Data are adapted from Bowen (1979).

[b] Mean ± standard deviation.

Table 4.2 Heterogeneity, HNO_3-extraction efficiency and r-value for 21 elements in Oostanaula Creek and Pond Creek soils

Element	Oostanaula Creek (n=54)				Pond Creek (n=43)			
	% CV		HNO_3-ex		% CV		HNO_3-ex	
	Total	HNO_3	Efficiency	r	Total	HNO_3	Efficiency	r
Al	34	25	30	0.30	38	38	56	0.78
Ba	41	51	33	0.56	35	83	76	0.72
Ca	152	181	68	0.70	46	52	**90**	0.95
Co	33	34	**91**	0.87	34	38	**94**	0.65
Cr	27	24	34	0.26 [a]	172	40	38	-0.18
Cu	34	81	30	0.25	83	51	**86**	0.92
Fe	34	28	67	0.84	43	41	**88**	0.90
K	35	37	9	0.09	26	44	26	0.65
La	38	42	40	0.08	45	56	65	0.52
Li	25	35	24	<0.01	25	36	43	0.55
Mg	39	74	29	0.37	36	38	58	0.70
Mn	61	62	**94**	0.96	56	63	**94**	0.96
Nd	34	42	**91**	0.53	54	67	70	0.80
P	58	63	66	0.97	60	62	**89**	0.98
S	76	67	63	0.25	–	71	–	–
Si	46	21	48	0.37	–	–	–	–
Sr	40	105	19	0.23	37	68	39	0.75
Ti	18	77	1	0.07	23	64	24	0.26
V	–	–	–	–	36	38	61	0.80
Zn	53	47	51	0.51	44	43	**86**	0.91
Zr	28	45	4	-0.20	22	39	7	0.23

[a] No significance correlated for HNO_3-ex relative to total if |r| value is less than 0.3 (bold number).

Table 4.3 Geochemical association for major and trace elements for Oostanaula Creek and Pond Creek soils in east Tennessee

	Oostanaula Creek	Pond Creek
Group 1	**Al**, **Fe**	**Al**, **Fe**
Group 2	Ba, Rb, Zr, Zn	Ba, Co, Nd, Li, Sr, La, V, Zr, Zn, Cr
Group 3	Co, Nd, Mo, Cr, Li, Sr, La, Cu, V	**Mg**, **Mn**, **P**, **Ti**
Group 4	**Mn**, **Ti**, **P**, Sr	**Ca**, **K**
Group 5	**Ca**, **K**, **Mg**	
Group 6	**Si**	

*Bold-faced are the major elements.

Appendix 9: Figures in Chapter 4

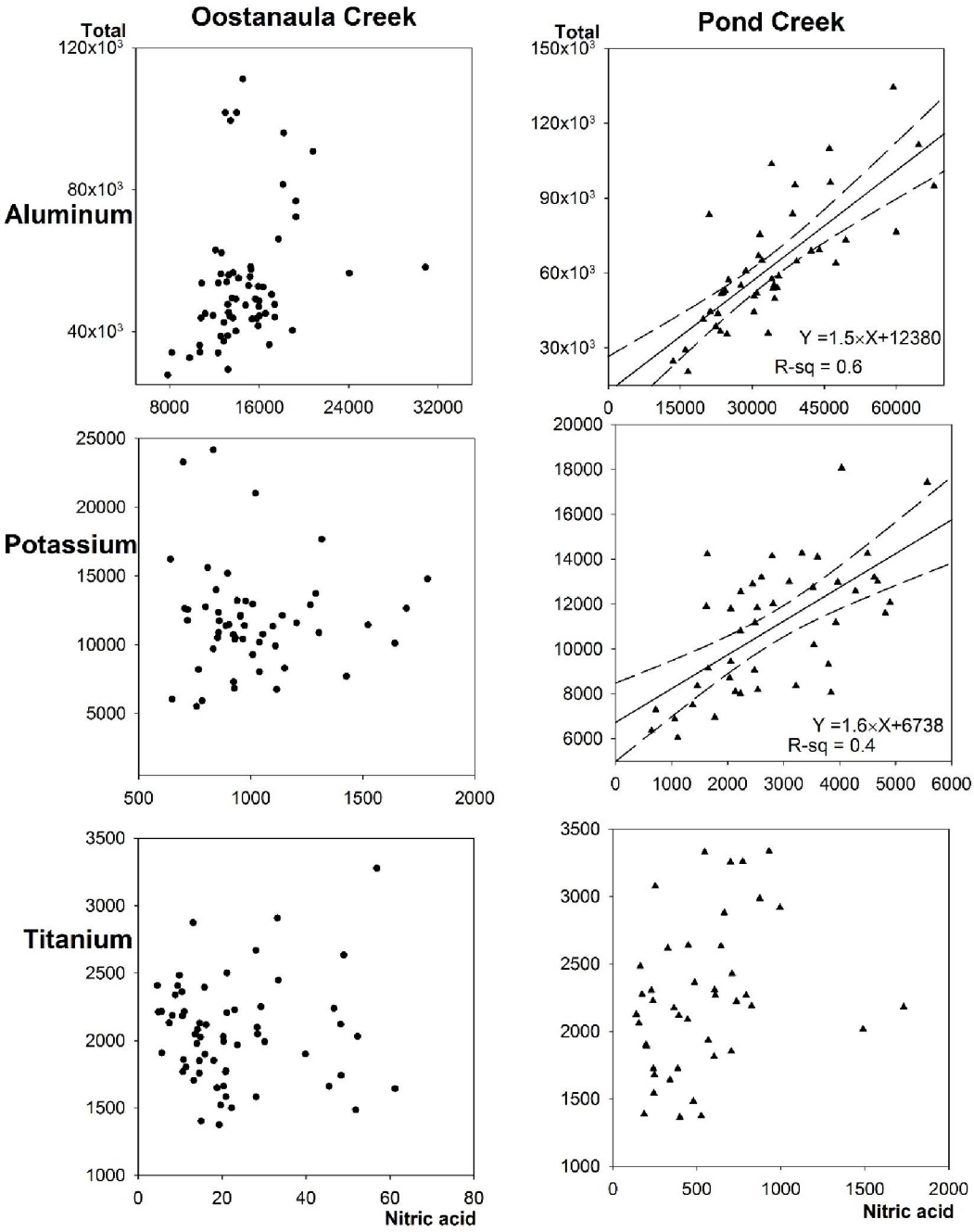


Figure 4.1 (a) Correlation and regression plots for Al, K, and Ti between total dissolution and nitric acid extraction for Oostanaula Creek and Pond Creek watersheds

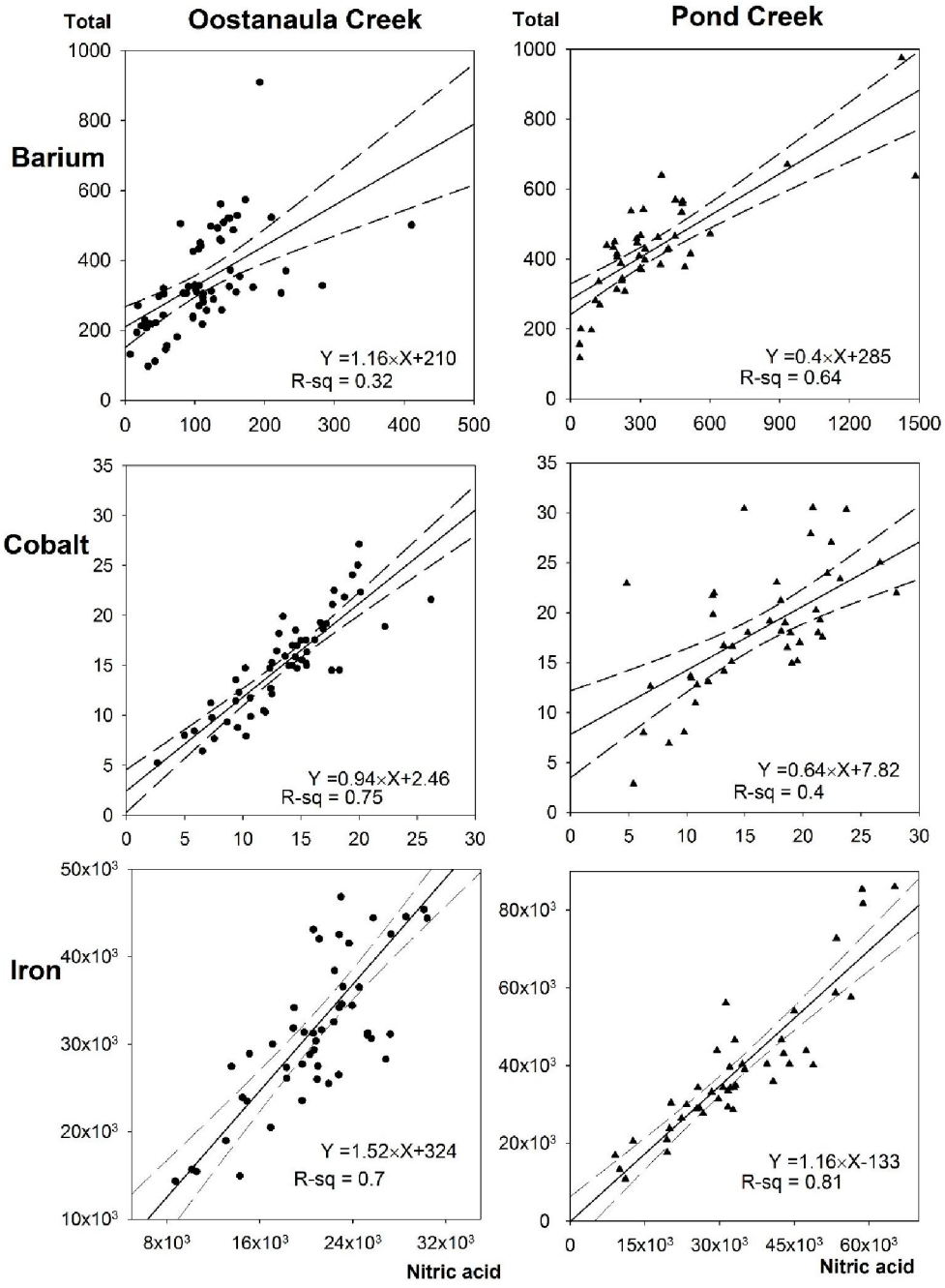


Figure 4.1 (b) Correlation and regression plots for Ba, Co, and Fe between total dissolution and nitric acid extraction in Oostanaula Creek and Pond Creek watersheds

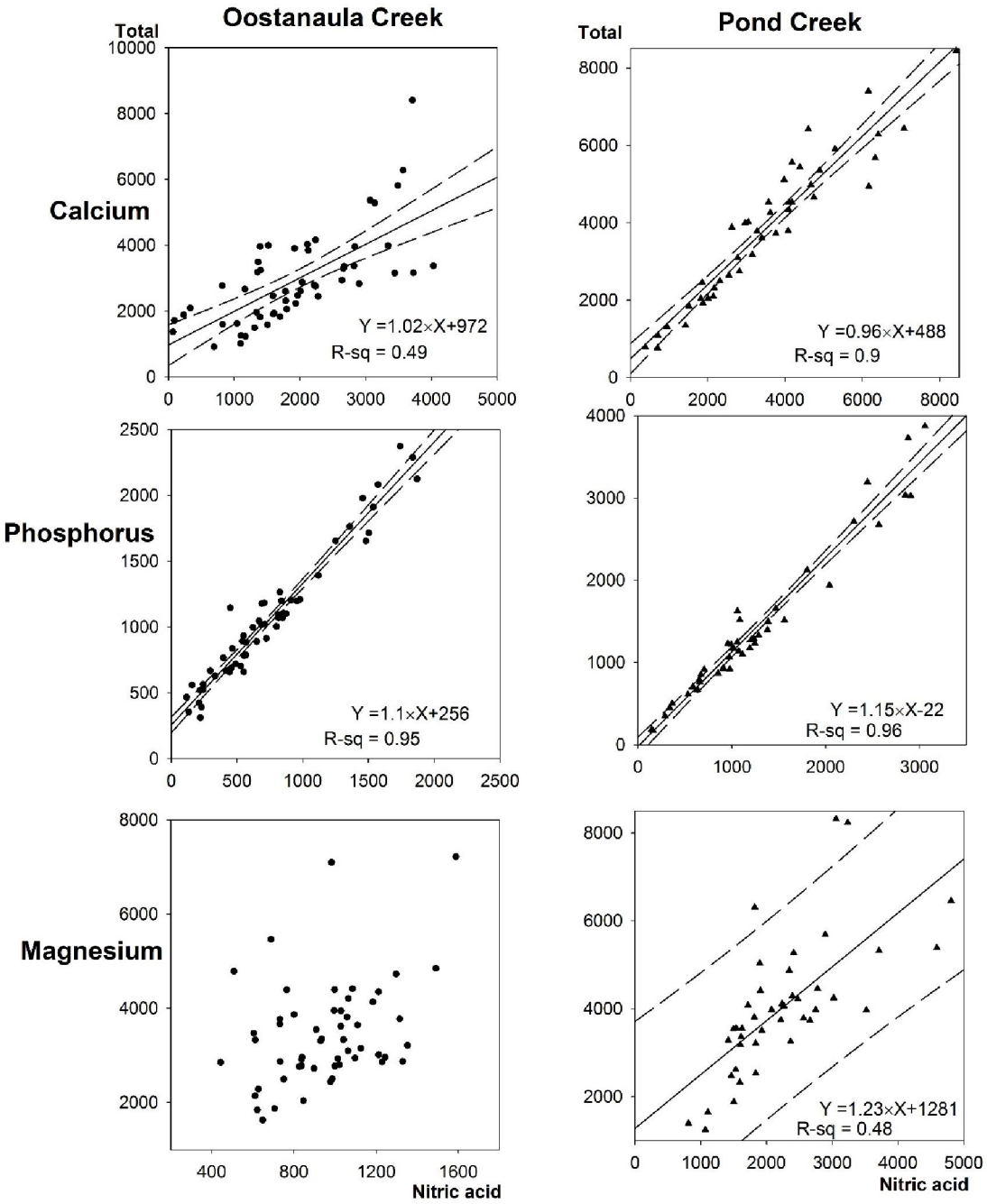


Figure 4.1 (c) Correlation and regression plots for Ca, P, and Mg between total dissolution and nitric acid extraction in Oostanaula Creek and Pond Creek watersheds

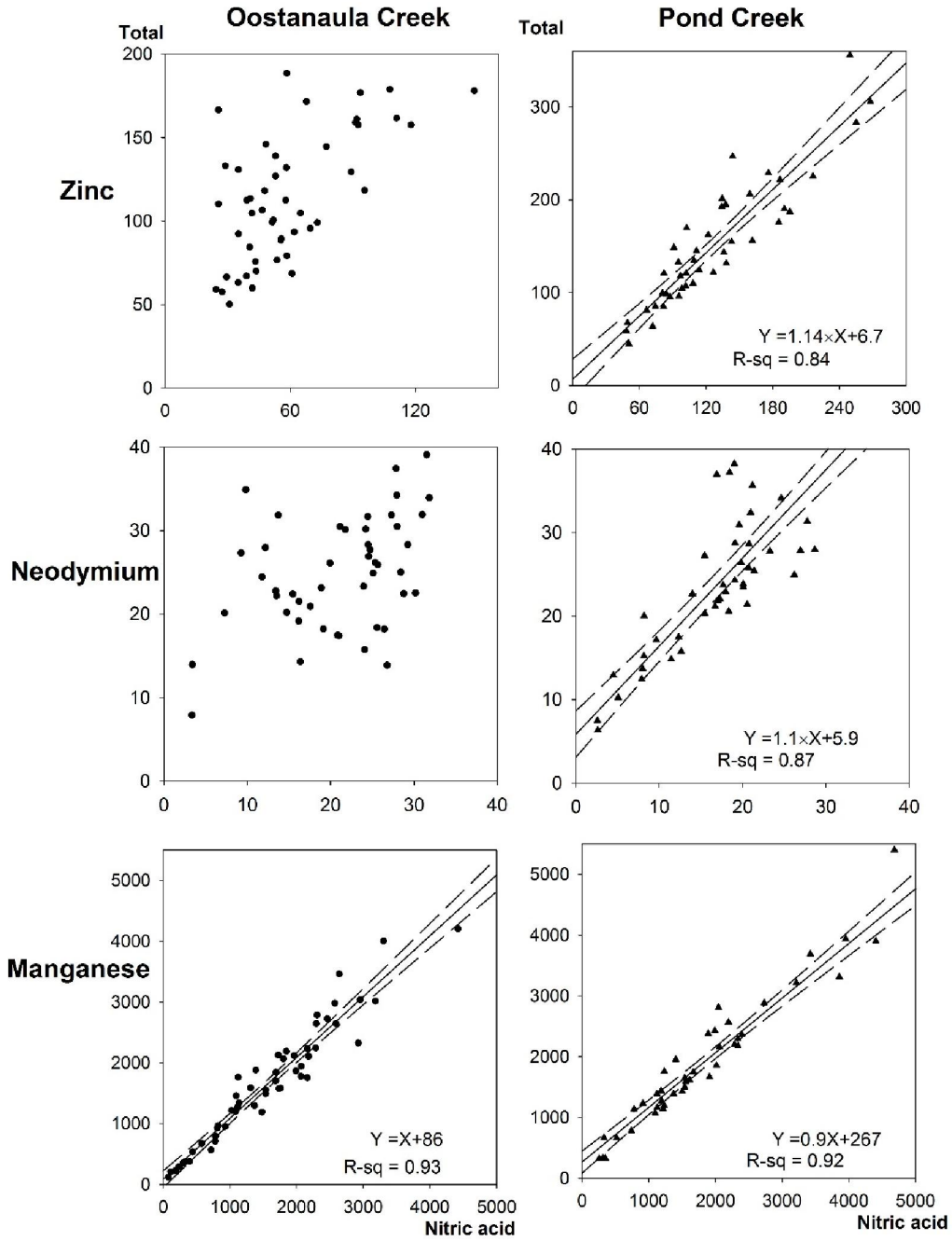


Figure 4.1 (d) Correlation and regression plots for Zn, Nd, and Mn between total dissolution and nitric acid extraction in Oostanaula Creek and Pond Creek watersheds

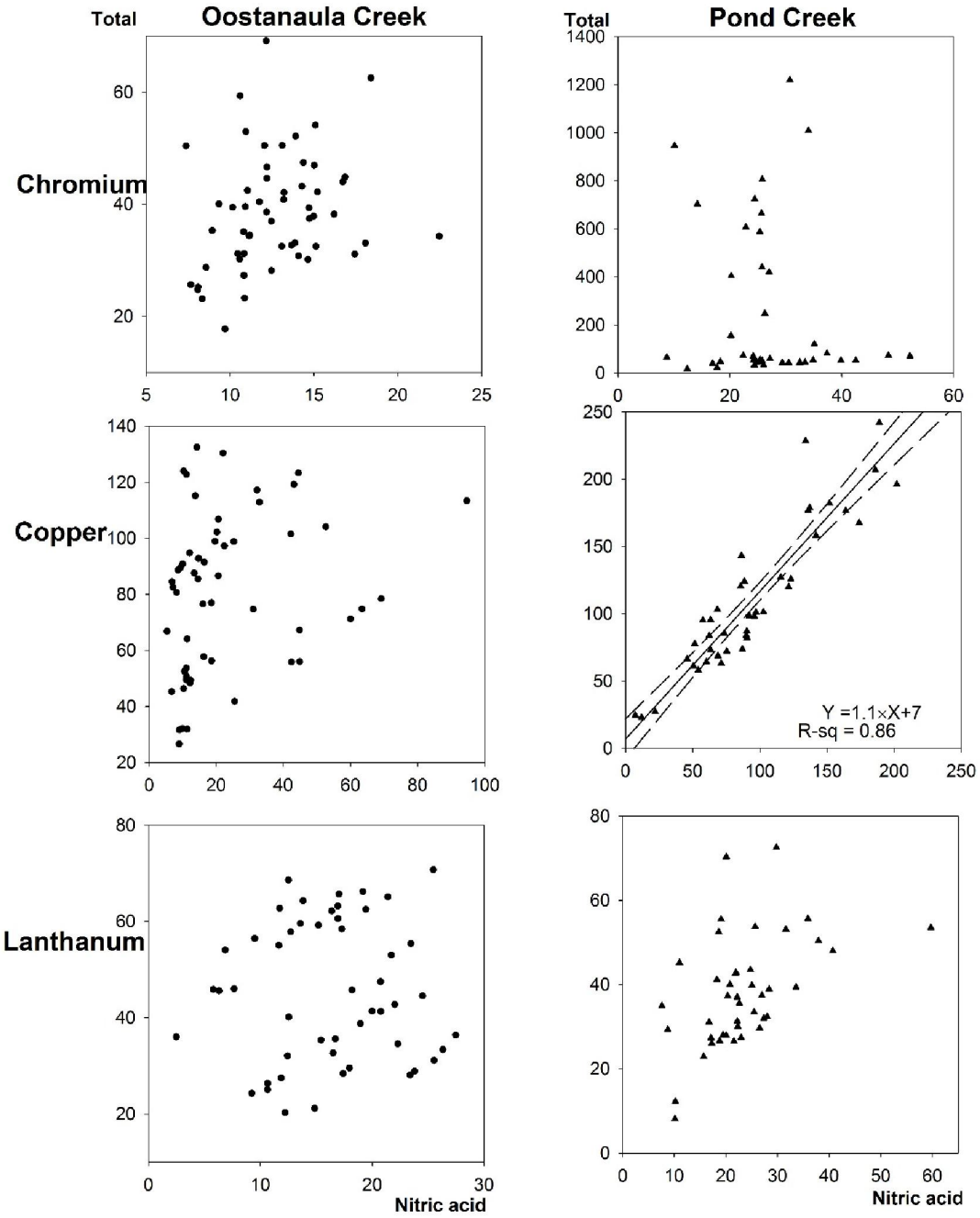


Figure 4.1 (e) Correlation and regression plots for Cr, Cu, and La between total dissolution and nitric acid extraction in Oostanaula Creek and Pond Creek watershed

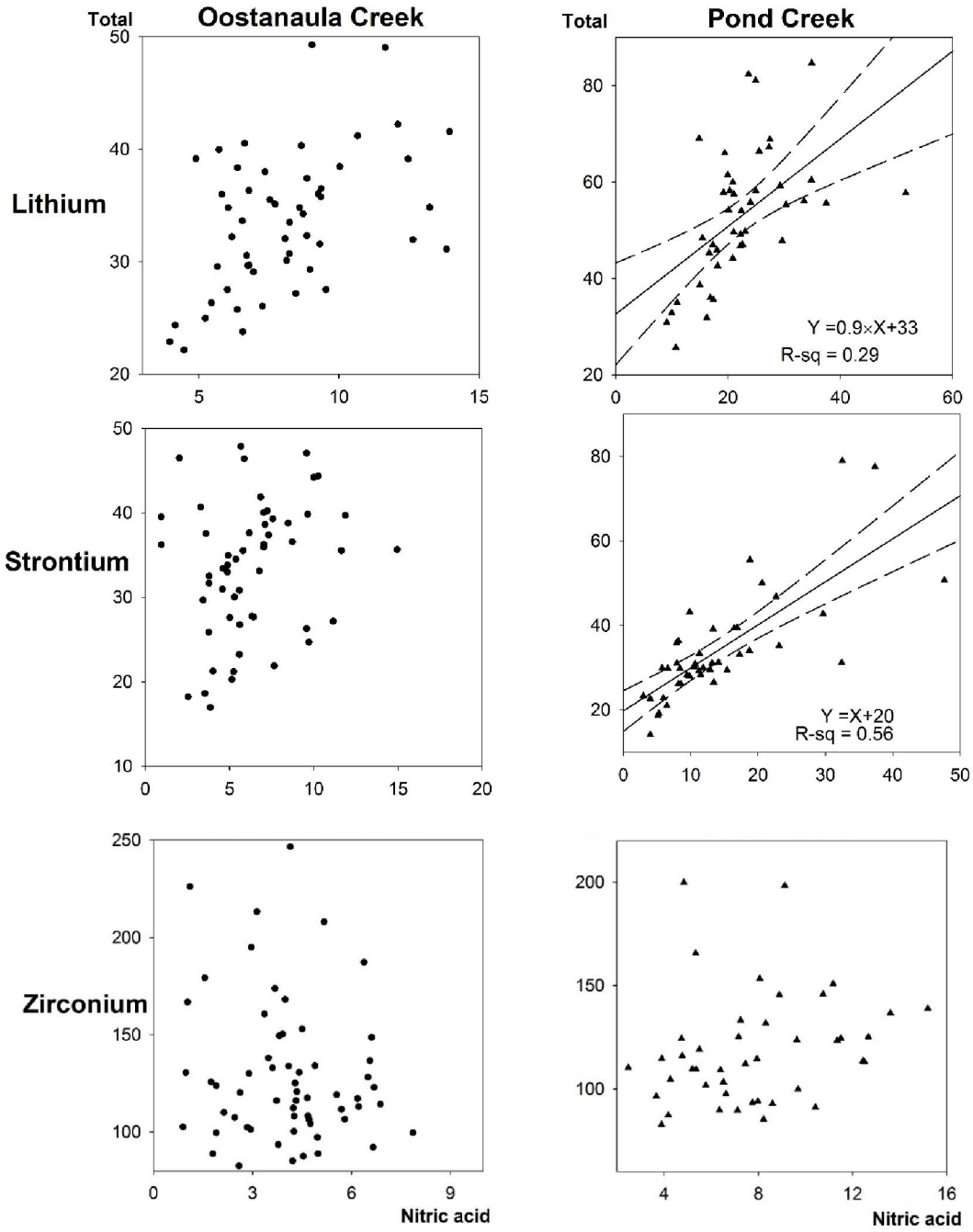


Figure 4.1 (f) Correlation and regression plots for Li, Sr, and Zr between total dissolution and nitric acid extraction in Oostanaula Creek and Pond Creek watersheds

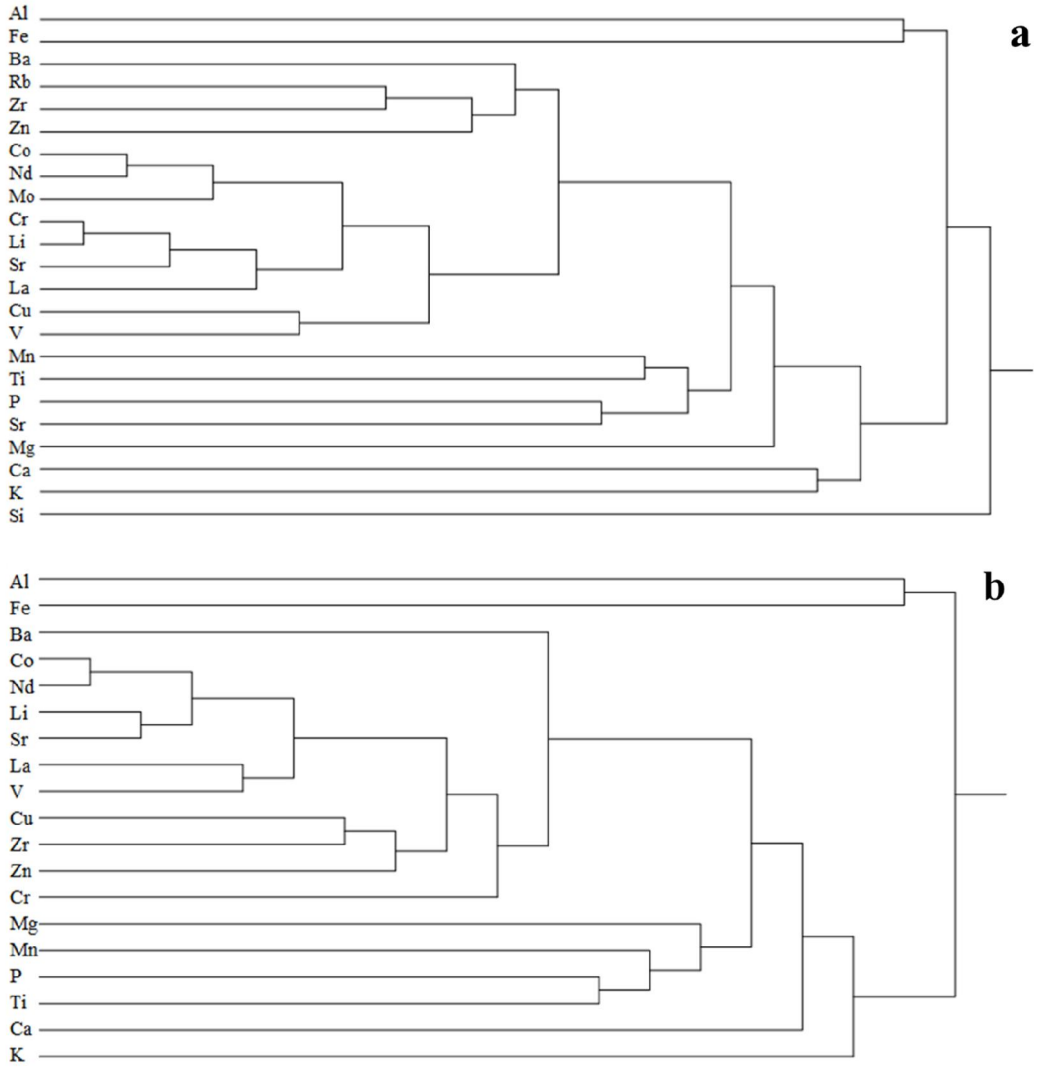


Figure 4.2 Total dissolution element dendrograms for measured elements in total dissolution for Oostanaula Creek (a) and Pond Creek (b) soils. The horizontal axis of the dendrogram represents the even spacing distance between clusters.

CHAPTER 5: CONCLUSIONS

More robust techniques for sediment source tracking are needed. Sediment bacteria metagenomics provide a powerful tool for assessing the complex microbial communities of sediment as well as eroding source materials. Sediment-MST herein refers to the direct tracking of microbial communities of sediment conglomerates by using prior knowledge of the characterization of the microbial communities for different land-based sediment sources materials (e.g., manure, upland and stream bank soils). In Chapter 2, it was shown that parent eroding soils and suspended sediment possess dissimilar bacterial communities. These varying bacterial community structures were employed diagnostically to assess the relative importance of eroding banks, using a Bayesian based model (SourceTracker). The results confirmed upland soils were likely significant sediment bacterial contributions to streams. These results indicates that the bacterial community, particularly with future improvements in the depth and scope of metagenomic sequencing, may be useful in the effort to better identify sources of suspended sediment and certainly warrants testing on a larger scale. The future benefit of sediment-MST will depend on the ability to demonstrate an apportioned link between the microbial community structure of suspended sediment and source materials in watersheds of various sizes. Such benefit may assist watershed managers to more efficiently target and implement best management practices (BMPs) that reduce non-point sources of both fecal source and sediment surface water contamination.

A novel approach for validating the sediment elemental fingerprinting technique was presented in Chapter 3. Specifically, the relative importance of different digestion procedures, objective source groupings, and methods for statistical tracer selection were

evaluated using predefined mixtures of sediment sources collected from a sediment impaired watershed. Sediment elemental data distinguished different coarse categories of sediment source materials, specifically surface versus subsurface and upland versus bank soils. However, sediment elemental fingerprinting was not effective in a small watershed for differentiating between finer categories of upland sources (cropland, pasture, and cattle paths).

The conclusions reached in Chapter 2, using bacterial metagenomic data, and Chapter 3, using sediment elemental fingerprints, identify different principal sources of sediment in an impaired watershed in southeastern Tennessee: upland soils in Chapter 2 and eroding banks in Chapter 3. While these findings appear contradictory, the errors associated with these two methods with limited sampling scope, are large, and this must be considered when interpreting the meaning of these apparent results. For this watershed, the methods are useful in clearly illustrating that eroding banks soils are an important source of stream suspended sediment and must be the focus of any water quality restoration effort.

Future sediment source tracking studies using both metagenomic data and sediment element fingerprints should be conducted within large watersheds with more readily deniable and distinct geological regions. Particle size fractions should be taken into consideration in future evaluations of sediment digestion procedures, objective groupings and statistical tracer selection. A narrower particle size range for the target sediment, e.g., 2-10 μm, 10-20 μm, and 20-30 μm, may provide more discriminatory power between different source groups. The results present in Chapter 4 clearly indicate

the safer and less expensive HNO_3 extraction procedure can be used for the sediment element analysis in these future studies.

VITA

Yanchong (Benjamin) Huangfu was born in Quwo, Shanxi Province, China in 1988, the son of Yuanzhou Huangfu (graduated from Tsinghua University in 1979) and Yingying Su (a medical doctor – internist in China). He relocated to the city of Xi'an in 1999 with his parents. He attended Xi'an Gaoxin No.1 Middle School and graduated in 2005. Then he started his undergraduate study in Hong Kong. He had a summer job at the DNC General Store at Yellow Stone National Park in 2007. He earned a Bachelor of Engineering degree in Civil Engineering in The Hong Kong Polytechnic University in 2009. He also completed his master study in the same university with a Master of Philosophy degree in Environmental Engineering. Before moving to the United States again, he used to work as an engineer in a construction company in Hong Kong and also a sewage treatment plant in mainland China.

In the spring of 2013, he started his doctoral program in the Department of Biosystems Engineering and Soil Science at The University of Tennessee – Knoxville. During his doctoral study, he has been a student member of several societies including the American Water Resources Association (Tennessee section), the Society for Applied Microbiology (in the United Kingdom), and the Soil Science Society of America. He will be receiving his Doctor of Philosophy degree in Biosystems Engineering from The University of Tennessee – Knoxville in December of 2018.